The Journal of

Gemmology

Volume 29 No. 1
January 2004

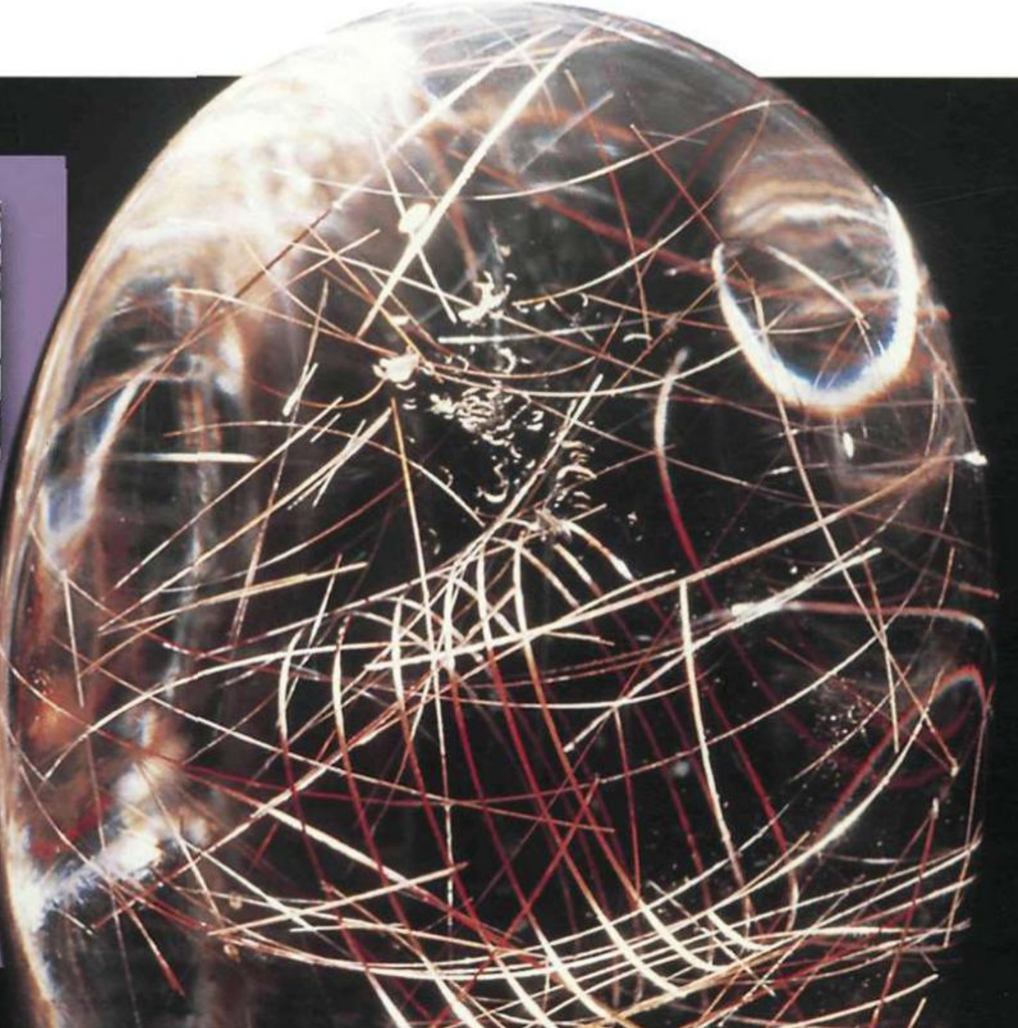

Colour zoning and composition of ruby-sapphire

Red and green labradorite feldspar

Microstructure of cultured blister pearls

The Gemmological Association and Gem Testing Laboratory of Great Britain

Gemmological Association and Gem Testing Laboratory of Great Britain

27 Greville Street, London EC1N 8TN
Tel: +44 (0)20 7404 3334 • **Fax:** +44 (0)20 7404 8843
e-mail: gagtl@btinternet.com • **Website:** www.gem-a.info

President: Prof A T Collins

Vice-Presidents: N W Deeks, R A Howie, D G Kent, R K Mitchell

Honorary Fellows: Chen Zhonghui, R A Howie, K Nassau

Honorary Life Members: H Bank, D J Callaghan, E A Jobbins, H Tillander

Council of Management: T J Davidson, R R Harding, L Hudson, I Mercer, J Monnickendam, M J O'Donoghue, E Stern, I Thomson, V P Watson

Members' Council: A J Allnutt, S Burgoyne, P Dwyer-Hickey, S A Everitt, J Greatwood, B Jackson, L Music, J B Nelson, P J Wates, C H Winter

Branch Chairmen: Midlands – G M Green, **North East** – N R Rose, **North West** – D M Brady, **Scottish** – B Jackson, **South East** – C H Winter, **South West** – R M Slater

Examiners: A J Allnutt MSc PhD FGA, L Bartlett BSc MPhil FGA DGA, S Coelho BSc FGA DGA, Prof A T Collins BSc PhD, A G Good FGA DGA, J Greatwood FGA, S Greatwood FGA DGA, G M Green FGA DGA, G M Howe FGA DGA, S Hue Williams MA FGA DGA, B Jackson FGA DGA, G H Jones BSc PhD FGA, Li Li Ping FGA DGA, M A Medniuk FGA DGA, M Newton BSc DPhil, C J E Oldershaw BSc (Hons) FGA DGA, H L Plumb BSc FGA DGA, N R Rose FGA DGA, R D Ross BSc FGA DGA, E Stern FGA DGA, S M Stocklmayer BSc (Hons) FGA, Prof I Sunagawa DSc, M Tilley GG FGA, C M Woodward BSc FGA DGA, Yang Ming Xing FGA DGA

The Journal of Gemmology

Editor: Dr R R Harding

Assistant Editors: M J O'Donoghue, P G Read

Associate Editors: Dr C E S Arps (Leiden), G Bosshart (Zurich), Prof A T Collins (London), Dr J W Harris (Glasgow), Prof R A Howie (Derbyshire), Dr J M Ogden (Hildesheim), Prof A H Rankin (Kingston upon Thames), Dr J E Shigley (Carlsbad), Prof D C Smith (Paris), E Stern (London), Prof I Sunagawa (Tokyo), Dr M Superchi (Milan)

Production Editor: M A Burland

Vol 29, No.1, January 2004

ISSN: 1355–4565

Coiled 'rutile' whiskers in a quartz single crystal

Ichiro Sunagawa[1], E. Alan Jobbins[2] and Emma Tinnyunt[3]

1. *Yamanashi Institute of Gemmology and Jewellery Arts,*
   Tokoji-machi 1955-1, Kofu, 400-0808 Japan
   e-mail (home): i.sunagawa@nifty.com
2. *Caterham, Surrey, CR3 6BA UK*
   e-mail: alan.jobbins@btinternet.com
3. *Hackney, London E2 8ET*
   e-mail: gemmyemma@MSN.com

Abstract: *'Rutile' whiskers showing a range of habits in a single crystal of quartz from Mogok, Myanmar, are described. The whiskers are thin and sometimes solid or thicker and hollow and may be straight, slightly curved or tightly curved into coils or spirals. The thicker whiskers are hollow tubes with the walls composed of aggregated thin fibres of 'rutile'. Their mode of formation by dislocation leading to the Eshelby twist, and their incorporation into the later-growing quartz are discussed. Later weathering is considered to cause pale brown axial and spotty peripheral staining.*

Keywords: *bundle whiskers, coiled whiskers, growth mechanism, rutilated quartz, rutile whiskers*

Introduction

Crystals sometimes exhibit habits very different from those expected from their structural characteristics. When NaCl or KCl crystals grow in a bulk aqueous solution, they take the cubic form bounded by {100} faces, i.e. the structurally expected form. When a supersaturated aqueous solution of NaCl or KCl is kept in a wineskin in dry shade, extremely elongated needle-like NaCl or KCl crystals bounded by {100} faces appear as if they are sprouting up from the outer skin. In this case, the needles are hollow, but many other crystal species can occur as solid needles. Taking examples from natural minerals, we may mention for example jamesonite, $Pb_4FeSb_6S_{14}$, millerite, NiS, and hair silver, Ag. A wide variety of artificial compounds is also known to show such morphology, e.g. metals: Fe, Cu, Ag, Sn; semiconductors: Si; sulphides: NbS_3; selenides: $NbSe_3$; carbides: SiC; nitrides: Si_3N_4; and oxides: Al_2O_3. Such crystals with extreme length to breadth ratios are called whiskers and have attracted both scientific and technological interests (Doremus *et al.*, 1958; Givargizov, 1986); they have also been called anisotropic crystals but this could be potentially confusing where optical properties may also be discussed.

ISSN: 1355–4565

Scientific interest arises from pure curiosity to understand how such unusual morphology is realized. Technological interest comes from the fact that whiskers have much higher crystal structure perfection and thus are elastically stronger than 3D bulk crystals. The high perfection of whiskers leads to potential materials to strengthen composites.

As to the mechanism of whisker formation, various hypotheses have been put forward, among which well established mechanisms are (1) the Vapour-Liquid-Solid (VLS) mechanism (Wagner and Ellis, 1964), and (2) the capillary mediated mechanism (Aoki, 1972). In the VLS mechanism, which was originally put forward for Si whiskers, Si supplied in the vapour phase (V) reacts with solid gold particles placed on a solid substrate of silicon and forms an Au-Si eutectic liquid droplet (L). Since the phase to nucleate and grow in such a eutectic liquid is determined by the liquid composition, only Si nucleates and grows (S) in the liquid droplet. There is only one growth site for Si in the Au-Si eutectic droplet, the crystal grows in one direction only and takes an extremely elongated needle habit. In the VLS mechanism a sphere of solidified eutectic Au-Si liquid always remains at the top of a Si whisker even after the completion of growth. The capillary mediated mechanism is applicable to KCl and NaCl whiskers. These are grown from a supersaturated solution which is kept in a wineskin and oozes through the skin by capillary action. As soon as the solution comes out on the skin surface, it evaporates, becoming more supersaturated; this results in immediate crystallization around the tiny capillary channel outlets. Crystallization continues perpendicular to the skin as a cylinder for as long as the capillary remains open and the solution is supplied continuously. Therefore, the whisker becomes a hollow one.

Figure 1: Polished quartz with numerous 'rutile' whiskers. Note the central thick coil and faint, much thinner coil at upper left and lower right (arrows). A partial loop, part of a widely spaced coil, is also visible at lower left centre. Height 56 mm.

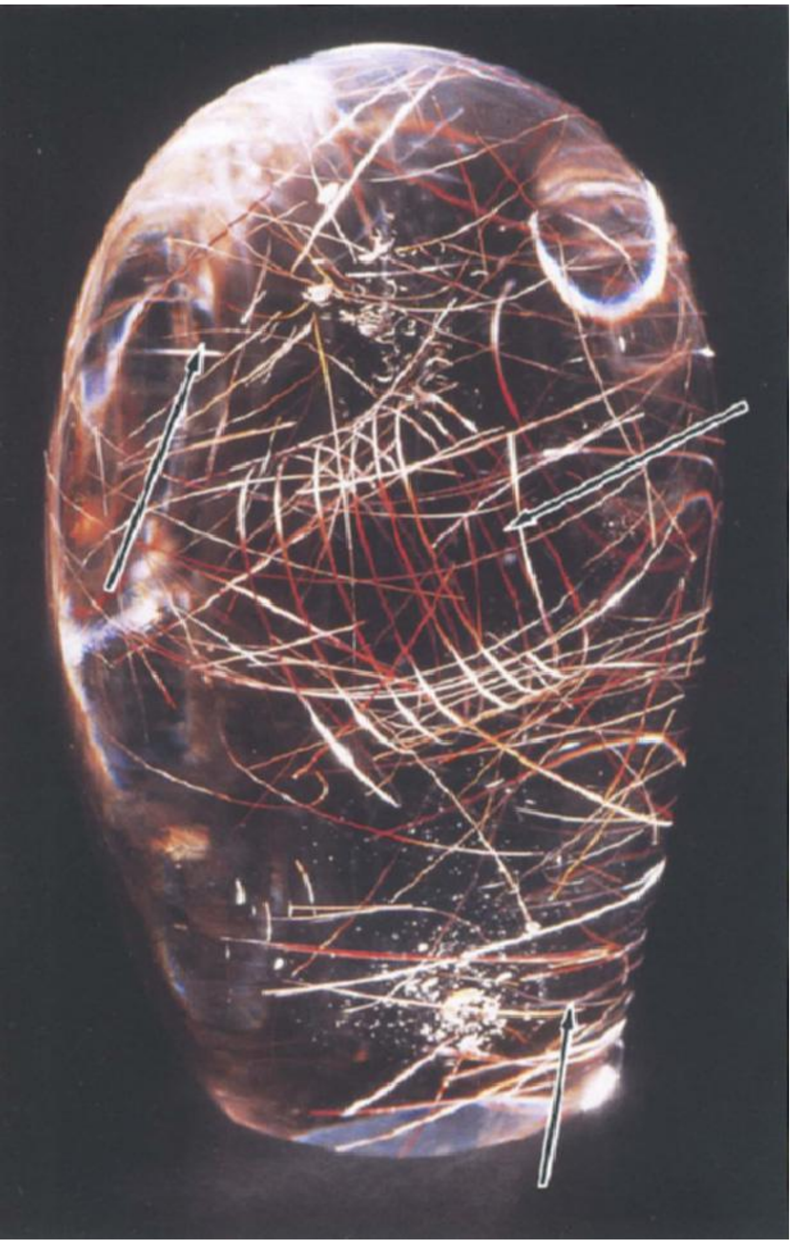

Whiskers have long been known in the mineral kingdom. Hair silver, millerite, and jamesonite are representative examples. Also known are pyrite FeS_2 and galena PbS, but these occur only rarely in whisker forms. Rutile (TiO_2) is another example showing whisker morphology that gemmologists often encounter in rutilated quartz (Gübelin and Koivula, 1986). The structurally expected polyhedral form of this rutile is short and prismatic, bounded by prisms {110} and pyramids {111}, but in rutilated quartz, they are whiskers and hitherto, gemmologists have not realized or been aware of their significance.

Most whiskers observed in natural crystals are straight, with aspect ratios (length *vs* thickness or height *vs* diameter) of a few tens

Figure 2a: Photomicrograph of the central thick coil. Note the axial pale brown line. Straight and slightly curved whiskers much thinner than the coil are also visible. Bar 0.5 mm.

to a few hundreds. Kinked (pyrite and galena), twisted (jamesonite) or ribbon (hair silver) whiskers are also known. But whiskers showing helical, coil, rope and other unusual morphologies in natural crystals have not to our knowledge been reported.

Recently, in 2001, when one of the authors (ET) visited Mogok, Myanmar, she obtained a specimen of colourless quartz full of needle inclusions polished in the form of an elongate egg. Most rutile whiskers in quartz are straight, but in this specimen there are some which show very unusual coil habits. Since whiskers with this spiral habit have not been reported from natural gem-quality mineral crystals, the sample was studied to try and understand its possible growth mechanism. This paper reports the results of observations on the sample, and presents an hypothesis for its origin.

Sample description

The sample is polished as an egg shape, maximum length 56 mm, maximum width 33 mm and weighs 75.45 g, with inclusions of straight, curved and coiled whiskers. *Figure 1* is a photograph of the specimen showing a distinct thick coil with an inclined axis, upper right to lower left, a faint but larger coil around the edge of the specimen, top right, together with slightly curved and straight whiskers. Arrows indicate coiled whiskers.

The RI of the specimen is approximately 1.54-1.55. The optic axis is at an angle to the length of the specimen, but a uniaxial figure is just visible and shows a typical quartz interference figure with a 'hollow' centre. The specimen is thus unambiguously identified as a single crystal of quartz. A small feather which reaches the polished surface shows a series of tiny spiky two-phase (liquid/gas) inclusions. Between crossed polars, the large coil appears a dull brownish-red, but is not noticeably birefringent. However, some straight and slightly curved whiskers (with sparse or no enclosed reddish deposits) are birefringent in first order grey colours.

Figure 2a shows an enlarged photograph representative of the central thick coil. The length, diameter and the spacing of the coil are 9 mm, 15 mm, and 1.8 mm, respectively, with 6 turns. There is also a much thinner, less visible coil at upper right of

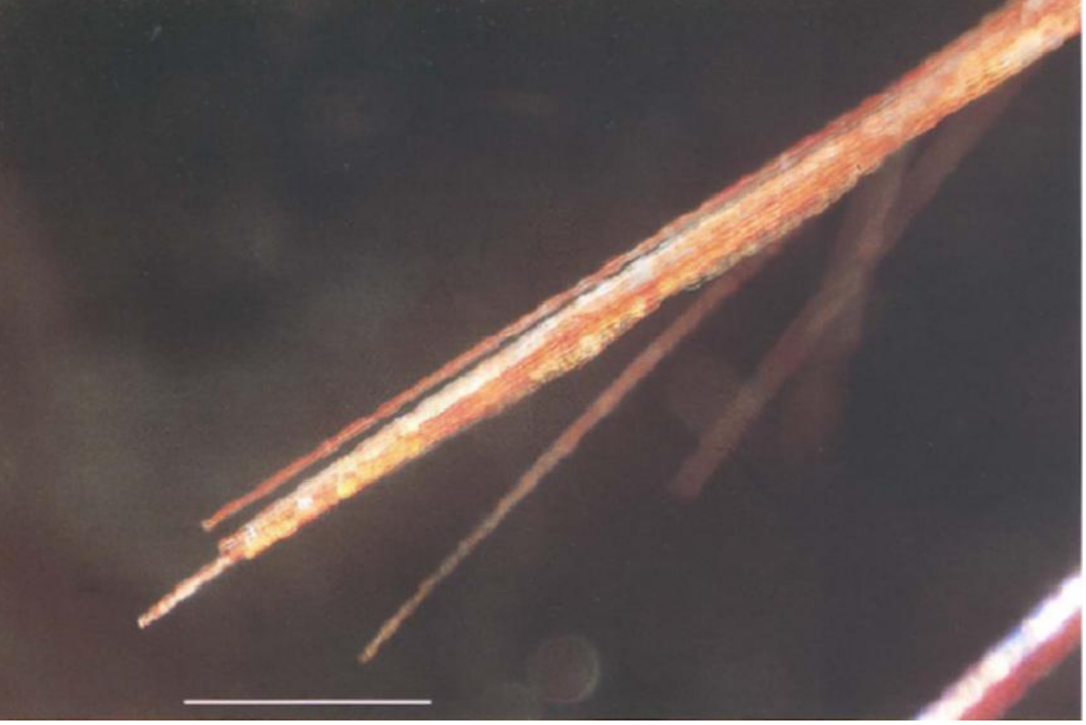

Figure 2b: One end of a hollow tube showing the splitting into several discrete and finer whiskers. Bar 0.1 mm.

Figure 1, with length, diameter and spacing of 9 mm, 10 mm, and 1.5 mm, respectively, and with only three turns. At both ends of these coils the curvatures change and divert from the turn of the coil. The ends of both hollow coils split into several discrete and finer whiskers (see *Figure 2b*). Some straight whiskers with elongations of 20 to 30 mm are 0.1 mm thick while others of similar length may be as thin as 20 μm. Most whiskers are hollow and many show ends split in to several finer whiskers.

In *Figure 3* are photomicrographs of the thick coil (*a.* view perpendicular to the elongation; *b.* oblique view). The two photographs indicate that the thick coil is a hollow tube with a pale brownish deposit on the wall surface of the hollow and sporadically distributed brownish dots within the wall layer. They also indicate that the thick coil is not an isolated and independent whisker, but a bundle of whiskers. Brown coloration may or may not be present in the thin straight whiskers. In *Figure 3a* the arrow in the upper centre indicates where the straight and coiled whiskers cross. A noteworthy point is that the straight whisker shows a distinct prism face and does not have a pale brown axis. Compared with the single crystalline nature of the straight whisker, the coiled whisker with the brown axial deposits is hollow and seems to represent a bundle of whiskers. The coil is 50 to 100 μm thick.

After the initial study of the specimen it became apparent that the inclusions were different from the usual rutile needles encountered in gemstones. Because of the specimen's size and its rounded surface, precise identification of the needles was not easy, but Professor Andy Rankin of Kingston University offered to attempt to check their identity using Raman techniques. This was carried out on fibres 10 to 50 microns below the surface and on two with a surface outcrop. Because of the fine needle form confirmation was lacking, but in his experience the rutile peak at 610 cm^{-1} is often very weak on such needles. Thus the presence of rutile is not disproven, but confirmation of actual rutile could not be substantiated. Strong fluorescence encountered above 500 cm^{-1} may have obscured the rutile peak – or weathered material in the tubes might have caused this.

We have had useful discussions with other gemmologists and mineralogists regarding the nature and origin of this specimen. We do not agree with suggestions that the coils could have been produced by computer-controlled laser beams, nor do we think that the coils are pseudomorphous after plant or other organic life. It has also been suggested that the existing coils are replacements of the original mineral.

Discussion

These inclusions show unusual habits for a crystalline material. The thicker whiskers are hollow with pale brown deposits, and some thinner whiskers are solid, so in order to understand how they formed, the following questions need to be answered: (1) whether the inclusions are crystalline or amorphous, and (2) whether they were formed before or after the growth of the host quartz crystal.

If the inclusions were formed before the growth of the quartz, they are whiskers, and the observed coil habit represents the original as-grown morphology of whiskers which was not modified to any significant extent by the later growth of quartz. If they were formed after the growth of the quartz, their formation must have an intimate relationship with dislocations in the quartz structure. Since there is more strain along dislocations than elsewhere in the structure, dislocations are preferable sites for later chemical attack. Dislocations which were subject to later chemical attack and show axial deposition of foreign material are called decorated dislocations. A method to decorate dislocations by appropriate metals deposited from a vapour phase was used as a powerful method to visualize dislocations in the earlier days of dislocation studies.

Very elongated needles of rutile are commonly observed inclusions in single crystals of quartz. They are usually straight and may be in ordered arrangements, or in random distribution and orientation. Growth-induced dislocations in single crystals of quartz usually show characteristic features such as divergent bundles starting from solid inclusions and running nearly perpendicularly to rhombohedral or prism faces. The needles in this specimen of quartz occur at random and do not show such characteristic distribution. We therefore believe that the rutile inclusions in quartz showing random frequency and orientation are not decorated growth-induced dislocations, but must have been formed before the growth of their host crystal, with little, if any, modification of morphology by the later growth of quartz.

Recently, whiskers showing unusual spiral morphology (Kishi *et al.*, 1995), microcoil (Motojima, *et al.*, 1995), ring (Tanaka, *et al.*, 1999, 2000), Möbius strip (Tanda *et al.*, 2002) and figure-of-eight crystal strip (Tanda and Tsuneta, 2002) have been observed on metal (Cu), sulphide and selenide (TaS_3, NbS_3, $NbSe_3$, $TaSe_3$) and nitride (Si_3N_4) crystals. All these whiskers are synthesized by CVD (chemical vapour deposition) methods. These have attracted renewed interest as topological materials and/or potential materials for CDW (charge-density-wave) interference, superconducting electron and two-component electron systems.

VLS mechanisms (Wagner and Ellis, 1964) or quasi-VLS mechanisms have been suggested as possible growth mechanisms for most of

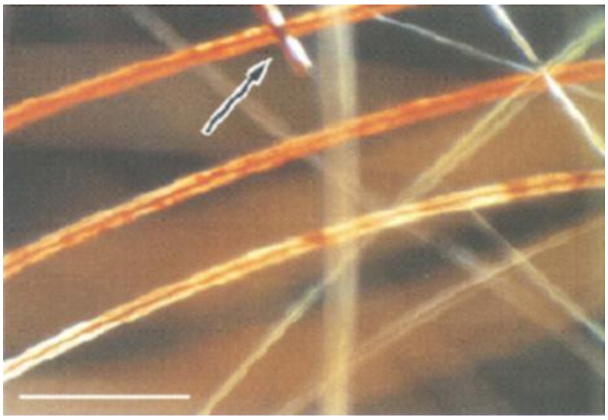

Figure 3a: *Part of the thick coiled whisker showing axial and sporadically distributed pale brown deposits. Note crossing of coil and straight whiskers at the upper centre of the picture (arrow). Bar 0.2 mm.*

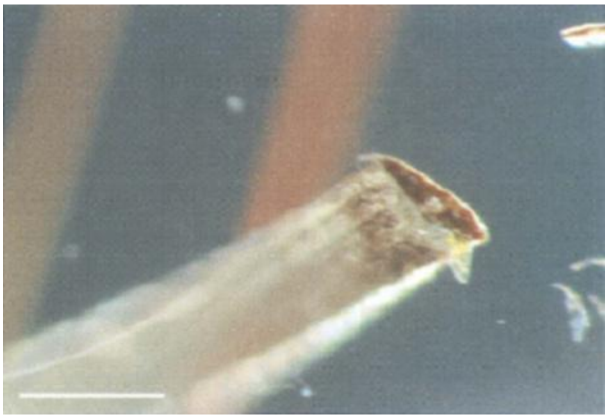

Figure 3b: *Relatively thick coiled whisker very near the quartz surface and showing fibres making up the walls of a hollow cylinder. Bar 0.05 mm.*

these whiskers. Cu whiskers may grow via a thin liquid layer of copper iodide (CuI), which is supplied by CuI vapour; the formation of a Si_3N_4 micro-coil whisker is activated by the presence of impurity, Fe or Co, from SiO-NH_3-H_2-Ar gas mixture; sulphide and selenide whiskers are synthesized by reacting nutrients Ta or Nb and S or Se in powder form in an evacuated quartz tube at elevated temperatures, which forms a eutectic liquid droplet of impurity component + Ta or Nb+S or Se.

Another possible mechanism for the formation of hollowed needles and whiskers is morphological transition of interface roughness due to adsorption of impurity on the tip surface of a prismatic crystal. This has recently been demonstrated for TiO_2 needles and whiskers grown by the LPE (Liquid Phase Epitaxy) method (Kawamura *et al.*, 2001). Due to substitution of Ti^{4+} ions by trivalent cations with similar ionic radius, oxygen ions around Ti^{4+} in the structure are destabilized to maintain electrical neutrality, resulting in breaking the Periodic Bond Chains (PBC) in the {111} face (Hartman and Perdok, 1955). This results in the transition of the {111} interface originally containing one PBC to a rough interface containing no PBC. This roughness occurs on the surface at the tip of a prismatic crystal, while the prism {110} faces remain unchanged as smooth interfaces, each containing two PBCs. As a result of this smooth to rough interface transition at the tip, growth proceeds rapidly in the direction of the *c*-axis, resulting in needle or whisker morphology. Formation of a hollow tube rather than a solid needle is due to preferential two-dimensional nucleation along the edges of the tip and prism faces. In both the VLS mechanism and the roughening transition on the tip surface, impurity cations play an important role, and these cations appear to be the essential reason why rutile crystals adopt a whisker morphology. However, since we have so far not observed direct evidence of the presence of a frozen liquid droplet at the tip of a whisker, we can not be certain that the VLS mechanism is the explanation. Various models have been proposed for the origin of the unusual habits of whiskers such as spirals, coils, Möbius strips and figures-of-eight. For those shown by sulphide and selenide whiskers, encircling of growing whiskers around a S or Se liquid droplet was suggested (Tanda and Tsuneta, 2002; Tanda *et al.*, 2002). For Si_3N_4 micro-coils, the beginning of curling occurs at a lump-like deposit on a straight whisker, which is assumed to be a liquid droplet with impurities such as Fe or Co. According to Motojima *et al.* (1995), all straight whiskers are single crystals of Si_3N_4, but micro-coils give electron diffraction patterns of an amorphous state. Moving from straight, via slightly curved, to micro-coil, the structural state changes from entirely single crystalline (straight) to axial centre single crystalline and peripheral amorphous (slightly curved) to amorphous and polycrystalline (beginning of coil) and eventually amorphous (micro-coil). In contrast, whiskers of sulphides and selenides showing unusual morphology are all single crystalline, and not amorphous.

Although no diffraction work has been done on 'rutile' inclusions in the present study we think that they were originally crystalline. If whiskers are thin and straight, they may be single crystals of rutile. These whiskers are not hollow tubes. Hollow tubes are only seen among the thicker whiskers. Thick whiskers are bundles of much thinner, single whiskers. If whiskers are bundled, they are more likely to be curved, twisted, curled or coiled in habit rather than straight. When a single whisker contains an axial dislocation, strain associated with the dislocation may cause an Eshelby twist. If Eshelby-twisted whiskers grow together in a bundle, it is highly possible that the bundle may take a helical or coil habit.

Stimulated by the observation of coiled 'rutile' whiskers, one of the authors (IS) re-examined other samples of twisted, curved, helical, coiled and rope-like bundles of whiskers of amphibole in the druse of a Japanese skarn. Micro-area XRD investigations of these whisker bundles indicate that they are all crystalline, and not amorphous. The results of investigations on these amphibole whiskers showing unusual morphology will be reported in a forthcoming paper (Sunagawa *et al.*, 2003).

Brown deposits in the axes of whiskers and spots around their margins are considered to be of secondary origin, formed by later weathering processes.

Conclusion

An unusual coil morphology exhibited by 'rutile' whiskers in single crystal quartz is reported. We conclude that both straight and coil whiskers were formed before the growth of the quartz crystal, and that their original forms have survived unmodified. There are thin single whiskers and thicker bundles of thin whiskers. The bundles consist of thin whiskers aggregated in a cylindrical manner with a hollow axis but the thin whiskers are solid. It is postulated that impurity cations influenced formation of rutile whiskers through destabilizing the tip interface and transforming it to a rough interface. As to the origin of the coiled morphology, twist caused by dislocation and strain in whisker structure is suggested. Later weathering of bundles of whiskers caused formation of brown axial deposits and sporadic peripheral brown spots.

Acknowledgement

We thank Professor Andy Rankin for his Raman work on the inclusions and several colleagues for useful discussions.

References

Aoki, Y., 1972. Growth of KCl whiskers on KCl crystals including the mother liquids. *J. Crystal Growth*, **15**, 163-6

Doremus, R.H., Roberts, B.W., and Turnbull, V. (eds), 1958. *Growth and perfection of crystals*. John Wiley, New York

Givargizov, E.I., 1986. *Highly anisotropic crystals*. D. Reidel, Dordrecht

Gübelin, E., and Koivula, J.I., 1986. *Photoatlas of inclusions in gemstones*. ABC, Zurich, 193, 313

Hartman, P., and Perdok, W.D., 1955. On the relation between structure and morphology of crystals. *Acta Cryst.*, **8**, 49-52, 521-4, 525-9

Kawamura, F., Yasui, I., and Sunagawa, I., 2001. Investigations on the growth and morphology of TiO_2 in the TiO_2-$Na_2B_4O_7$ system with and without impurities using a new LPE method. *J. Crystal Growth*, **231**, 186-93

Kishi, K., Nanaba, O., Jo, S., and Kabashima, T., 1995. The surface structure of spiral Cu whiskers. *Phys. Low Dim. Struct.*, **10/11**, 157-64

Motojima, S., Yamana, T., Araki, T., and Iwanaga, H., 1995. Preparation of micro-coiled Si_3N_4 fibres by impurity metal activated chemical vapour deposition and their mechanical properties. *J. Electrochemical Soc.*, **142**, 3141-8

Sunagawa, I., Takahashi, Y., Imai, H., and Yamada, S., 2003. Helical, coil, curl, ribbon and rope whisker bundles of amphibole and frost column of quartz. *Mineral. Mag.* (submitted)

Tanaka, S., Kawamoto, H., Shiobara, S., Okajima, Y., and Yamaya, K., 1999. Ring-shaped crystals of $NbSe_3$ and $TaSe_3$. *Phys. IV, France*, 9 (Pr 10-379)

Tanaka, S., Kawamoto, H., Shiobara, M., Sakurai, Y., Yasuzuka, S., Okajima, Y., and Yamaya, K., 2000. Single-crystal rings of $NbSe_3$: a system for CDW interference? *Physica B*, 284-288, 1657-8

Tanda, S., and Tsuneta, T., 2002. Topological materials. *KOTAIBUTSURI (Solid State Physics)*, **37**, 527-36 (in Japanese)

Tanda, S., Tsuneta, T., Okajima, Y., Inagaki, K., Yamaya, K., and Hatakenaka, N., 2002. A Möbius strip of single crystals. *Nature*, **417** (No. 6887), 397-8

Wagner, R., and Ellis, W.C., 1964. Vapour-Liquid-Solid mechanism of single-crystal growth. *Appl. Phys. Lett.*, **4**, 89-90

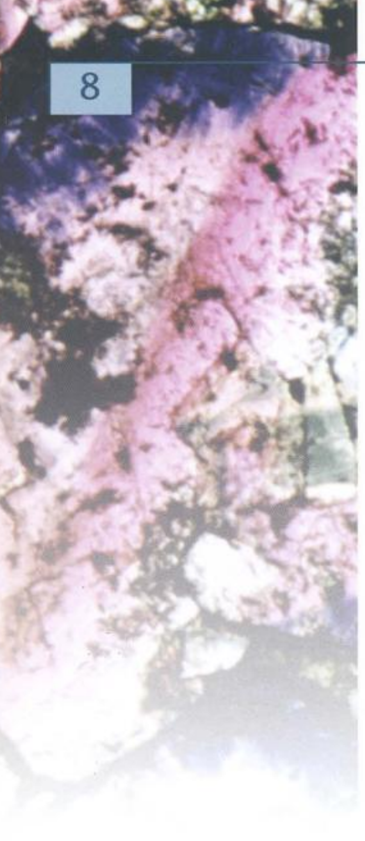

Colour zoning and composition of ruby-sapphire from Westland, New Zealand

Rodney H. Grapes and Paul W. O. Hoskin

Institut für Mineralogie, Petrologie und Geochemie, Albert-Ludwigs-Universität Freiburg, D-79104 Freiburg, Deutschland/Germany
e-mail: rodney.grapes@minpet.uni-freiburg.de

Abstract: *Ruby rock ('goodletite') is a ruby-sapphire-bearing fuchsite-margarite rock from the Southern Alps of New Zealand. The typically barrel-shaped ruby-sapphire shows a spectacular diversity of colours including rose-red, carmine, deep purple-red, pale-pink, pale-blue, deep-violet, as well as colourless examples that can be related to variable concentrations of* Cr_2O_3 *together with minor (typically <0.5 wt.%) iron oxide and* TiO_2*. Most crystals are colour-zoned, having pink or blue centres and colourless terminations. Individual ruby-sapphire crystals can exhibit extreme Cr-zonation, for example from 2.67 to 6.24 wt.%* Cr_2O_3 *in one example documented in this paper. Substitution of Cr into the corundum structure is a function of Cr-rich metasomatism involving reaction between Cr-poor quartzofeldspathic schist and ultramafic rock at elevated temperature and pressure. Substitution of iron (*Fe^{3+} *and* Fe^{2+}*) +* Ti^{4+} *to form sapphire rather than ruby corundum probably correlates with diminished* Cr^{3+} *concentration in the fluid phase during crystal growth.*

Introduction

During the 1890s rare boulders of a unique 'ruby rock' (informally named 'goodletite') were found (and continue to be found) in moraine derived from the Southern Alps in north Westland, New Zealand (McKay 1893; Ulrich 1894; Bell and Fraser 1906; Morgan 1927; Mason 1989; Grapes and Palmer 1989, 1992, 1996; Brown and Bracewell 1996; Grapes 1999). The rock consists of clusters of ruby-sapphire crystals set within a matrix of emerald-green chromian muscovite (fuchsite), margarite, with accessory chlorite, chromite, Ti-magnetite, and with dravitic tourmaline forming single crystals that overgrow the micaceous matrix and also occur in veins (see Figure 2 of Grapes and Palmer, 1996). Bulk rock and mineral analyses are given in Grapes and Palmer (1996).

The corundum was originally described by Ulrich (1894) as 'oriental ruby', presumably from the fact that some of the crystals were, as he described, "*... a fine rose-red, approaching carmine ...*", although most "*... are of a deep purple-red and rather dull, the larger ones generally showing dark, dull terminations with clearer portions of brighter red intermediate. Perfectly clear and finely coloured grains can, however, easily be picked out for proving the characteristic strong pleochroism of the ruby.*" Morgan (1927) records one crystal of nearly 25 mm in diameter that is "*... of a beautiful red transparent colour.*"

ISSN: 1355–4565

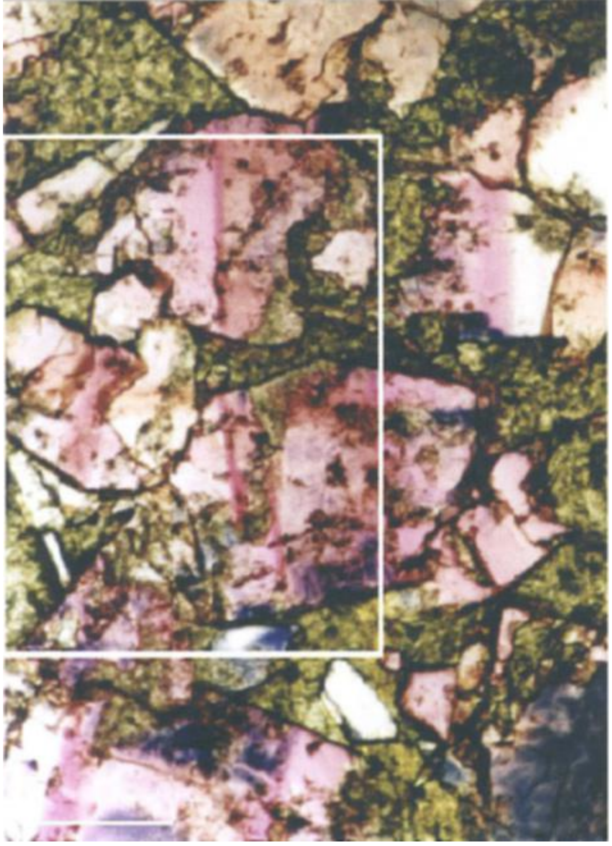

Figure 1a: Thin section photomicrograph (plane polarized light) of ruby-sapphire crystals within a matrix of margarite and chromian muscovite (fuchsite). The thin section is 0.035 mm-thick. Thin, darker-pink lamellae have the highest Cr-content (up to 12.9 wt.% Cr_2O_3) and abundances decrease with lighter-pink coloration, to <0.3 wt.% in colourless parts of the crystals. Areas of blue sapphire (see bottom-right crystal) contain 0.04-0.6 wt.% TiO_2. White box delineates area shown in (b). Scale bar is 0.5 mm.

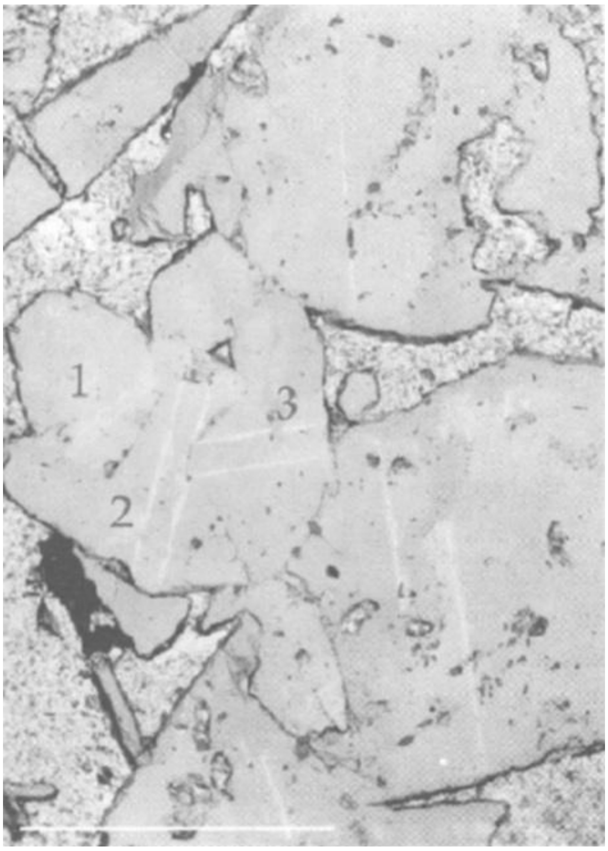

Figure 1b: A backscattered electron image of the outlined area in (a) showing three inter-penetrating crystals (labelled 1, 2 and 3), each with two parallel Cr-rich lamellae (white lines) in the central parts of the crystals. Scale bar is 1 mm.

Although the ruby rock is a rare and highly prized jewellery-grade ornamental stone, individual crystals of the ruby-sapphire corundum are typically strongly colour zoned, often intergrown, contain inclusions of the mica matrix, and commonly fractured, so that they are seldom of gem quality.

Crystal habit and colour zoning

Mineral separates from lightly crushed samples of the 'ruby rock' indicate that the corundum generally has a barrel-shaped habit with hexagonal dipyramids; some crystals have very small rhombohedral faces. Individual crystals are highly variable in size and typically range from 2–6 × 1–2 mm. The crystals are horizontally striated and many occur as interpenetrating clusters as shown in *Figures 1a and 1b*.

In 0.035 mm-thick thin section, the New Zealand corundum is invariably spectacularly coloured and in the red range, may be pale-pink/pinkish-orange/carmine/dark ruby-red; in the blue range it may be pale-blue/bluish-green/deep-violet (*Figure 2*). In sections approximately parallel to the *c*-axis the corundum is often colourless at both extremities and shows a gradual increase in pink coloration towards the central part where there are usually two thin parallel ruby-red bands separated by a thicker central band of either pale-pink or blue/violet colour (*Figures 1a and 2*). While pink and blue growth zoning is clearly present, the development of partial rims of sapphire in many crystals appears to be a replacement that extends inwards along parting planes (*Figure 3*). The patchy distribution of blue coloration such as that shown in *Figure 3* is also suggestive of replacement. As separates, such grains appear dark bluish-grey.

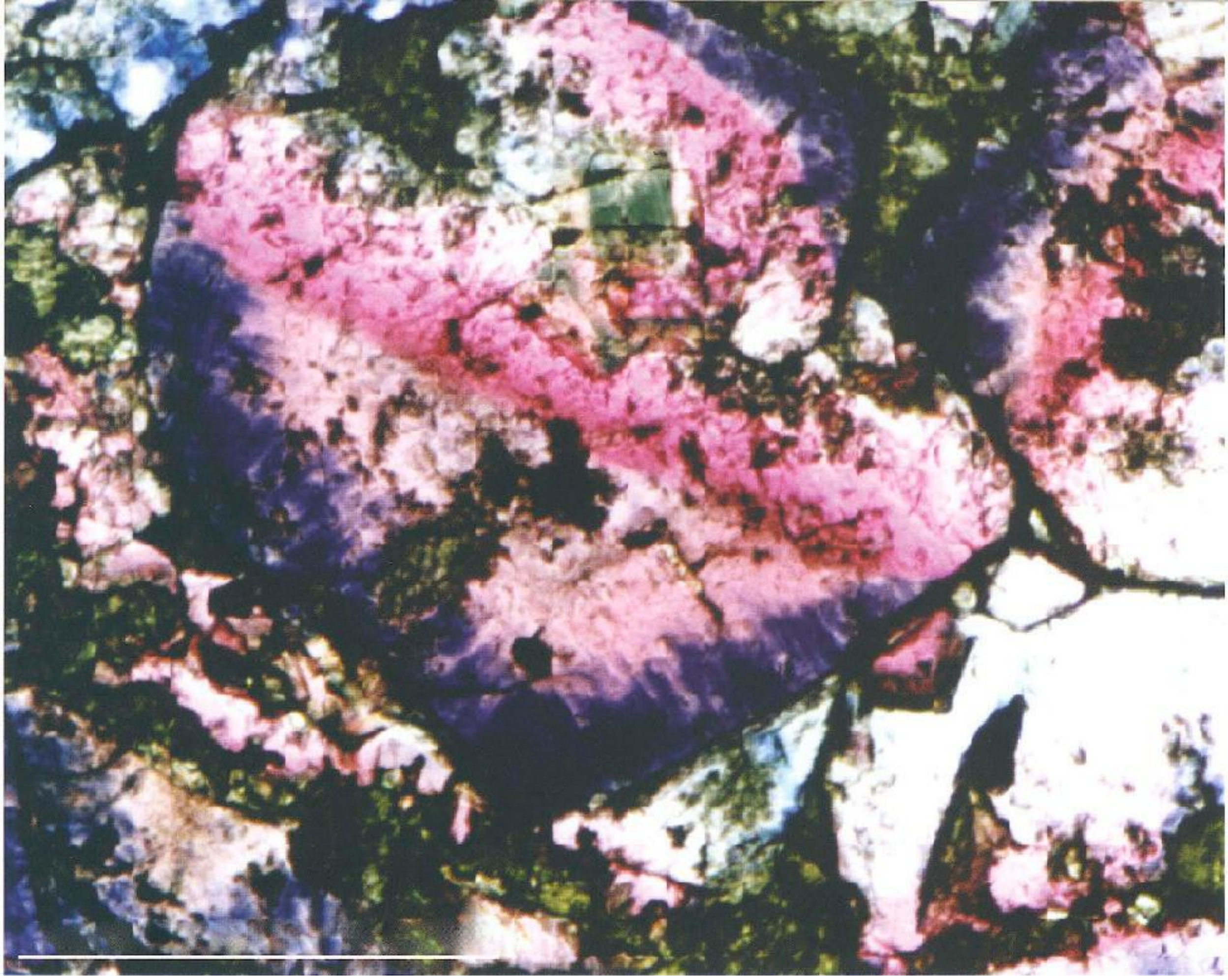

Figure 2: Thin section photomicrograph (plane polarized light) of a zoned corundum crystal showing marginal sapphire (blue) zoning and possible inward replacement along parting planes. Scale bar is 2 mm.

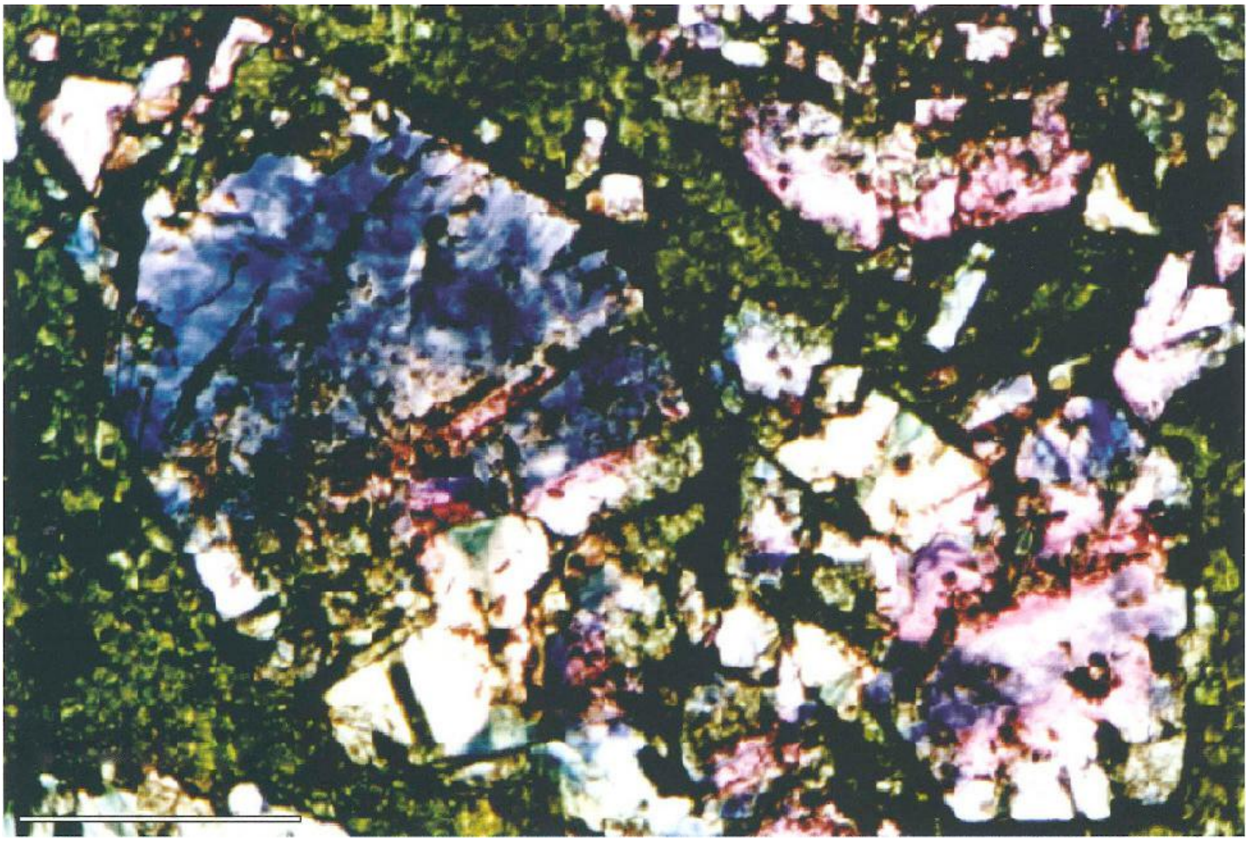

Figure 3: Thin section photomicrograph (plane polarized light) showing patchy blue coloration in pale pink-colourless corundum crystals within a chromian muscovite-margarite matrix. Scale bar is 2 mm.

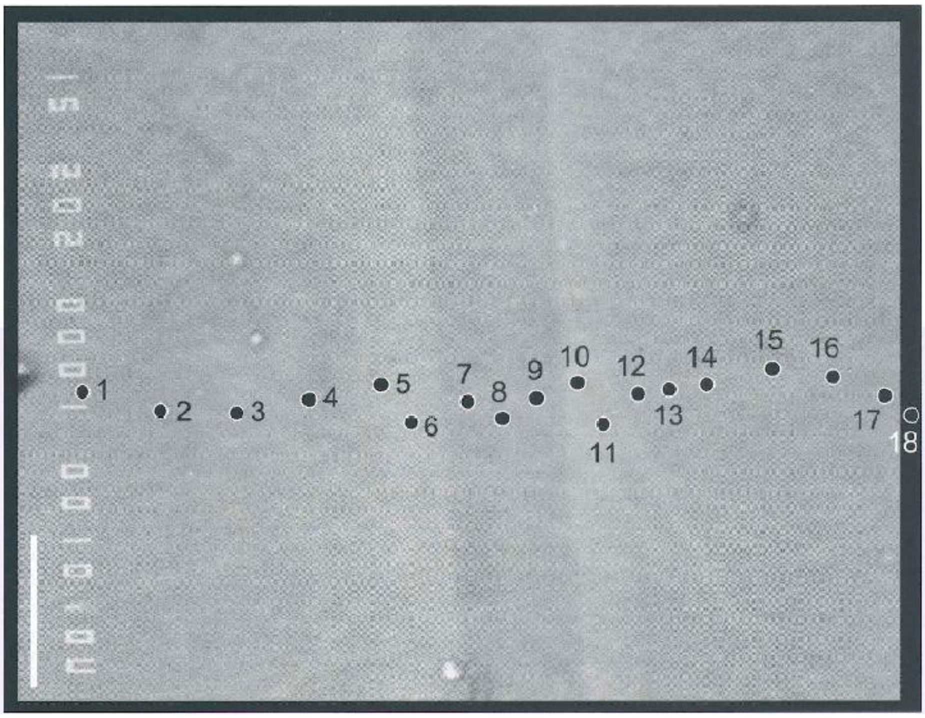

Figure 4: Backscattered electron image of the central part of a zoned corundum crystal. In plane polarized light, the central dark grey band is blue (analyses 7–9); the light grey marginal zones are dark ruby-red (analyses 5, 6, 10 and 11); the remainder of the crystal is pale to very pale-pink. Numbered spots are locations of electron microprobe spot analyses listed in Table I and plotted in Figure 5. Scale bar is 10 μm.

Chemical Composition

Electron microprobe analyses across the central part of a zoned corundum crystal (*Figure 4*) are given in *Table I* and show that Cr_2O_3 ranges from 2.67–6.24 wt.%, Fe_2O_3 (as total iron) from 0.13–0.54 wt.%, and TiO_2 from 0.01–0.18 wt.%. Compositional variation across the zoned crystal is shown in *Figure 5*. The central blue band has the lowest Cr and highest Fe and Ti contents; adjacent thin red bands have the highest Cr and lowest Fe and Ti contents. Chromium progressively decreases outwards from the central red bands and iron increases in the very pale pink areas of the crystal furthest away from the red bands. These variations may result from a number of possible substitutions, such as, $Cr^{3+} \leftrightarrow Al^{3+}$, $Fe^{3+} \leftrightarrow Al^{3+}$, and $Fe^{2+} + Ti^{4+} \leftrightarrow 2Al^{3+}$.

The spot analyses listed in *Table I* also indicate the presence of SiO_2 ranging from 0.06–0.14 wt.%. These values are significantly higher than microprobe values of between 0.005–0.02 wt.% in corundum recorded by Schmetzer and Bank (1981). However, ruby corundum (0.98–3.83 wt.% Cr_2O_3) from O'Briens Claims, Zimbabwe, analysed by Schreyer *et al.* (1981), lack iron and have between 0.02 and 0.94 wt.% TiO_2 and between 0.00 and 0.66 wt.% SiO_2. An inverse relation between Ti and Si in two analyses listed by Schreyer *et al.* (1981) suggests that Si may proxy for Ti according to the substitution $Si^{4+} \leftrightarrow Ti^{4+}$. However, the data from the New Zealand corundum show no such inverse relationship (*Table I*), and the status of Si in corundum remains problematical. Backscattered electron imaging of many corundum crystals indicates the presence of 'ghost-like' crystal shapes of matrix mica (muscovite and margarite) from which the corundum grew (e.g. see Figure 7 of Grapes and Palmer, 1996). This suggests that some or possibly all SiO_2 analysed in the corundum (*Table I*) is due to contamination caused by the electron beam impinging on subsurface mica in the 0.035 mm-thick thin section. Although not routinely analysed for,

Table I: Electron microprobe analyses (wt.% oxide) of a colour zoned corundum‡.

Analysis	**1**	**2**	**3**	**4**	**5**	**6**	**7**	**8**	**9**
	PP	PP	PP	P	DP	DP	B	B	B
TiO_2	0.02	0.01	0.04	0.02	0.01	0.03	0.18	0.17	0.15
Al_2O_3	96.50	96.35	96.62	96.22	94.08	93.97	96.31	96.71	96.31
Fe_2O_3†	0.20	0.23	0.18	0.17	0.19	0.24	0.47	0.52	0.54
Cr_2O_3	3.17	3.62	3.73	4.05	5.52	6.09	2.67	2.69	2.72
Total	**99.89**	**100.18**	**100.57**	**100.46**	**99.80**	**100.33**	**99.63**	**100.09**	**99.72**
SiO_2	0.07	0.06	0.11	0.09	0.12	0.11	0.09	0.10	0.13
$Fe_2O_3^*$	0.18	0.22	0.14	0.15	0.16	0.21	0.29	0.35	0.39
FeO^*	0.02	0.01	0.04	0.02	0.01	0.03	0.16	0.15	0.13
Analysis	**10**	**11**	**12**	**13**	**14**	**15**	**16**	**17**	**18**
	DP	DP	P	P	P	PP	PP	PP	PP
TiO_2	0.01	0.04	0.03	0.02	0.01	0.04	0.03	0.02	0.03
Al_2O_3	93.77	94.56	95.01	95.70	95.16	95.98	95.68	95.95	96.35
Fe_2O_3†	0.18	0.16	0.20	0.13	0.24	0.21	0.18	0.23	0.26
Cr_2O_3	6.24	5.44	4.20	4.01	4.00	3.68	3.41	3.45	3.31
Total	**100.20**	**100.20**	**99.44**	**99.86**	**99.41**	**99.91**	**99.30**	**99.65**	**99.95**
SiO_2	0.13	0.14	0.09	0.12	0.13	0.08	0.11	0.06	0.06
$Fe_2O_3^*$	0.17	0.12	0.15	0.10	0.20	0.15	0.13	0.18	0.11
FeO^*	0.01	0.04	0.03	0.02	0.01	0.04	0.03	0.02	0.03

‡Analysis numbers correspond with locations shown in backscattered electron image (*Figure 4*).
†All iron as Fe_2O_3
* FeO and Fe_2O_3 calculated on the basis of rhombohedral stoichiometry of 3 oxygens and 2 cations. SiO_2 values not included in the recalculation.
Colour observed in plane polarized light in a 0.035 mm thick microscope thin section. PP = pale pink; P = pink; DP = dark pink; B = blue.

detectable amounts of Ca and K in some corundum analyses would support this assumption.

Recalculation of the corundum on a rhombohedral oxide basis (i.e. 2 cations and 3 oxygens) gives stoichiometric amounts of FeO (0.01–0.16 wt.%) and Fe_2O_3 (0.10–0.39 wt.%) that are also given *Table I*, and the relation between Cr^{3+}, Fe^{3+} and (Fe^{2+} + Ti^{4+}) is shown in *Figure 6* and allows the intensity of pink coloration to be contoured.

Discussion

The observed colour of corundum is explained in terms of Cr, Fe, Ti and V (e.g. Loeffler and Burns, 1976; Schmetzer and Bank, 1981) which are often present in trace amounts. Red colour is due to the presence of Cr^{3+} (intensified by V^{3+}), green coloration is due to Fe^{3+}, and blue colour is caused by the presence of Fe^{2+} + Ti^{4+}. The most striking feature of the New Zealand corundum is its high chromium content and colour zonation. Grapes and Palmer (1996) showed that Cr contents in the corundum range from <0.5 to as high as 13 wt.% Cr_2O_3 with such variation occurring over only a few micrometres; a smaller range, but still significant is shown in *Figure 5*. The highest Cr-contents of the corundum are recorded in the thin ruby-red growth zones that typically occur on two opposing {0001} planes within the central parts of crystals and formed during the early stages of growth.

Figure 5: Plot of wt.% oxide versus distance (μm) along the electron microprobe traverse across the central part of the zoned corundum crystal shown in Figure 4. Analysis 1 is at 0 μm. Data are tabulated in Table I. Colour shading represents colours and colour intensity observed optically in plane polarized light.

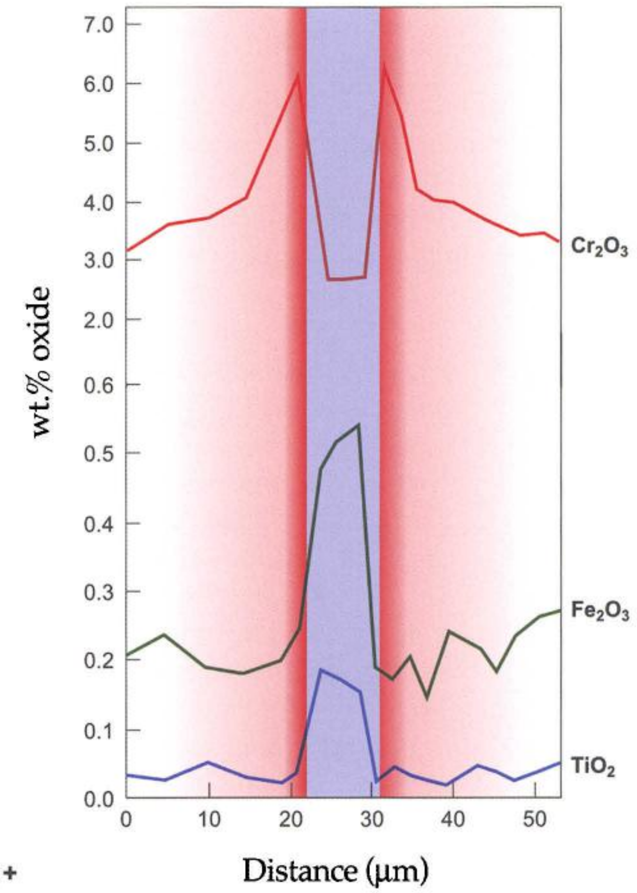

Subsequent growth to form the characteristic steep pyramidal terminations and barrel-shaped habits was accompanied by a decreasing amount of Cr-substitution, presumably reflecting gradually diminishing amounts of Cr in the fluid leading to the development of optically colourless corundum with <0.5 wt.% Cr_2O_3. The central blue sections of many crystals and areas of marginal sapphire replacement also have significant Cr_2O_3 ranging between 1.32 and 3.06 wt.%, TiO_2 contents of 0.04–0.63 wt.% and computed FeO contents of 0.13–0.25 wt.% (Grapes and Palmer, 1996) that can be related to intensity

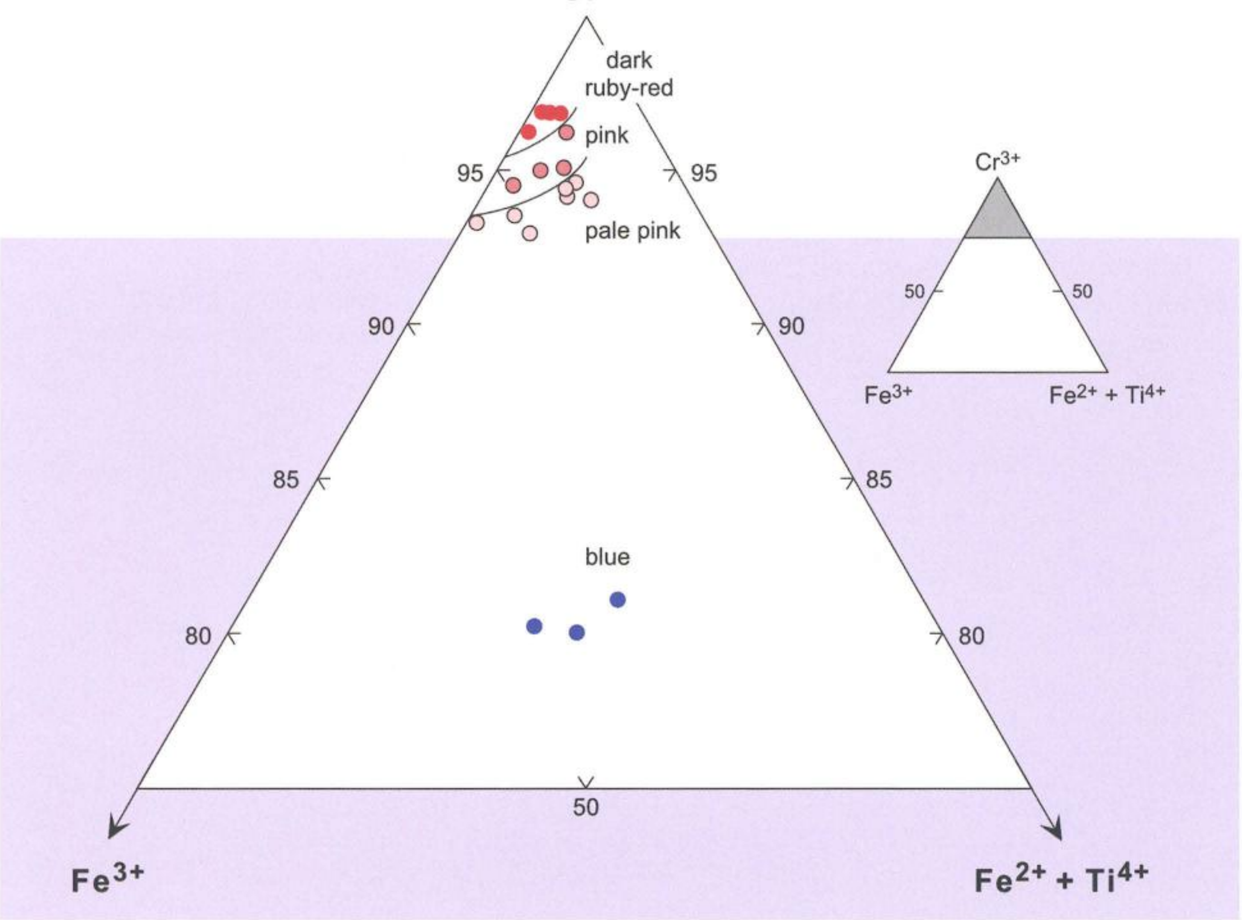

Figure 6: Plot of corundum compositions given in Table I in terms of Cr^{3+}, Fe^{3+} and (Fe^{2+} + Ti^{4+}) showing relationship to colours observed under plane polarized light in a microscope thin section with a thickness of 0.035 mm.

of blue coloration. A change in colour from pale-blue to dark violet-blue is associated with increasing Ti and Fe; in thin section this masks the usual pink coloration imparted by Cr^{3+} (*Figure 2*), but in hand-specimen it shows as a characteristic deep-purple in many crystals (e.g. see Figures 1 and 2 of Brown and Bracewell, 1996).

The Cr-rich environment in which the corundum grew is considered to be the result of metasomatic reaction between ultra-mafic rocks with a mean of 2023 ppm Cr and inclusions of Cr-poor quartzofeldspathic schist (mean of 45 ppm Cr); this took place under *T-P* conditions of 450±20°C and 5–6 kbar (Grapes and Palmer, 1996) to produce the corundum-margarite-fuchsite-tourmaline assemblage. While substitution of Cr into the corundum structure was clearly a function of the Cr-rich environment, the entry of iron (Fe^{3+} and Fe^{2+}) + Ti^{4+} may simply reflect periods at the initial and latest phase of corundum growth of diminished Cr^{3+} concentration in the fluid phase, rather than any change in redox potential.

Acknowledgement

We acknowledge the suggested changes and constructive comments on the manuscript by an anonymous reviewer.

References

Bell, J.M., and Fraser, C., 1906. The geology of the Hokitika sheet, North Westland quadrangle. *New Zealand Geological Survey Bulletin*, **1**

Brown, G., and Bracewell, H., 1996. Goodletite: a beautiful ornamental material from New Zealand. *Journal of Gemmology*, **25**, 211-7

Grapes, R.H., 1999. Ruby-sapphire from Westland: early and more recent discoveries. *Mineralogical Society of New Zealand Newsletter*, **10**, 3-9

Grapes, R.H., and Palmer, K., 1989. Goodletite further re-examined. *Geological Society of New Zealand Newsletter*, **85**, 31

Grapes, R.H., and Palmer, K., 1992. Ruby-kyanite rock from south Westland. *Geological Society of New Zealand Newsletter*, **95**, 35-6

Grapes, R.H., and Palmer, K., 1996. (Ruby-Sapphire)-chromian mica-tourmaline rocks from Westland, New Zealand. *Journal of Petrology*, **37**, 293-315

Loeffler, B.M., and Burns, R.G., 1976. Shedding light on the color of gems and minerals. *American Scientist*, **64**, 636-47

Mason, B., 1989. Goodletite re-examined. *Geological Society of New Zealand Newsletter*, **84**, 66

McKay, A., 1893. Geological explorations of the northern part of Westland. *Appendices of the House of Representatives, New Zealand*, C-3, 132-86

Morgan, P.G., 1927. Minerals and mineral substances of New Zealand. *New Zealand Geological Survey Bulletin*, **32**

Schmetzer, W., and Bank, H., 1981. The colour of natural corundum. *Neues Jahrbuch für Mineralogie, Monatshefte*, **Jg. 1981, H.2**, 59-68

Schreyer, W., Werding, G., and Abraham, K., 1981. Corundum-fuchsite rocks in greenstone belts of Southern Africa: petrology, geochemistry, and possible origin. *Journal of Petrology*, **22**, 191-231

Ulrich, G.H.F., 1894. On a discovery of 'oriental ruby' and 'margarite' in the province of Westland, New Zealand. *Mineralogical Magazine*, **10**, 217-9

Red and green labradorite feldspar from Congo

Michael S. Krzemnicki

SSEF Swiss Gemmological Institute, Basel, Switzerland
e-mail: gemlab@ssef.ch

Abstract: *Two red and one green transparent cut feldspars from the Democratic Republic of Congo have been investigated and are compared with similar material from Oregon (USA). The specimens from Congo display a deeper colour saturation, which make these new findings very attractive gemstones. The studied specimens belong to the labradorite variety of plagioclase feldspar. Microscopically the stones are rather clean, and only some twin lamellae, hollow channels and fine inclusions are present.*

The red and green colours in labradorites from both Congo and Oregon are due to copper, and the differences in colour are attributed to tiny copper colloids of different size. The Congo labradorites contain about 20× more copper than the Oregon stones.

General considerations about commercial terms and mineralogical nomenclature of feldspars are presented.

Keywords: *Congo, copper, feldspar, labradorite, plagioclase*

Introduction and sample description

Recently, the SSEF Swiss Gemmological Institute received two feldspars from Dr Laurent Sikirdji (Gemfrance, St.-Ismier, France) for testing. Specimen RC1 (1.967 ct) is intensely red and specimen GC1 (4.856 ct) is of a saturated green colour. A similar red specimen (RC2) of 2.969 ct was provided by Peter Salzmann (Lucerne, Switzerland). The location of the source is not yet exactly known; however, they are said to originate from the Democratic Republic of Congo (L. Sikirdji, pers. comm., 2003). The author has seen several faceted red feldspars from Congo up to 10 ct during the 2003 Tucson show. These feldspars (*Figure 1*) strongly resemble sunstone labradorite from Oregon in the USA (Pough, 1983; Hofmeister and Rossman, 1985; Johnston *et al.*, 1991), but display a more vivid and saturated colour than the latter. The occurrence of red and green plagioclase is not uncommon. Hofmeister and Rossman (1985) and Johnston *et al.* (1991) described in detail that such colours may even occur within a single specimen, often accompanied by a spangling effect (aventurescence or schiller) as a result of oriented small red platelets. The red and green samples examined in our study showed no spangling effect (aventurescence), although Fritsch (2002) observed such an effect in stones from the same general location.

ISSN: 1355–4565

Figure 1: Labradorite feldspar from Congo (two intense red stones on the left, and one intense green on the upper right) and Oregon (all other stones), showing the colour variations from intense red and green (Congo) to pale red, pale yellow, pale green and colourless (Oregon). © Dr Michael S. Krzemnicki, SSEF Swiss Gemmological Institute.

On the market (Tucson 2003), the red and green stones from Congo have been offered as red andesine (an intermediate member of the plagioclase feldspar solid solution series). In the literature, gem-quality red andesine from Congo was first mentioned by Fritsch (2002). Below, physical, chemical and spectroscopic data of the studied samples are compared to similar feldspars from other sources (Hofmeister and Rossmann, 1985; Johnston *et al.*, 1991; Laurs, 2002). Then the nomenclature of sunstone feldspar is discussed, taking into account the controversy among gemmologists in 1992 (Gübelin, 1992; Hanneman, 1992; Hoover, 1992; Johnston, 1992; Liddicoat, 1992a, 1992b).

Table I: Gemmological properties of labradorite and andesine from Congo and Oregon (USA).

	Labradorite from Congo	Andesine from Congo	Labradorite from Oregon
	(this study)	Fritsch (2002)	(this study)
weight	1.97 to 4.856 ct	1.04 to 8.95 ct	2.91 and 3.63 ct
SG	2.68 to 2.70	2.67	2.70 and 2.72
RI	RIα 1.553 to 1.555 RIγ 1.562 to 1.563	1.551 1.560	1.560 and 1.565 1.570 and 1.572
birefringence	0.007 to 0.011	0.009	0.007 and 0.010
optic nature	biaxial (positive)	biaxial (negative)	biaxial
colour	red (RC1 and RC2) and green (GC1)	red	pale red (RO1) and pale green (GO1)
pleochrosim	very weak (red samples RC1 and RC2) to distinct (green sample GC1)	very weak	very weak (red sample RO1) to distinct (green sample GO1)
transparency	transparent	transparent	transparent
LW-UV	weak to distinct orange	weak to medium orange	none
SW-UV	none	weak red	none
observations	milky turbidity green labradorite: red under incandescent light	'schiller' effect	slight 'schiller' effect

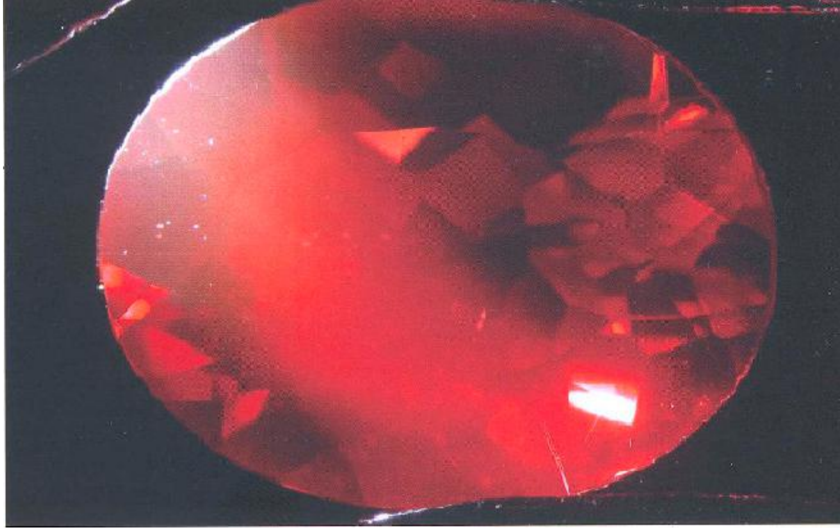

Figure 2: Red labradorite RC2 from the Congo revealing its milky turbidity. © Dr Michael S. Krzemnicki, SSEF Swiss Gemmological Institute.

Gemmological properties

The samples were first studied using classical gemmological equipment and methods, namely, the refractometer, hydrostatic balance, polariscope, long- and short-wave ultraviolet light (LW-UV and SW-UV) and microscope. RC1, RC2 and GC1 showed more or less equal values for refractive indices, birefringence and specific gravity (*Table I*). All samples were determined as optically biaxial positive. The red specimens (RC1, RC2) showed only very weak pleochroism, whereas the green sample (GC1) presented a distinct pleochroism from greenish-yellow to bluish-green. Hofmeister and Rossman (1985) also found only minor pleochroism in the red sunstone labradorites from Oregon (USA), but a distinct dichroism in their green samples. Under LW-UV, the red samples showed a weak orange glow, whereas the green stone appeared distinctly orange. Under SW-UV, no fluorescence was observed in RC1, RC2 and GC1, in contrast to Fritsch (2002) who reported a weak red fluorescence and even some surface related bluish luminescence in his stones from Congo.

Microscopic observations

All samples are rather clean with only a few inclusions. The red stones show a relatively uniform colour distribution, which was confirmed in immersion liquid. Specimen RC1 shows a step-like healing fissure along a cleavage direction. RC2 (*Figures 2 and 4*) contains several distinct twin lamellae and a few parallel hollow channels; in some parts along but not within the twin lamellae, very tiny particles were observed. These particles are responsible for a general milky turbidity, which may be concentrated in zones. No reflecting inclusions producing aventurescence were observed.

The colour of the green stone (GC1) is distinctly lamellar zoned. With high magnification, small parallel fluid channels and trails of tiny inclusions are visible. Furthermore, the specimen shows a milky turbidity and a reddish hue in white incident light (*Figure 3*).

UV-Vis spectroscopic analyses

Spectra were recorded with a Hitachi U-4001 spectrophotometer from 800 to 280 nm (UV-Vis) and from 2500 to 280 nm to record absorption in the near-infrared region.

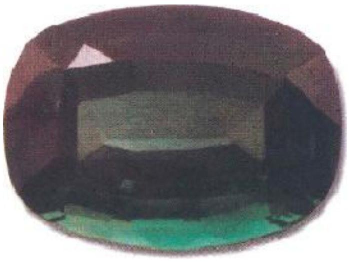

Figure 3: Green labradorite GC1 from the Congo displaying a trace of pale red in white incident light. © Dr Michael S. Krzemnicki, SSEF Swiss Gemmological Institute.

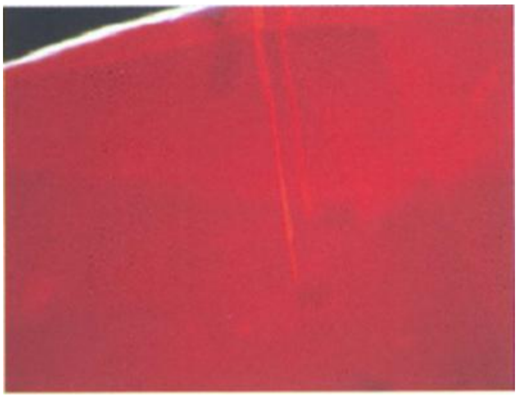

Figure 4: Lines of tiny inclusions and milky turbidity in specimen RC2 from the Congo. Magnification 50×. © Dr Michael S. Krzemnicki, SSEF Swiss Gemmological Institute.

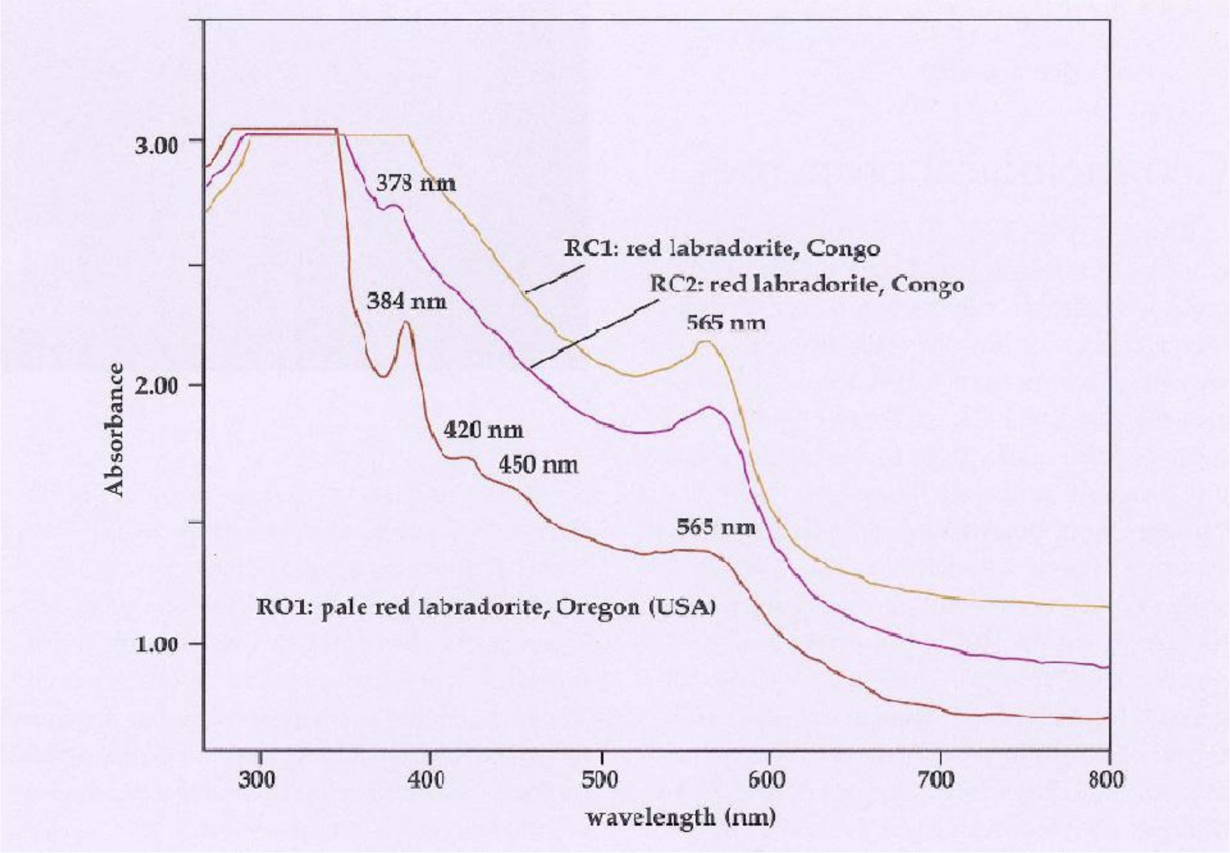

Figure 5a: Unpolarized UV-Vis spectra of red labradorite from Congo and Oregon (USA). Both curves are quite similar with a distinct absorption band at 565-580 nm due to copper.

The red specimens (*Figure 5a*) were measured without a polarizing filter, as only very weak pleochroism was observed. The UV-Vis spectra are characterized by a general increase in absorption towards ultraviolet (strong UV tail). However, two distinct absorption bands at 565 and 380 nm are present. In *Figure 5a* the spectra of RC1 and RC2 are compared with a pale red sunstone labradorite (RO1) from Oregon (USA).

The green sample (*Figure 5b*) shows two different absorption curves for the yellowish-green and bluish-green directions. The yellowish-green direction is a rather flat curve with a broad minimum at 620 nm and a small absorption band at about 430 nm, partly masked by the steep increase of absorption towards ultraviolet (total absorption at ~370 nm). The bluish-green direction shows no distinct minimum at 620 nm, and a broad absorption band is centred at 680 nm. The spectra of green labradorite from Oregon (sample GO1) are somewhat similar. However, if the bluish-green and green direction spectra are compared (*Figure 5b*), the broad absorption band is shifted towards 620 nm and is less pronounced. In the light red direction, no minimum is found at 620 nm, but there is a general decrease in absorption towards the near-infrared. Furthermore, the green labradorite from Oregon shows not only absorption at 420 nm, but also two bands at 450 nm (weak) and 380 nm.

Discussion of UV-Vis spectra and colour cause

According to Hofmeister and Rossman (1985) the colour in labradorites from Oregon (USA) is correlated with the concentration of copper. Red labradorites show the highest copper content (150-200 ppm CuO), whereas yellow varieties contain the lowest concentrations (0-40 ppm).

The colour is further dependent on Cu exsolution temperature, rate of Cu diffusion and aggregation (Cu^0 colloids) and state of copper (Cu^0 or Cu$^+$).

(a) Red labradorites

After Hofmeister and Rossmann (1985), the band at 560 to 585 nm combined with a general increase of absorption towards ultraviolet is attributed to intrinsic absorption by tiny Cu^0 particles which are too small to scatter light (< 22 nm), and produces a red colour. The band-shift from 560 nm towards shorter wavelengths, coupled with a broadening of the absorption band is related to increasing size of the Cu^0 colloids. As the spectra of the red samples from Congo (RC1 and RC2) are very similar to that from Oregon (RO1) in the 565 nm spectral region, the copper colloids are most probably of a very similar size and measure only a few nanometres (Hofmeister and Rossman, 1985).

According to Hofmeister and Rossman (1985), the bands at 380, 420 and 450 nm are due to Fe^{3+} in tetrahedral sites in the feldspar structure. In the samples from Congo, the band at 380 nm is present but smaller, and those at 420 nm and 450 nm are absent. The latter, however, may be masked by the strong UV absorption, probably resulting from a much higher copper concentration in stones from Congo (up to 0.329 wt.% CuO in RC1) compared to material from Oregon (0.015 wt.% CuO in RO1). When extending the spectra into the near-infrared (NIR) up to 2000 nm, the samples from Congo show a broad absorption band at about 1260 to 1310 nm. According to Hofmeister and Rossman (1985), this absorption band can be attributed to Fe^{2+}.

(b) Green labradorites

In 1985, Hofmeister and Rossman presented several models involving tiny copper clusters (i.e. pairs of Cu^0 atoms) or Cu^0 – Cu$^+$ intervalence charge transfer to explain the green colour, but still the cause of the green colour in copper-bearing labradorite remains rather an enigma.

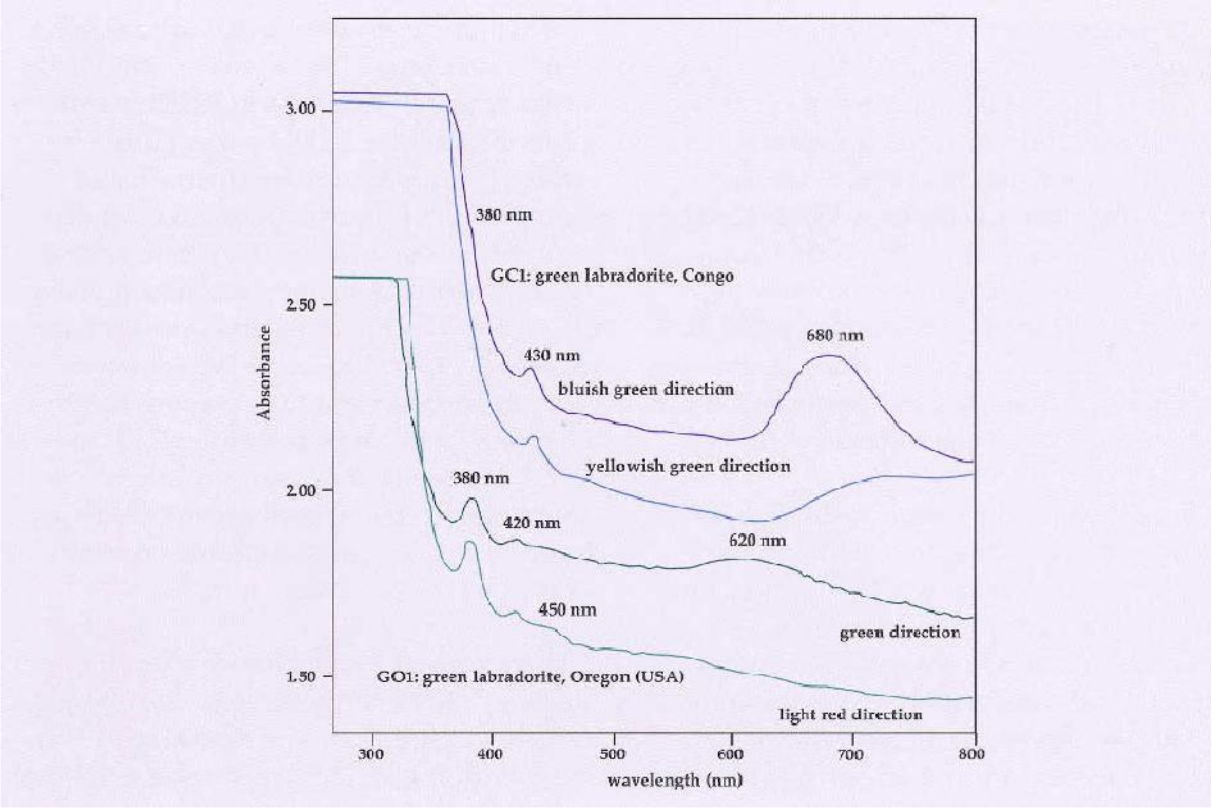

Figure 5b: Polarized UV-Vis spectra of green labradorite from Congo and Oregon (USA). Both labradorites are characterized by distinct pleochroism.

Table II: Chemical compositions of labradorites from Congo and Oregon, USA.

Sample	**RC1***	**RC2***	**GC1***	**RO1**	**Johnston 1991**	**GO1***
Colour	red	red	green	pale red	pale red	green
Origin	Congo			Oregon, USA		
SiO_2	53.865	55.958	57.570	51.56	51.83	52.370
Al_2O_3	30.182	28.139	25.612	30.23	30.51	31.018
CaO	9.766	10.018	10.845	13.53	13.43	11.902
Na_2O	5.051	4.950	4.914	3.78	3.74	3.744
K_2O	0.195	0.097	0.098	0.02	0.11	0.197
MgO	b.d.	b.d.	b.d.	0.16	b.d.	b.d.
TiO_2	0.149	0.160	0.141	0.02	0.043	0.081
Fe_2O_3	0.448	0.470	0.549	0.48	0.03	0.641
MnO	0.001	0.002	0.004	0.06	0.010	0.021
Cr_2O_3	0.007	b.d.	b.d.	n.a.	n.a.	0.010
V_2O_3	0.007	b.d.	0.006	n.a.	n.a.	b.d.
CuO	0.329	0.205	0.260	0.015*	0.011	0.010
ZnO	b.d.	0.001	0.001	n.a.	n.a.	0.006
Total	**100.00**	**100.00**	**100.00**	**99.83**	**99.73**	**100.00**
anorthite%	52	53	55	66	66	64
albite%	48	47	45	34	34	36

*determined with ED-XRF
n.a. not analysed; b.d. below detection limit

The green colour in labradorite sample GC1 from Congo is also attributed to copper and, as in the red labradorites, this causes strong absorption towards the ultraviolet. The band at 430 nm is attributed to Fe^{3+}, whereas the other iron bands at 450 and 380 nm, which are present in the UV-Vis spectrum of green labradorite from Oregon, may be masked by the strong absorption. Again, this is due to the higher copper content of the Congo stones compared to those from Oregon (0.26 vs. 0.01 wt.% CuO respectively).

The difference in pleochroism of green labradorite from Oregon (GO1) and the specimen from Congo (GC1) is clearly illustrated in the spectra. In sample GC1, the minimum at 620 nm combined with an increase in absorption towards the near infrared (800 nm) is responsible for the yellowish-green hue, whereas the green specimen from Oregon (GO1) shows a constant decrease in absorption towards the near-infrared, thus resulting in a pale red pleochroic colour.

When using incident light, the red specimens from Congo display an off-white milky turbidity (*Figure 2*), which is attributed to scattering (Steffen, 2000) by tiny particles (probably copper) apparently not large enough to produce aventurescence. Similar incident illumination of the green sample (GC1) produces a distinct red, most probably due to the presence of relatively larger copper colloids (a few nm to 22 nm in diameter); these are also thought to be responsible for the colour of the red labradorites RC1 and RC2. These colloid clusters add their red component to the overall green colour, produced by smaller Cu^0 clusters and possibly Cu^0 – Cu^+ intervalence charge transfer.

In conclusion, it can be stated that the causes of colour in these feldspars are quite complex. Hofmeister and Rossman (1985) and Johnston *et al.* (1991) established that 100 ppm copper is sufficient to cause a red colour in sunstone labradorite from Oregon. In the studied samples from Congo, the Cu concentration exceeds this value by a factor of >20 (2000 – 3300 ppm Cu), and could explain the much more pronounced UV absorption of these stones.

Chemical investigations

Semi-quantitative chemical analyses were carried out with a Spectrace 5000 Tracor ED-XRF on three cut stones from Congo. The results are listed in *Table II*, together with analyses of Oregon stones. Apart from the main constituents Si and Al, the specimens reveal calcium dominating sodium (about 10 wt.% CaO versus 5 wt.% Na_2O). Potassium is only a minor constituent. Furthermore, all samples contain minor amounts of copper (up to 0.33 wt.% CuO), iron (0.55 wt.% Fe_2O_3), titanium, and traces of Mn, Cr, V and Zn.

Most feldspars may be classified in the ternary K-Na-Ca-diagram (*Figure 6*) with the end members orthoclase (potassium-feldspar), albite (sodium-feldspar) and anorthite (calcium-feldspar). The classification of feldspar is rather complex, involving variation of both chemical composition and structural state (ordering of Si and Al on distinct tetrahedral sites), the latter depending on the temperature of crystallization and on subsequent thermal history (Deer *et al.*, 1992; Hänni, 1989). At high temperature, there is solid solution between albite and orthoclase (alkali feldspar series) and between albite and anorthite (plagioclase series), respectively. At lower temperature, there are some miscibility gaps, which result in exsolution of different feldspar phases, often causing optical effects such as iridescence and light scattering. The plagioclases are classified chemically into the varieties albite, oligoclase, andesine, labradorite, bytownite and anorthite, characterized by a gradual increase in RI and SG towards the calcium end member anorthite. The intermediate plagioclase varieties are basically defined for convenience and have no structural significance (Deer *et al.*, 1992).

The investigated feldspars from Congo are very low in potassium and thus belong to the plagioclase series. When calculating their composition and their place in the plagioclase solid solution series, the Congo feldspars lie in a range slightly over the 50% mark of the anorthite component, which is the limit between andesine and labradorite. In *Figure 6* they are plotted together with labradorite samples from Oregon. Their position in the labradorite field is near the andesine boundary, and thus they may be considered as sodic labradorite, in contrast to the calcic labradorites from Oregon. This conclusion is supported by RI and SG values, which are at the lower end of the labradorite range. As these samples from Congo are very close to the andesine/labradorite boundary, it is possible that further sampling of red and green feldspars from Congo may reveal a wider range of chemical compositions which could extend into the andesine field of the ternary feldspar plot (Fritsch, 2002; L. Sikirdji, pers. comm., 2003).

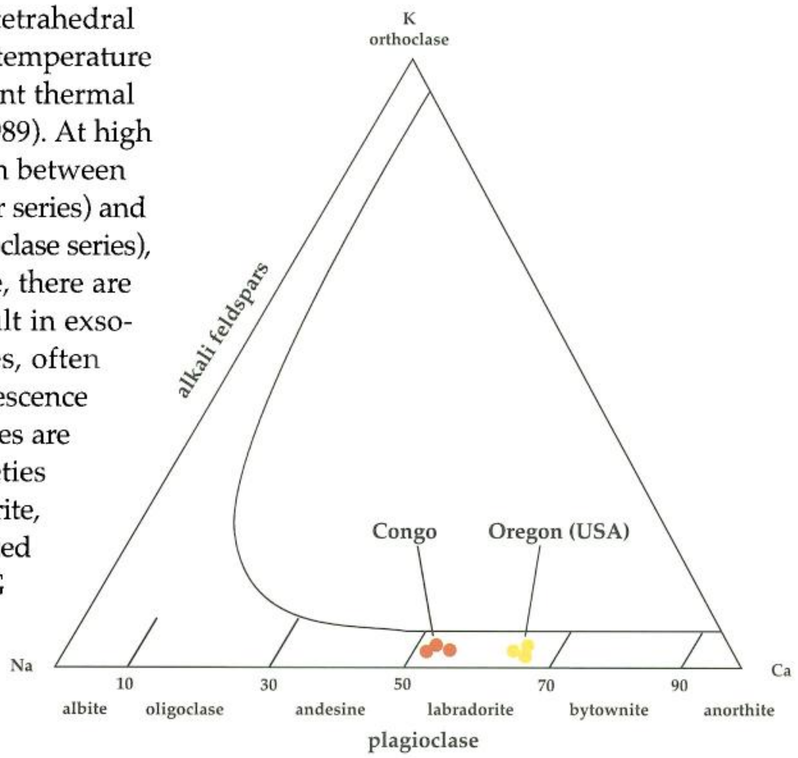

Figure 6: Ternary feldspar plot indicating the composition of the samples from Congo and Oregon (USA).

The labradorites from Congo are in many aspects very similar to the material from Oregon (USA), but have a lower anorthite content (less Ca, see *Table II*), also reflected by slightly lower RI values (Congo: RI 1.553 to 1.563; Oregon: RI 1.560 to 1.572).

Discussion of feldspar nomenclature in gemmology

There are many commercial names for different feldspar varieties such as sunstone, moonstone, spectrolite, amazonite, etc. These names are generally based on the appearance of the feldspar, but more or less connected also to the chemistry, structure and inclusions. The discussions about sunstone or heliolite as a commercial name for the material from Oregon (Gübelin, 1992; Hanneman, 1992; Hoover, 1992; Johnston, 1992; Liddicoat, 1992a, 1992b) have illustrated that the use and correct designation of names remains a matter of discussion in the gemmological community.

Since the term sunstone is merely a matter of appearance, describing golden to red feldspars with more or less schiller (aventurescence) due to tiny inclusions (e.g. hematite platelets, copper colloids), it is well fitted to be used in the trade for many varieties of feldspar in both the plagioclase and alkali feldspar ranges (see Hänni *et al.*, 2003). It is suggested, however, that the commercial name should be followed by the correct mineralogical name, e.g. sunstone labradorite, variety of feldspar.

The term moonstone, however, should be restricted to alkali feldspars (Deer *et al.*, 1992; Hänni, 1989) showing a filmy white to pale blue sheen; this is due to scattering of light from tiny domains caused by perthitic exsolution (irregularly-shaped intergrowth of potassium-rich and sodium-rich feldspar). Stones resembling these but with a plagioclase composition (also called peristerites) may display a white sheen or a rainbow-coloured iridescence, depending on the sizes of the submicroscopic intergrowths of the calcium-rich and calcium-poor plagioclase lamellae (Deer *et al.*, 1992). When the lamellae are thick enough, multiple reflections produce iridescence (labradorescence). If all spectral colours are visible, these iridescent plagioclases (labradorites) may be called spectrolite, regardless of how much ore mineral inclusions are providing a dark background. Such iridescent plagioclases should not be called moonstones for three reasons, they differ not only in appearance (pale blue sheen vs. iridescence), but also in their structure (perthitic exsolution vs. peristeritic lamellar intergrowth) and chemical composition (alkali feldspar vs. plagioclase feldspar).

In conclusion: it is recommended that commercial names for feldspar varieties should be linked with the correct mineralogical names to avoid any confusion.

Acknowledgements

The author would like to thank Dr Laurent Sikirdji (Gemfrance, St.-Ismier, France) and Peter Salzmann (Lucerne, Switzerland) for the loan of samples. ED-XRF analyses were kindly done by Peter Giese at SSEF Swiss Gemmological Institute. Further thanks go to Professor Dr Henry A. Hänni who provided reference samples from Oregon and other sources and to Dr Lore Kiefert who reviewed this manuscript (both from SSEF Swiss Gemmological Institute).

References

Deer, W.A., Howie, R.A., and Zussman, J., 1992. *Rock forming minerals. 2nd edition.* Longman, England

Fritsch, E., 2002. Gem News: Red andesine feldspar from Congo, *Gems & Gemology*, **38**(1), 94-5

Gübelin, E., 1992. 'Misnomer' in American gemology. *Gems & Gemology*, **28**(3), 149

Hanneman, W.Wm., 1992. More on 'misnomers' in gemology, *Gems & Gemology*, **28**(4), 220

Hänni, H.A., 1989. Les feldspaths. *Revue de Gemmologie*, 101, 19-20

Hänni, H.A., Koivula, J.I., and Tannous, M., 2003. Gem news: star sunstone from Tanzania. *Gems & Gemology*, **39**(3), 235-6

Hofmeister, A.N., and Rossman, G.R., 1985. Exsolution of metallic copper from Lake County labradorite. *Geology*, **13**, 644-7

Hoover, D.B., 1992. Another perspective: history of heliolite. *Gems & Gemology*, **28**(4), 220-1

Johnston. C.L., Gunter. M.E., and Knowles, C. R., 1991. Sunstone labradorite from the Ponderosa Mine, Oregon. *Gems & Gemology*, **27**(4), 220-33

Johnston, C.L., 1992. Confusion at the top? Heliolite vs. sunstone. *Gems & Gemology*, **28**(4), 221, 288

Laurs, B., 2002. Gem News: Sunstone feldspar from Tanzania. *Gems & Gemology*, **38**(2), 177

Liddicoat, R.T., 1992a. In reply: 'Misnomer' in American gemology. *Gems & Gemology*, **28**(3), 149

Liddicoat, R.T., 1992b. What did you say the name was? *Gems & Gemology*, **28**(4), 219

Pough, F.H., 1983. Heliolite, a transparent, facetable phase of calcic labradorite. *Journal of Gemmology*, **18**(6), 503-14

Steffen, G., 2000. *Farbe und Lumineszenz von Mineralien*. Enke im G. Thieme Verlag, Stuttgart

SPECIAL OFFER • SPECIAL OFFER • SPECIAL OFFER

- **Can measure faceted gems with RIs 1.43-3.10**
- **Speedy identification – no contact liquid necessary**
- **Supplied with standard quartz and CZ to ensure correct calibration**
- **Portable – powered by two AA batteries**

THE BREWSTER ANGLE METER

Usual price £1200*

Special offer £960*

while stocks are available

(*Prices exclusive of VAT, postage and packing)

For further information on this instrument see
'A new Brewster angle meter for gem identification' J. Gemm., 1999, 26 (8), 539-42

Gem-A Instruments, 27 Greville Street, London, EC1N 8TN
t: **+44 (0)20 7404 3334** e: **gagtl@btinternet.com** w: **www.gem-a.info**

GEM DIAMOND PRACTICAL CERTIFICATE

Gain a diamond practical qualification in just six days

An intensive diamond grading course plus Certificate exam which provides students with the best possible preparation for the day-to-day handling of diamonds in any area of the trade.
No prior diamond experience is necessary.

The course includes:

- Clarity grading using a 10x loupe
- Colour grading with emphasis placed on grading by eye
- Aspects of cut including symmetry and proportions
- Simulants and treatments
- Description of rough crystals

Next course to be held at the Gem-A London headquarters:
Wednesday 5 May to Wednesday 12 May (weekdays only) with the Examination on Thursday 13 May.

The fee of £750 includes
tuition, examination fees, a 10x loupe, stone cloth, stone tweezers and a practical book.

For further course dates contact the Gem-A Education Office on **+44 (0)20 7404 3334**
e-mail: **gagtl@btinternet.com** or visit the Gem-A website at **www.gem-a.info**

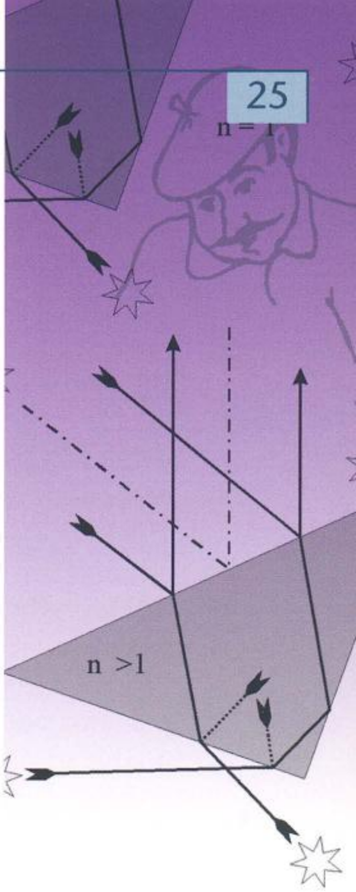

Optimizing faceting for beauty

Anton V. Vasiliev[1]

Translated by Bruce L. Harding[2]

from the *Russian Gemological Bulletin*, 2002, 5(2), 33-41

1. LAL Scientific & Industrial Firm, Moscow, Russia
2. E. Brookfield, MA, USA

Abstract: *Demands for beauty of a gem are related to the level of cutting technology that has been attained. Working the stone unavoidably results in its loss of weight, so the beauty of a gem is in conflict with its potential value. The appearance of a faceted stone is produced by optical effects; therefore the problem of optimizing the faceting of a stone is reduced to determining the criteria which affect its beauty and defining the faceting parameters which best satisfy those criteria. A correctly faceted stone is a compromise between different criteria.*

This selection of optimum parameters is affected by the physical properties of the gem and how it will be used. A faceted gem is an optical device which transforms light sources into light specks on the surface, which is different for each position of a viewer. The stone will be set in a jewellery article which will most probably be seen from certain directions, thus its appearance should be optimized for the most likely combinations of viewer and light source positions. For example, for a viewer looking perpendicularly into the table, one can determine the directions of light sources which are visible in the stone. In optimizing the directions of light sources it is important to consider the influence of the viewer's head and body, which are not light sources. The body of the observer can lead to asymmetrical distribution of light on the surface of the stone and incorrect facet slopes can lead to 'dead' regions of the gem.

To optimize the arrangement of facets an artist will consider the appearance of the entire item.

Translator's Note

It is impossible to translate exactly. Word-for-word does not read properly and re-phrasing requires some word changes. In technical writings many terms have unique meaning in the subject field and are different from those in dictionaries or not listed at all; in such cases the translator must interpret the best meaning from context. It is necessary to know the subject and, ideally, the author and his intent. In this case we were fortunate to talk often with the author via Internet to clarify meanings, and ultimately, to have him review the translation.

ISSN: 1355–4565

The history of faceting

The desire for beauty has been a characteristic of mankind throughout his history. This is shown by cave paintings and archeological excavations. Natural stones have played an enormous role in evolution of society; note the term 'Stone Age'. However, the ways of using minerals for adornment, their variety and popularity, have depended on methods of working them at the time.

The earliest stones used for adornment were probably water-worn alluvial pebbles. Later, for greater lustre, their surfaces were polished with abrasives. Because men were unable to sort abrasives by grain size, final polishing was probably done with a soft abrasive-carrier such as leather or wood. It was impossible to achieve a perfect flat surface but convex surfaces were relatively easy to polish. The hardness of accessible abrasives did not exceed that of alumina (Al_2O_3), which limited the variety of workable materials. Such materials were not valued then as they are today. Archeological discoveries and etymological studies of the names of precious stones[1, 2] show that before mastery of fine polishing techniques was common, only vividly coloured opaque minerals were popular – lazurite, turquoise, jasper, nephrite, jadeite, coloured chalcedony, etc. It was easy to approach fine polishing of the surfaces of most cryptocrystalline minerals in this list. Materials such as ruby, sapphire or emerald, and especially diamond, probably were not used then.

The next step must have been the flattening of one side of a pebble to facilitate its attachment to the surface of everyday objects, weapons or adornments. Thus arose an early form of gem-cutting called the 'cabochon'. The skills of working different stones improved considerably: carving appeared on hematite and chalcedony, and work began on transparent stones. At this time diamond was still not valued or used in adornments. Although diamond is sometimes found in nature as a well-formed octahedral crystal, the configuration of its natural faces, in combination with its optical properties, means that it does not effectively show its 'fire' (colour flashes) so valued in modern diamond cuts. Stones with convex surfaces, however, showed the phenomena caused by oriented inclusions such as 'asterism' and 'chatoyancy' very well. Stones with these effects were most highly-valued until the development of faceting with flat faces. The values of such stones were uncommonly high in regions where the quality of faceting remained poor until recently.

You need only to turn over a transparent cabochon – so that the base faces upward – to see that it looks better, that it reflects more light into the eye of the observer. Note the similarity of the form of faceted stones from regions with less advanced faceting with the form of the inverted cabochon. The evolution of cutting by flat faces is entirely natural – from the cutting of cabochons the cutters learned that a perfectly smooth rounded surface was harder to obtain than the interrupted surface formed by flat faces of arbitrary form. To form truly flat faces it is necessary to use a flat metallic disc (copper, tin or lead), like that used by a potter, for grinding and/or polishing. Initially the arrangement of facets was random, determined largely by the shape of the rough. The criterion of quality was the beauty of the external view of the gem. Cutters noticed that some stones looked better than others and tried to repeat the special features of the more beautiful ones. Thus evolved, by trial-and-error, good (but certainly not the best) proportions for faceting[3]. This was before the first attempt to mathematically define these forms. The irregular shapes of crystal fragments and alluvial pebbles did not suggest symmetrical arrangement of the facets; exceptions were the elongated crystals of beryl and tourmaline, the shape of which became the basis of the baguette and emerald cuts.

Generally the evolution of faceting follows the example of diamond[4]. Actually, when man first thought to polish the top of the diamond octahedron, the faceting of other minerals was already well-known and the proportions of these stones sufficiently perfected. Fortunately, the cubic face is the softest for diamond. The slopes of the octahedron faces were so imperfect that it was necessary to polish a facet at the opposite end – the culet[5] – of significant size, but still the stone did not look good. Therefore cutters began to change the slopes of all the faces and, in embellishing the stone, added additional bevels with reduction and gradual disappearance of the culet. The resulting arrangement of facets is due to the four-fold symmetry of the initial octahedron. Thus was born the modern arrangement of diamond facets, with the shape of the girdle being defined by the square form inherited from its original octahedron. This style of cutting is now called 'antique' or 'cushion'. Only the tendency to form the diamond like other faceted stones explains the cutting-off of the top, for one, and subsequent efforts to alter the natural octahedron. The start of its faceting was the key to the destiny of diamond; as a result diamond acquired exceptional popularity and high price universally. As cutting experience was gained, the proportions of the gem changed and its beauty increased. In the course of time, beauty of the gem gained greater importance than its weight whereby, in modern cutting, the girdle of the most popular diamond cut, the standard round brilliant (SRB) has become perfectly circular. Here, for the first time, we see conflict between the weight and beauty of the gem; this subject will be pursued in detail later. The first attempts to calculate the parameters of faceting were made in the 18th century[6, 7], and best-known in our time came the book of Marcel Tolkowsky in 1919[8, 9]. Despite some errors[9] it was an attempt to mathematically explain the successful solution which had, by that time, already been found by the best cutters in the trade. The wide reputation of this book explains its timeliness – it appeared when the public was ready to consider that diamond should be cut only with precisely correct proportions. However, the main merit of this book is that it drew attention of a wider audience to the problem of correct parameters for faceting and served as the source of ideas for a series of other studies[10-12]. Tolkowsky's SRB solution became the basis of several standards, including some modern systems for appraising the cut-quality of diamonds. Similar studies were also conducted in Russia[13, 14].

Beauty and value or value vs. beauty

The faceted gem may serve one of two main purposes. On the one hand, the gem is the embodiment of beauty and part of jewellery, whose primary purpose is to please the eye. On the other hand, there is its material value as an investment, when it is, perhaps, kept in a bank. Strictly speaking, for the second purpose the stone can exist by itself and need not be seen – there are only important documents confirming its existence and indicating its characteristics which determine its value. Very frequently for trading (especially wholesale) there is the need for commercial transactions without seeing the stones or by people incapable of determining their quality. For this there are special systems to define and evaluate the qualitative and quantitative parameters of the stone. In modern systems the quality of cutting is appraised by separate parameters. A specialist-expert appraises the stone according to one of these systems (certification) and issues a correspondingly designed form (certificate). The illusion can result that the criteria by which the stone is certified completely represents its beauty and desirability to a consumer, which is generally not true. Certainly they try to select grading system parameters so that they do not conflict with the consumer's perception of the stone, but complete agreement is impossible to attain. The main problem of any system of certification is to provide simple and universal guidelines as to how to rank the stones. In this sense it is not required that the certification criteria fully characterize beauty, which is a very complex property of the gem and depends upon too many environmental factors including our subjective perception. The beauty of a stone and its cost are two aspects of the same thing; we should not blindly subjugate beauty to cost, or to an appraisal system unless the stone is cut exclusively for investment purposes. More than any other mineral, the beauty of diamond suffers from this double standard. From here on we will consider only questions related to achieving beauty, not looking for the best compromise of beauty and cost, but developing each cut according to artistic taste, preference, experience and objectives.

Let's now list the four cases where existing systems of appraisal and trade operate at the expense of beauty.

1. Shape vs. weight

The sum total of beauty, rarity and durability determines the attractiveness of a stone and its price. Demand for beauty of a cut stone has changed according to changes in technology of cutting and the results which it made attainable. For people outside the gem cutting industry the beauty of gems was determined only by their colour and size (weight). Since the beginning of gem-cutting, form has become a large factor, unavoidably accompanied by its loss of weight. Form began to play an especially important role in the faceting of transparent gems. Historically, in regions where the technology of faceting lagged, the main consideration was conservation of the stone's weight. However, in countries with developed faceting technology, the priority is the correct shape of the faceted gem. Thus the majority of Indo-Chinese and Indian cutters do not favour losing weight when cutting rubies and sapphires like diamonds and European and American jewellers have a problem mounting stones in jewellery which are faceted in this way from Southeast Asia. We expect that the correct shape of the stone and its resulting beauty will improve in the course of time.

2. Weight vs. size

It is understandable that a dimensionally larger stone pleases the eye more than a small one. But people have become accustomed to buying goods by weight; they typically do this both with potatoes and with precious stones! However, the weight of a stone is not always proportional to its visible size. Round stones faceted in a country with developed faceting technology, having the same girdle diameter (that is, the same visible size) will be lighter but more beautiful than some faceted in Southeast Asia. Unfortunately some cutters cut a gem worrying only about retention of its weight, not taking its beauty into consideration. The consumer suffers. Judge for yourself – you get a heavier stone for more money, but less beautiful. For less beauty the buyer is forced to pay more money! This approach is most common in those countries where the cutters do not know how to cut or cut badly; they sell them as a certain substance by weight (they can pour more than 100 stones into one bag); in such cases the price of the finished stone differs little from the cost of the raw material from which it is made. This is like appraising a painting by the cost of its paint and canvas (this approach is justified for some paintings!). Thus stones sell by weight, not that weight is their best characteristic, but because weight is a simpler quantity to measure, and is the tradition.

3. Discrete price lists

To price stones the trade creates price lists, which are sometimes complex tables in which, as a collection of charts, the parameters of stones are divided into discrete intervals. The price of a stone jumps when it crosses an interval boundary. For example, on all price lists the price of a stone weighing 0.99 carat is considerably less that a stone weighing 1.01 carat. If the faceting of these stones is identical they cannot be visually distinguished from each other. Cutters, concerned with profit, cut stones to dimensions which correspond approximately to carat sizes, but to obtain the larger profit will deviate from the best proportions and, to be sure not to miss, will try to add a little extra; thus the beauty of the stone may suffer considerably. Similar step-grading is also used for other parameters of the stone.

4. Restriction of shape and other parameters

Systems for appraising the quality of cutting for diamonds use the standard set by Tolkowsky which, although good, is not best for specific jewellery articles. Its very specific arrangement of facets is accepted as the standard, therefore the faceting of a more beautiful stone with small deviations from these parameters can cause a reduction in its price. Non-standard faceting, even if more beautiful, is often met with hostility by stone dealers although the jeweller, to implement his design ideas, may need gems of non-standard shape and facet arrangement.

Two approaches to improving the form of faceted gems

Faceted gems involve rather complex optics. Two fundamentally different approaches are possible for the solution of any complex problem.

1. *General* (also called 'synthetic') consists of examining the problem as a whole. This method applies to improving the appearance of a faceted gem. A cutter, after completing his work on the stone, can evaluate the result by critically examining the item; it is possible to determine the best combination by comparing stones faceted with different parameters. So, by trial-and-error, experimenting cutters searched for their favourite solutions. This method is good in that it uses the exact 'image' of the faceted gem! However, this approach involves expenditure of raw material and time, although, under conditions of production manufacture this can be minimized by controlled variations in faceting parameters of individual stones. This is exactly how M. Tolkowsky found the solution which he tried to verify in his book[8]. Appearance is subjective but we can photograph a real stone in real lighting, and quantitatively evaluate its real image.

   Only recently, with the advent and wide acceptance of computers, did it become possible to mathematically simulate a faceted stone with sufficient accuracy [15-18], to draw and analyse its image by program[17, 18]. Speed and elimination of raw material loss are the advantages of this method. It is possible to criticize many possible re-reflections of rays (to discuss the finer points) taking into account partial polarization of refracted beams, and similar small deficiencies, but we must acknowledge that the best of such programs provide quality representations and make it possible to draw valuable practical conclusions[18]. The results are very entertaining and produce an especially strong impression on unenlightened people. However, the computer image, at best, only approximates an appearance of a real gem; therefore, with this method, in principle, it is not possible to gain more information than by cutting and studying real stones. Most important – a single external view does not give direct answers to numerous questions, such as: why this stone, under certain conditions behaves one way and not another. Having received answers to such questions, it is possible to learn how to design a faceted gem.

2. An *analytical* approach consists of separating the total problem into less complex components and examining them separately; for example, analysis of rays incident to the stone from a specific chosen direction, or a single row of facets, or only in one plane. It is possible to study only the influence of table size on the appearance of the stone or separately calculate only the ability of the gem to return light to the eye of the viewer. Until now the majority of researchers have adopted this approach and 'could not see the forest because of the trees'. Usually one researcher would focus on one method of solving only one part of the problem without considering other aspects. Even precise answers to the question – why does this facet work precisely so, in this condition, and not otherwise? – does not make it possible to estimate the beauty of the entire stone.

In reality these approaches are never encountered in such pure form. Even those who attempt to evaluate appearance by the method of computer simulation, divide the problem into smaller parts; for example, they separately evaluate light return and dispersion colours of rays. Even here there is unavoidable simplification – limitation to a number of re-reflections of rays, or the number of colours in the spectrum, etc. Those who choose the analytical approach must, in the end, combine the solutions of all the components of the problem. The best results in this case are obtained by those researchers who are intimate with all aspects of gems

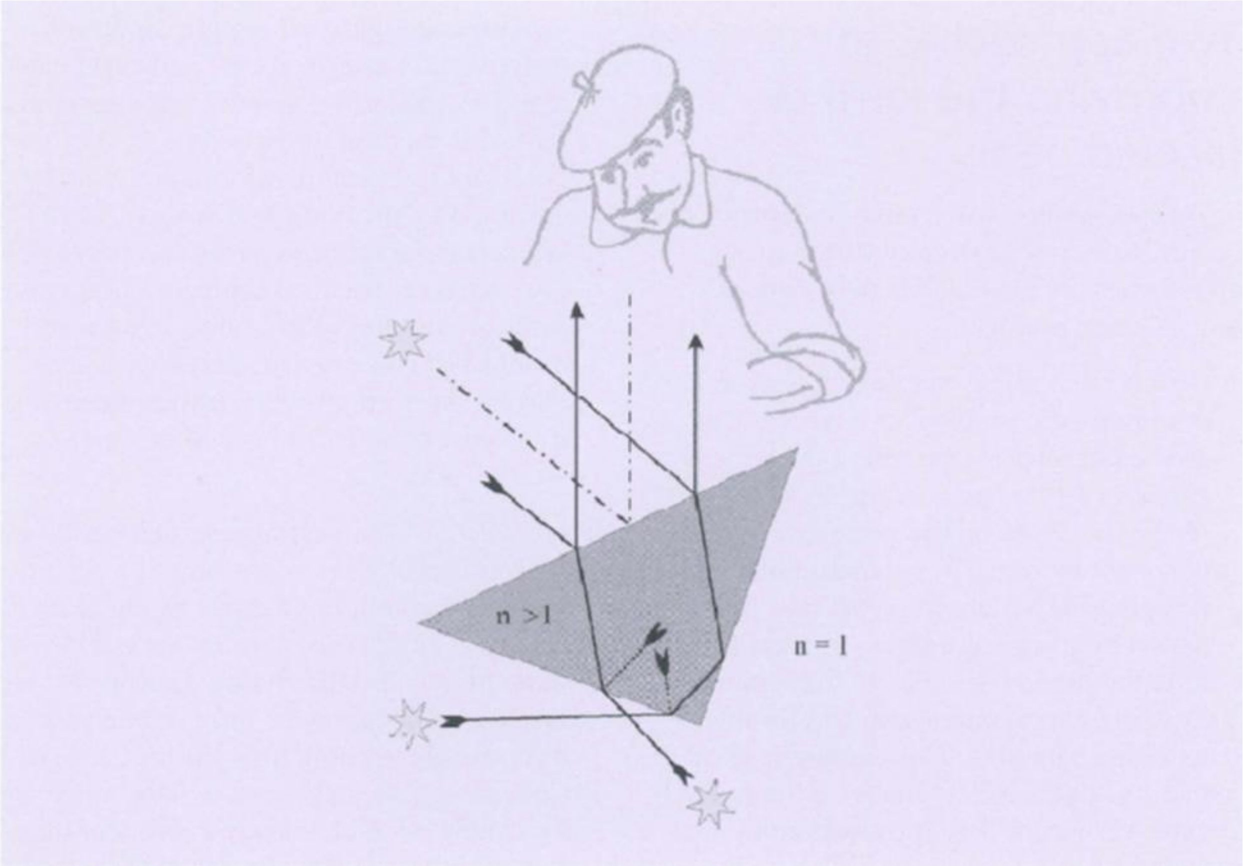

Figure 1: Light rays in a faceted gem of arbitrary shape.

from physics and mathematics to the cutting and manufacture of finished products (Marcel Tolkowsky, Bruce Harding, Anton Vasiliev*).

From here we will attempt to find how to optimize the form of a faceted gem to achieve its maximum beauty by using both approaches. One must treat the results of such studies not as the final truth, but only as tools, similar to the brushes and paints of the artist. The artist is required to create beauty, and he can use any combination of brushes and paints.

What we see in faceted stones

The appearance of a faceted stone, despite the subjectivity of the concept of beauty, is defined by optical effects. Therefore the problem of optimizing the stone by its facets is reduced to determining criteria on which its beauty depends, and to selecting faceting parameters (shape, facet slopes, and their arrangement) to best satisfy the selected criteria.

First of all, let us list what we generally see in a faceted gem, which is a convex polyhedron of arbitrary form, bounded by flat surfaces. First, consider only stones in air, of faceted, colourless, optically isotropic material with a refractive index more than one. After defining the position of the stone and the observer (*Figure 1*) we can then trace the path of each ray that leaves the stone and enters the pupil of the viewer's eye. For such rays to exist the following three factors are necessary:

1. source or sources of light;
2. the stone itself;
3. the viewer.

Usually the distance from the eye to the stone is much more than the size of any facet, the distance to the light source is still more, and the width of the light source exceeds any

---

*Vasiliev added by translator

facet of the gem. What the viewer sees in each part of the stone can be defined by extending all rays from the eye to the gem to their intersection with surrounding objects (*Figure 1* shows these as stars). If, in this direction, there is an object radiating light, we will see a speck of bright light in the corresponding place on the stone. If a dark object is encountered, the corresponding spot on the stone will be dark. Since the eye of the viewer is focused on the stone, a sharp picture is focused on the retina (the rear focal plane of the eye's lens) which is a mosaic of these light and dark spots. Each spot corresponds to one (or more) objects surrounding the stone. Consequently we see in the stone only reflected and refracted images of the surrounding space. Directions (relative to stone) to objects visible in the stone can be assigned corresponding angles, for example by azimuth and inclination. *Thus the faceted stone is an optical device which converts a distribution of light sources into the pattern of light specks seen on its surface.* The geometry of the faceted stone defines the manner of this conversion.

The more bright specks of light we see on the surface of the stone, the stronger it will shine. Let's call this quantitative characteristic the 'brightness' of the stone (the concept of 'brightness' is used here in the everyday sense, not in the physics sense). We can optimize the stone's brightness: if lights are placed in the same directions as each ray, the entire surface of the stone will shine! If they are moved the stone will become dark. Thus the degree of brightness of the stone depends not on its form but on the arrangement of the light sources. It depends on the form of the stone only where the light sources must be in specific places. We obtain the paradoxical conclusion that there is no poor faceting, only unsuccessful arrangement of the light sources!

It is a simple fact that the task to optimize faceting of a stone to increase its brightness for the most general case, does not make sense. There cannot always be 'ideal' cutting; it is possible to optimize one faceting parameter or another to achieve greater beauty only for given specific conditions. Now let us put limits on relative positions of light, stone and viewer.

Light return

A real faceted stone is an adornment, more precisely part of an adornment because it is rarely used for this purpose in loose form. Therefore we will study the faceted stone fastened to the surface of jewellery or other article. Let us represent this surface with a plane which passes through the stone, dividing all surrounding space into two halves. Momentarily, let us call these halves the top and bottom so that the major part of the jewellery article is found in the lower half and the viewer and light sources in the upper. Since the light source and viewer are found in the same half of space, to return light rays to the viewer the stone must *reflect* them. Simple refraction is usually insufficient to make them hit the eye of the viewer.

The polished surface of any crystal will shine by directly reflecting light. This Fresnel partial reflection does not depend on the shape of the stone (the reflected beam does not enter the stone) – it is determined by the refractive index (and angle of reflection) – therefore there is no sense in trying to optimize this lustre. Total reflection can be ensured by spraying on a metallic reflecting film, an amalgam coat, or a simple layer of foil under the stone; however, all such reflective layers are destroyed in the course of time, violating a criterion of treasure – its eternity. In most modern types of faceting the reflection of light into the eye of the observer is achieved by double total internal reflection by the facets of the pavilion. We will examine other methods of recovering light in future publications.

Let us trace the path of a ray, shown in *Figure 2*, via two opposing pavilion facets inclined at angle α from the plane of the girdle (the 'belt' of the gem). The conditions for total internal reflection of both facets are satisfied only for rays whose directions of incidence lie inside angle ϕ formed by limiting rays A-A and B-B. (Note that this range of directions ϕ inside the stone will be broader outside the stone because of refraction.) Total internal reflection is lost for ray C-C at the

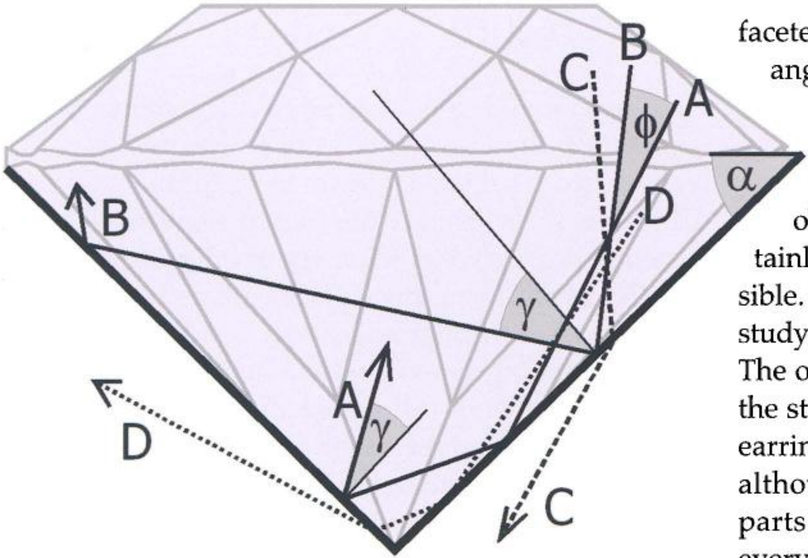

Figure 2: Internal reflections from pavilion facets.

first facet and for ray D-D at the second. Violation of total internal reflection does not mean that the ray does not entirely cease to be reflected, but the portion of the beam which is reflected drops rapidly as the angle of incidence reduces below the critical angle γ. The range of directions for all incident beams which satisfy the condition for total internal reflection can be calculated:

$$\phi = 180° - 2\gamma - 2\alpha \quad (1)$$

where $\gamma = \arcsin(1/n)$ – the critical angle for total internal reflection for the given material with refractive index n. It follows from this expression that as α decreases, ϕ increases, and the more incident rays in the stone are turned back, the greater is the possibility of their being seen, with consequently greater brightness of the stone. However, this slope (α) cannot be decreased below a certain limit. If we make the slope of these faces less than the critical angle, with the stone viewed perpendicular to its table, everything located below the stone is visible through it and all regions of the gem under the table become transparent. As a result, perception of the stone's solidity is lost and it looks 'like glass'. When tilting the stone one or more faces of the pavilion may become transparent, (especially with low refractive index) but if condition $\alpha > \gamma$ is met, only a small part of the total number are transparent, which is not as noticeable as transparency of the entire middle. In the opinion of experimental faceters[23] slope α must exceed the critical angle by 1.5-2 degrees:

$$\alpha > \gamma + 2° \quad (2).$$

The direction of the view of the observer perpendicular to the table is certainly important but not the only view possible. The priority of viewing directions for studying a stone depends on its application. The owner of a ring will most likely examine the stone perpendicular to its table. Stones in earrings are viewed from various directions, although mainly from the front (i.e. those parts not enclosed by the mount). Notice that everyone except the wearer sees a ring stone from arbitrary positions that the wearer does not.

Figure 2 shows the advantages of open-sided settings for holding gems; since parts of the casting leave the pavilion accessible to ambient light, rays D-D cannot be considered lost. This is especially advantageous for colourless stones since the absorption of such rays is less (their path through the stone is shorter, therefore they are lighter) and dispersion – that is, caused by the dispersivity of the material of the gem – is sometimes higher than usual. Consideration of rays D-D demonstrates that the optimum form of faceting depends also on how the stone is held in the jewellery.

In order to see a ray reflected by the stone, it is necessary not only to return it via the pavilion, but also to ensure its exit to air through the top of the gem. If the slope β of the crown facets is too great, instead of leaving the gem, the ray will be reflected back into it, as shown in *Figure 3*. Although faceting methods were proposed[20], by calculations for repeated internal reflections (6 and more times), it is unlikely that the authors actually tried this in practice; the effects of imperfect polishing, inaccurate geometry and un-flatness of facets in real gems accumulate with an increase in the number of reflections, and the path of a ray becomes unpredictable. It is possible to avoid internal reflection by the crown facets if we cut them at slope angle β not exceeding...

$$\beta < \gamma + 90° - 2\alpha \quad (3).$$

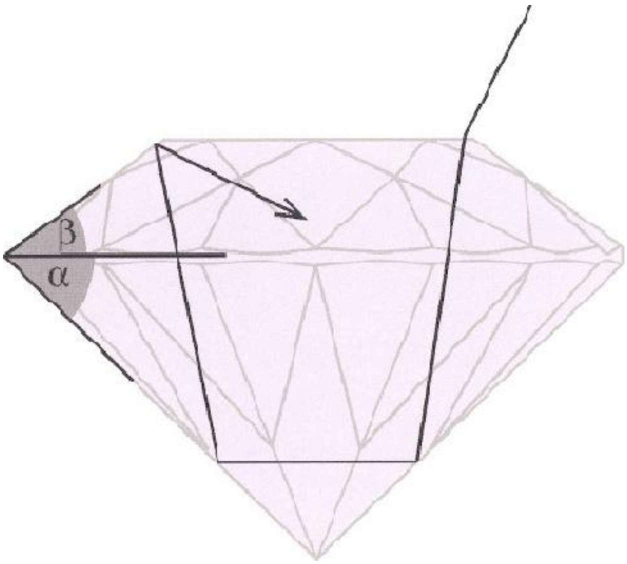

Figure 3: Total reflection of ray from crown back into gem.

Effect of the viewer

The presence of a viewer puts additional limits on arrangements of light sources. The fact is that the head and body of the viewer are not light sources (at least not bright). The head is in the same direction as the eye but has a significant angular size (usually the light source is farther from the stone than the viewer), it is desirable to facet so that the viewer will not see reflections of his own head in the stone. Areas of the gem which reflect the viewer's head will be dark for any positions of the light sources. The shape of the head and arrangement of the eyes vary for different people; shapes and sizes of hairdos and headwear even more so. To simplify analysis, we consider the head as a sphere with an eye in the centre. Thus light rays exiting the stone must diverge from their direction of entry by more than half the angular size of the head. Ignorance of this fact lead to the design of Johnsen[10-12], which calculated, in essence, that the viewer would see only his reflection and only the lamp saw all of the light specks. To this day, researchers fall into this trap[21]. Divergence of the exiting ray from the entering ray must be assured for the three possible paths of the ray through the gem:

1. Entry through the table and exit from the same.
2. Entry through the table but exit from the bezel (side facets of the crown). According to the principle of reverse ray-tracing, this is the same as entry into the bezel and exit through the table.
3. Entry through one side of the bezel and out the opposite side of the bezel.

Consideration of the viewer's head was first presented by Bruce Harding in an article[19] as early as 1975. He cut a garnet according to a published recommendation (40° slope of the main facets, top and bottom[3]). Upon examining it closely (by a lamp behind his head) Harding noticed that, as the stone neared his face (increasing the angular size of his head) it darkened, but it brightened as it was moved away from himself. He investigated this effect and published an article with analytical expressions for calculations, and graphs whose coordinates were the slope angles of the pavilion and bezel facets. He shaded those areas which did not provide sufficient divergence of the exiting beam (similar to *Figure 4*), assuming that the viewer looks into the top of the stone perpendicular to the table. To illustrate this, Harding later (1986) wrote a computer program which showed the paths of rays through the stone. The author became aware of this work in the early 80s and expanded the results to include the case where the viewer looks at the stones from other directions[22].

Figure 4 shows shaded areas designated by letters **E**, **G** and **F** for faceted corundum, inside which facet slopes do not assure 10° ray divergence, for arbitrary positions of the viewer, for the three routes cited above, respectively. These areas are somewhat wider than those presented by Harding and more severely limit the acceptable regions, but they ensure the necessary beam divergence in those remaining regions for any inclination of the stone relative to the direction of viewing. Shaded areas **H** and **I** do not satisfy equations (2) and (3) respectively.

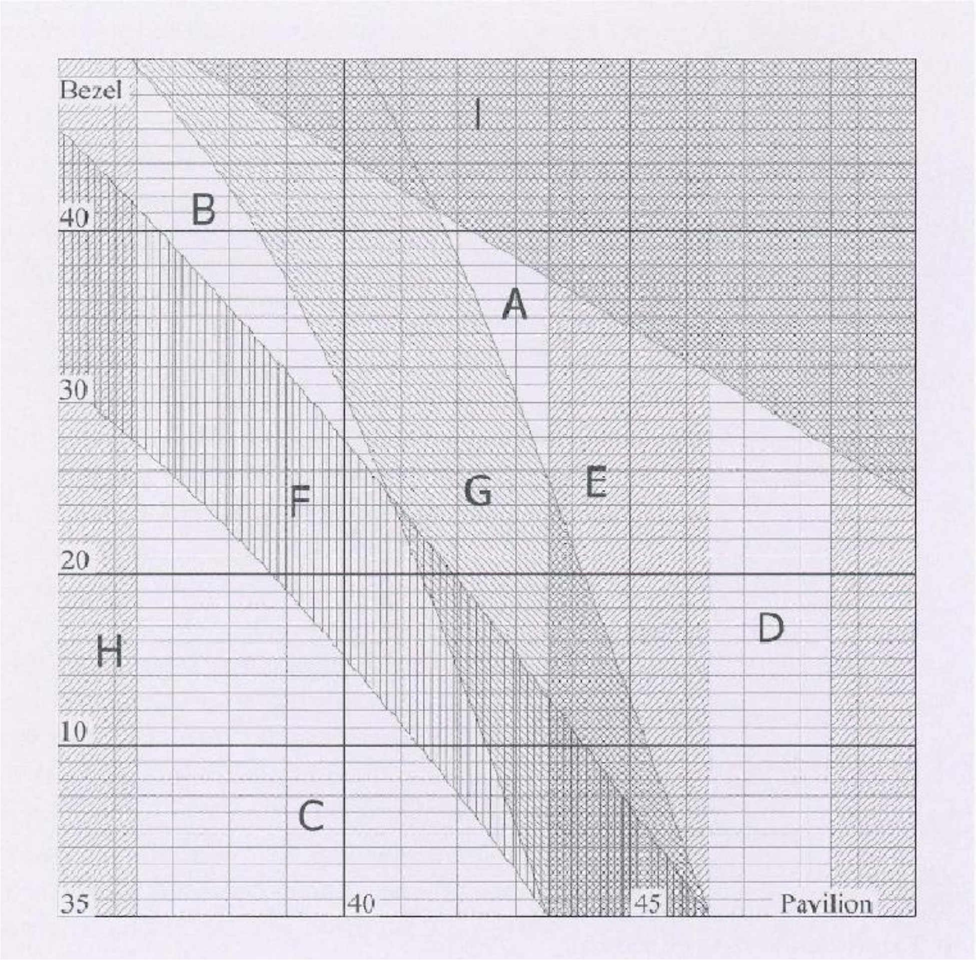

Figure 4: Regions of pavilion and bezel slope combinations.

Four regions – **A**, **B**, **C** and **D** – remain unshaded. To compare them it is necessary to consider the body of the viewer, which is also reflected in the stone and blocks light. For stones in regions **C** and **D** the body of the viewer is reflected predominantly only in one half of the stone (near to the viewer for **D** and away for **C**). This one-sidedness seriously affects the beauty of the stone, so we exclude such slope combinations as unsuccessful.

The location and shape of the remaining acceptable regions (**A** and **B**) depend on the refractive index of the material being cut and the angular size of the viewer's head – that is, the distance from which the gem is viewed. The final results of calculation for different materials and 10° minimum ray divergence, are shown in *Figure 5*. Other details are considered less important and are omitted in this diagram. In this diagram zone **B** does not exist for quartz; actually it appears only for minerals with refractive index greater than 1.62. For materials with lower refractive index there is only one region of solutions (**A**), which disappears if $\mathbf{n} < 1.47$. Apparently natural glass occupies last place in the list of minerals which can be faceted satisfactorily, and minerals such as fluorite and opal cannot satisfy the requirements we have defined.

Other things being equal, stones of region **B** have high brightness and give more rays, but those from region A have greater colour intensity. Without going into detail, let it be said that stones from the upper left of region **A** have the best colour dispersion of exiting rays. Although calculations are carried out only for rays in the plane of the paper in *Figures* 2 and 3, the results apply generally also to oblique rays (lying in other planes), with the exception of rays exiting into the air through bezel facets [formula (3)]. To avoid loss of skew exit rays it is necessary to use either additional facets (upper triangles of the crown = 'stars') or to use crown main facet slopes 3-5° below the upper boundary of region **A**. Small deviations beyond the recommended limits do not significantly affect the beauty of the gem; they are permissible.

In this article we examined only rays reflecting from facets which are opposite to each other. The majority of rays incident perpendicular to the girdle plane go exactly this way; however, other rays can enter adjacent or remote facets. In the latter case the path of a ray may change sharply and the majority of such rays pass through the stone by more complex routes, often with a large number of internal re-reflections. The number of such rays increases with tilting the gem; their main feature is a radical change in the mode and number of interacting facets by the tiniest rotation of the gem. The rays we studied comprise the majority and repeated part of all rays forming the exterior appearance of the gem. Therefore it is most important to consider them in the optimizing of faceting. If we seriously violate even one of the criteria set above, we will get a noticeable negative effect on the beauty of the stone. Precise calculation of all possible rays is possible but exceeds the scope of this article.

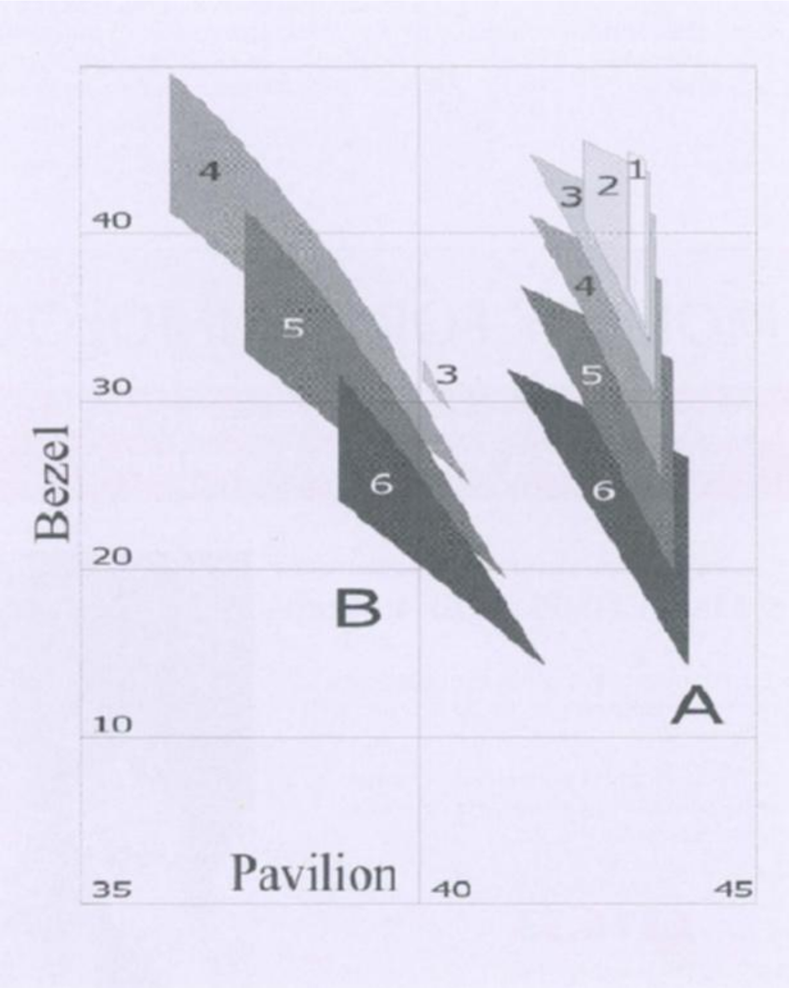

Figure 5: Best slope combinations for various gem materials:
1) obsidian *2) quartz* *3) topaz*
4) corundum *5) zircon* *6) diamond*

References

1. Smith, G., 1984. *Gem Stones*. Translated from English – M.: World, p.219
2. Dav, B.H., 1988. *Joy of Stones*. Murmansk, Murmansk Book Publisher
3. Sinkankas, J., 1989. *Gem Cutting: A Lapidary's Manual*. Translated from English – M.: World, p.409
4. Tillander, H., 1965. Six centuries of diamond design. *The Journal of Gemmology*, **9**(1), 1-2
5. Eppler, W.F., 1967. The significance of the culet of old brilliant-cut diamonds. *The Journal of Gemmology*, **10**(7), 218-23
6. Jeffries, David, 1756. *Abhandlung von den Demanten und Perlen*. Translated from English and French by Georg Marcus Knock, Danzig
7. Mawe, John, 1823. *Treatise on Diamonds*. London
8. Tolkowsky, M., 1919. *Diamond Design*. E. & F. Spon, London
9. Harding, B.L. *'Diamond Design' Revisited*. Written in 1975, privately circulated and first published at www.gemology.ru and www.cutstudy.com 2002
10. Johnsen, A., 1926. *Sber. Preuss. Akad, Wiss.*, 19, 322
11. Rosch, S. *Deutsche Goldschmiede - Zeitung*. Nos 5, 7, 9
12. Krumbhaar and Rosch, 1926. Mitteilungen aus dem Laboritorium für Diamantforschung. *Deutsche Goldschmiede - Zeitung*, 5, 48
13. Vutovski, B.V., 1952. Rational facet slope angles. *Bull. Tech. Inform. on Gemcutting and Jewelry Manufacture*, 2, 53
14. Vutovski, B.V., 1954. Rational slope angles for facet cutting and their calculation. *Transactions of Institute of Crystallography, Academy of Science, Union of Soviet Socialist Republics*, 9, 367
15. Dodson, J.S., 1978. *Optica Acta*, 25(8), 681, 693, 701
16. Hardy, A., Shtrikman, S., and Stern, N., 1981. A ray-tracing study of gem-quality. *Optica Acta*, 28(6), 801-9
17. Hemphill, T.S., Reinitz, I.M., Johnson, M.L., and Shigley, J.E., 1998. Modeling the appearance of the round brilliant cut diamond: an analysis of brilliance. *Gems & Gemology*, **34**(3), 158-83
18. Sivovolenko, S., 2000. www.gemology.ru and www.cutstudy.com
19. Harding, B.L., 1975. Faceting limits. *Gems & Gemology*, **XV**(3) 78-88. Reprinted at www.gemology.ru and www.cutstudy.com 2002
20. U.S. Patent No. 4,083,352
21. Noobin, B.B., and Shirokich, T.B., 1998. *Glass paste – imitation colored diamonds*. Smolensk PO 'Crystal' VI Science-Practical Conference, Status and Perspective of Development at Russian Diamond-Brilliant Complex
22. Vasiliev, A.B., 1995. Selecting Facet Slope Angles. *Acta Universitatis Wratislaviensis*, 1607, 143-6
23. Vargas, G. and M., 1977. *Faceting for Amateurs*. 2nd Edn

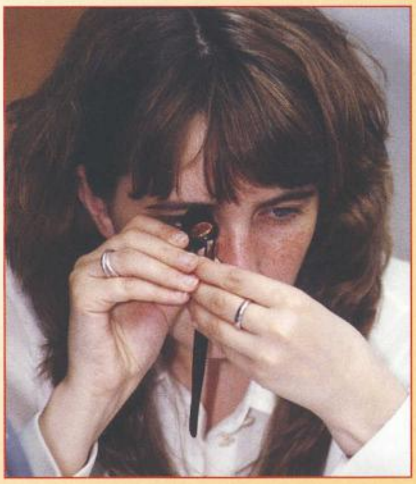

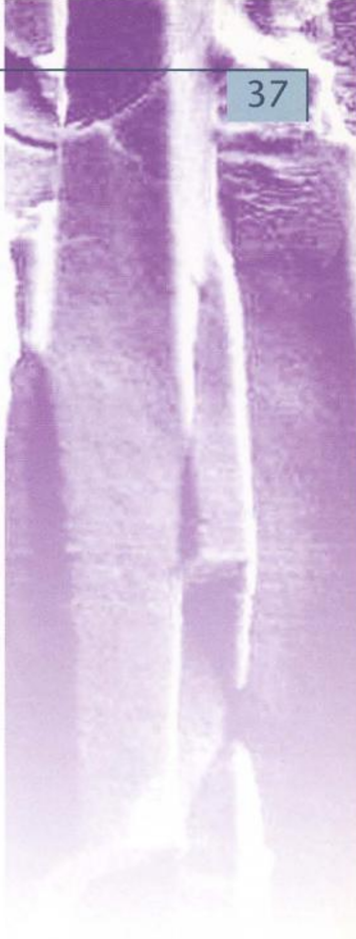

The microstructure of the shell and cultured blister pearls of *Pteria penguin* from Sanya, Hainan, China

Huang Fengming[1], Chen Zhonghui[1], Tong Hua[2],
Zhou Ying[1], Zhang Ziqi[1] and Yang Mingxing[1]

1. *Gemmological Institute, China University of Geosciences, Wuhan, 430074*
2. *Testing Center, Wuhan University, Wuhan, 430072*

Abstract: *The microstructure of the shell and cultured blister pearls of* Pteria penguin *from Sanya, Hainan, were examined using a scanning electron microscope and are described in detail. The results indicate that the shell of* Pteria penguin *consists of an outer organic layer (conchiolin), a middle prismatic layer and an inner nacreous layer. The prismatic layer shows multiple sub-layers (commonly 3 or 4) with a total thickness of 0.3-0.9 mm. Single calcite prisms are 13-55 μm wide, and show five- or six-sided sections. Organic matrix lies between the calcite prisms. The nacreous layer of the shell shows a characteristic step-like structure through labyrinthic structure (fingerprint-like) to spiral-like structure from the margin to the umbonal region of the shell. The nacreous layer consists of aragonite and organic matrix, with a total thickness of 1.0-1.5 mm. Single aragonite platelets have a thickness between 0.3 and 0.8 μm. The cultured blister pearls consist of a bead nucleus, a prismatic layer and a nacreous layer, the layers totalling 0.15-1.00 mm in thickness.*

Keywords: *conchiolin, cultured blister pearl, nacre,* Pteria penguin, *SEM, shell structure*

Introduction

Pteria or *Magnavicula penguin* (Röding) belongs to the *Phylum Mollusca*, Class *Pelecypoda*, Order *Anisomarya* and Family *Pteriidae* (Xie, 1995). The animals live in subtidal areas in the tropics and subtropics, such as the shores of Australia, Indonesia, Japan, New Caledonia, New Guinea, and Guangdong and Hainan, China (Zhang *et al.*, 1994; Xie, 1995; Meng *et al.*, 1995; Fu and Liang, 2000; Liang *et al.*, 2001). *Pteria penguin* is large in size, has great vitality and a fast growth rate, and their mantles have a strong capability for secretion. Therefore, they are ideal for producing large pearls, especially large blister pearls. The blister pearls grown in *Pteria penguin* are large in size, with a thick nacreous layer and a strong lustre, and so have a high commercial value. Reports involving development and artificial propagation of *Pteria penguin* have been published by Liang *et al.* (2001) and Yu *et al.* (2000), and of cultivation of blister pearls

ISSN: 1355-4565

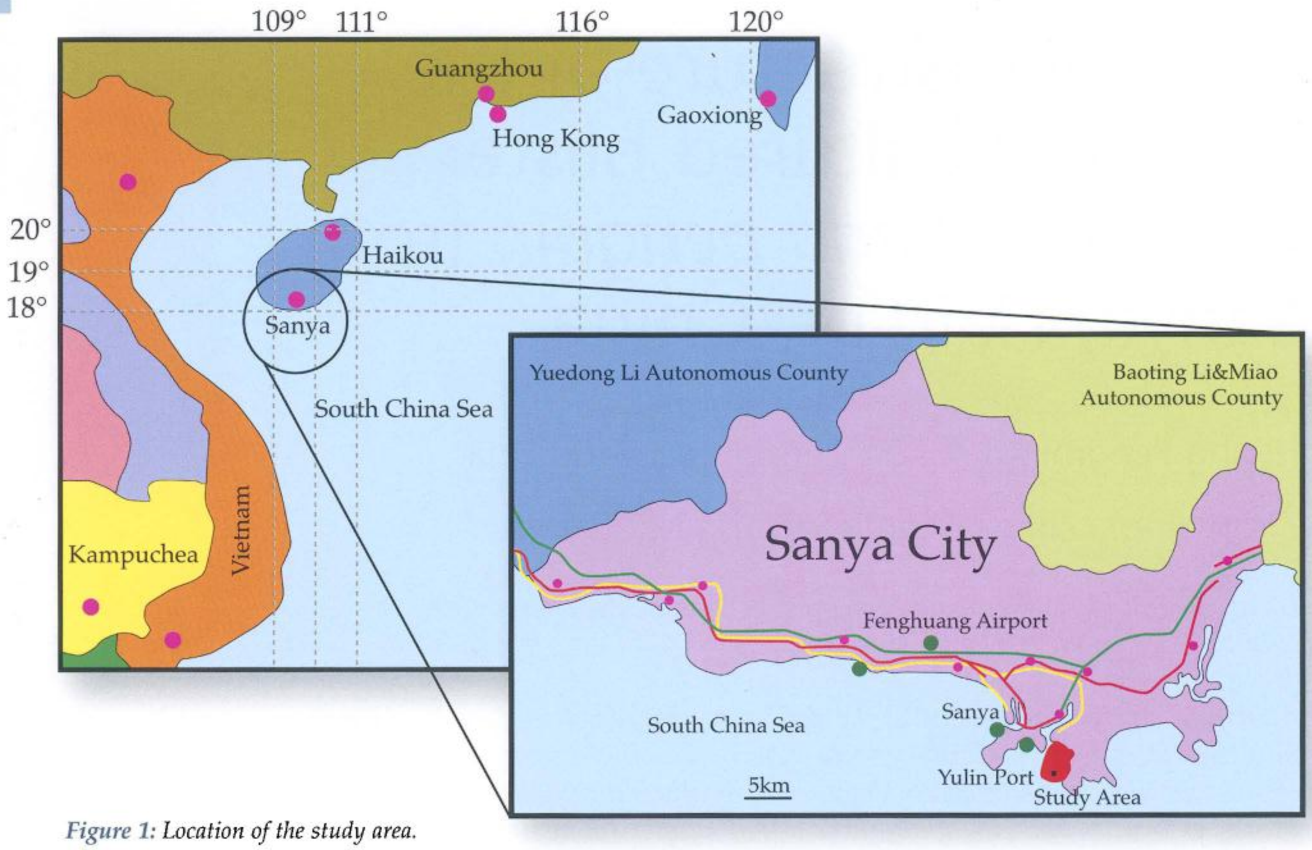

Figure 1: Location of the study area.

using *Pteria penguin* by Zhang *et al.* (1994), Xie (1995), Liang *et al.* (1998) and Fu and Liang (2000), but a study of the structure of the shells of *Pteria penguin* and blister pearls produced by *Pteria penguin* from China is lacking. The work presented here aims to fill this gap with a study, using a scanning electron microscope, of shells and cultured blister pearls of *Pteria penguin* from Sanya, Hainan Province.

Materials and Methods

The shells

The shells of *Pteria penguin* and the cultured blister pearls produced by *Pteria penguin* were obtained from Lupearl Aqua-culture Co. Ltd. in Sanya, Hainan Province. This cultured pearl farm is in the famous Yulin port, and is 20 km away from Sanya, about forty minutes drive by car *(Figure 1)*. The sea area of the farm is approximately 70 hectares and over 300 people are employed. At present, *Pteria penguin*, *Pinctada maxima* (white lip oyster) and *Pinctada margaritifera* (black lip oyster) are being reared. The growth rates of the oysters are controlled from incubation through to maturity. This produces a stock of oysters of similar maturity which are ready for the culturing operation at the same time.

The shells for this study were adult shells (more than two years old) and the cultured blister pearls had been grown for approximately six months. Both shells and blisters were first immersed in 5% NaOH solution for about ten minutes to remove some impurities, then washed with distilled water and dried in air. The shells were cut directionally for different purposes: ribbons of 2 cm × 0.5 cm were cut for observing the section structure and squares of 1 cm × 1 cm for observing the surface structure. For determining the change in surface structure of the nacreous layer, a continuous traverse from one margin to the other of a shell was preserved in six adjacent samples *(Figure 2)*. The specimens of cultured blister pearls were obtained by cutting the shells and removing the outer layers.

Equipment

A Hitachi Scanning Electron Microscope (SEM) was used to observe the surface and section structures of the shells and cultured blister pearls under the following conditions: an acceleration voltage of 20 kV, and beam current of 5 × 10^{-10}A.

Results

Shell

Nacreous layer: In the nacreous layer of the shell, the following three kinds of surface structures were observed: step-like, labyrinthic (fingerprint-like) and spiral.

In the step-like surface structure, the growth layers of aragonite crystals are parallel to each other *(Figure 3a)*, with a distance of about 13 μm between the neighbouring two growth layers of aragonite, measured from the Figure. The aragonite crystals have round outlines and occur in a range of sizes. At the front edges of the growth layers, the aragonite crystals appear as irregular and isolated crystals. Away from these growth edges, the crystals are unresolvable by the SEM and appear as a single mass *(Figure 3b)*.

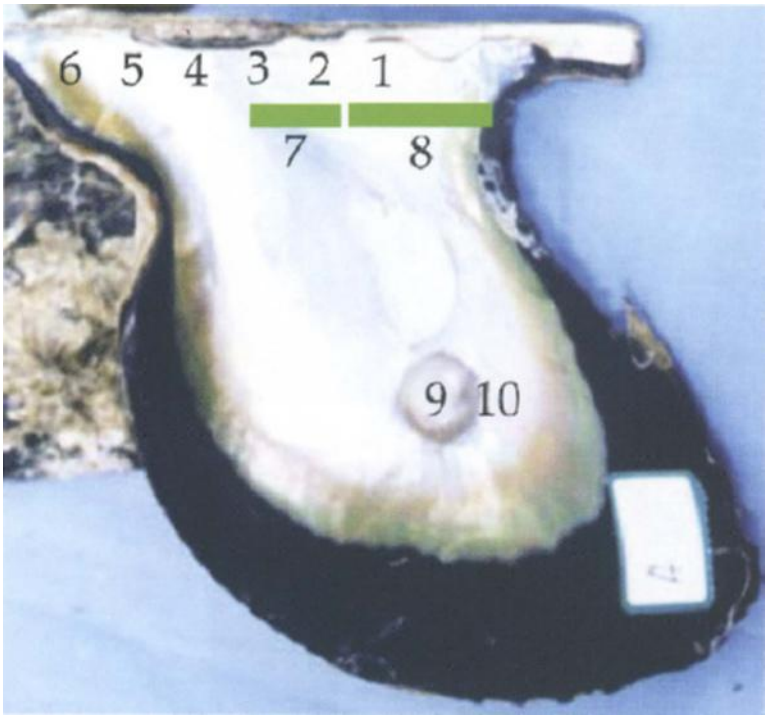

Figure 2: A diagram showing the locations of the specimens of the shell and cultured blister pearl.

1-6: Six adjacent specimens for observing surface structure of the nacreous layer, with 3 being the sample of the umbo.

7-8: Representative specimens for studying the thickness changes in the nacreous and prismatic layers.

9-10: Cultured blister pearl specimens.

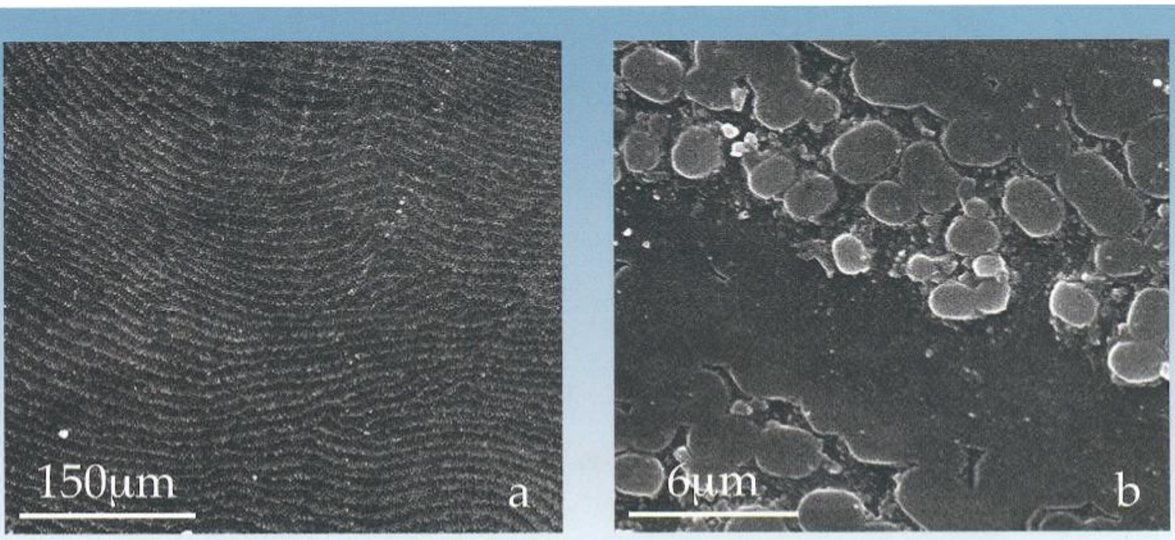

Figure 3a & b: Step-like surface structure of nacreous layer of shell.

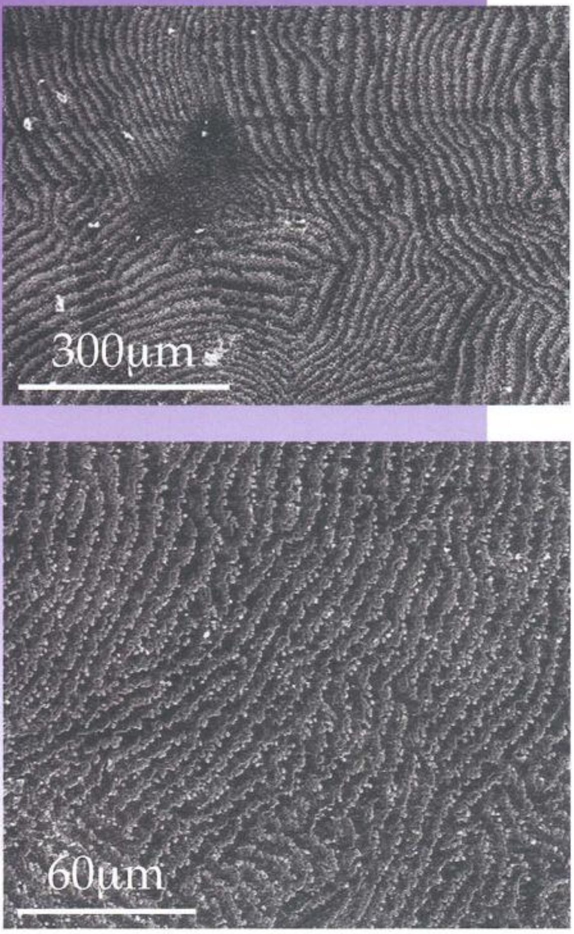

Figure 4: Labyrinthic surface structure of nacreous layer of shell.

In the labyrinthic (fingerprint-like) structure, the growth layers of aragonite overlap each other *(Figure 4)*, with a distance of 4–13 µm between the neighbouring two growth layers.

The spiral structure of shell is characterized by spiral growth layers of aragonite crystals *(Figure 5)*, including right-hand spirals and left-hand spirals, but usually right-hand spirals. Locally, several spirals may connect together. The distance between the neighbouring two growth layers of aragonite increases from outer to inner layers.

The surface structures observed in specimens 1–6 *(Figure 2)* show regular variations. Specimen 1 is characterized by step-like and labyrinthic (fingerprint-like) surface structures, while in specimens 2 and 4 labyrinthic structure predominates, with local development of spiral structure. Spiral structure dominates in specimen 3 and labyrinthic structure dominates in specimens 5 and 6. This indicates a regular variation from step-like surface structure through labyrinthic structure to spiral structure from the margin to the umbo of the shell.

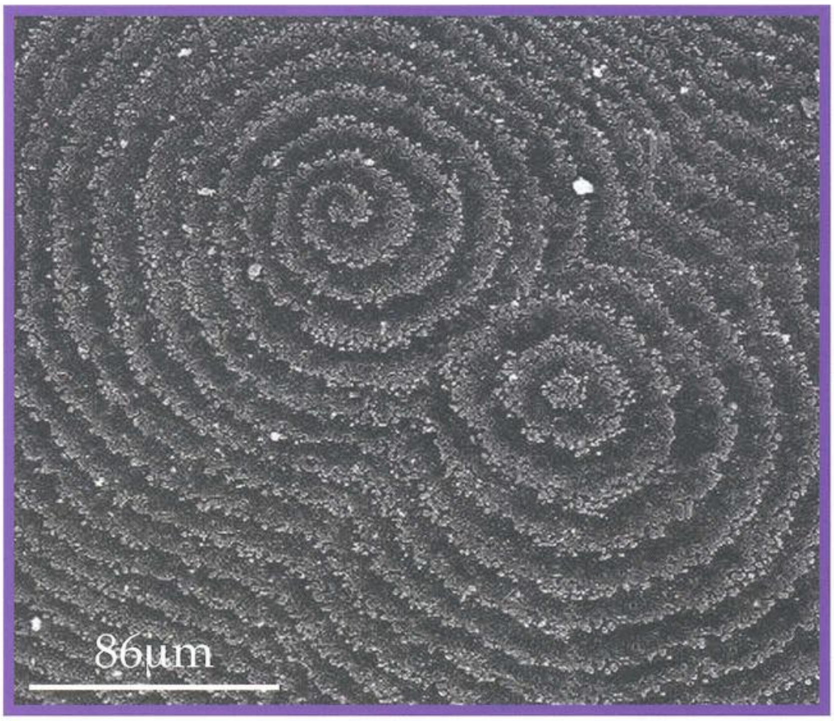

Figure 5: Spiral surface structure of nacreous layer of shell.

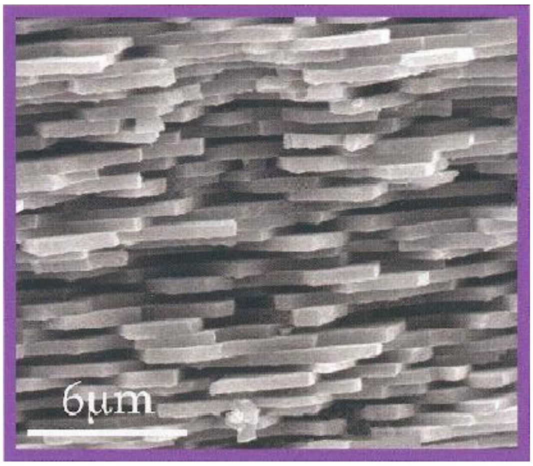

Figure 6: *The regular aragonite platelets of the shell.*

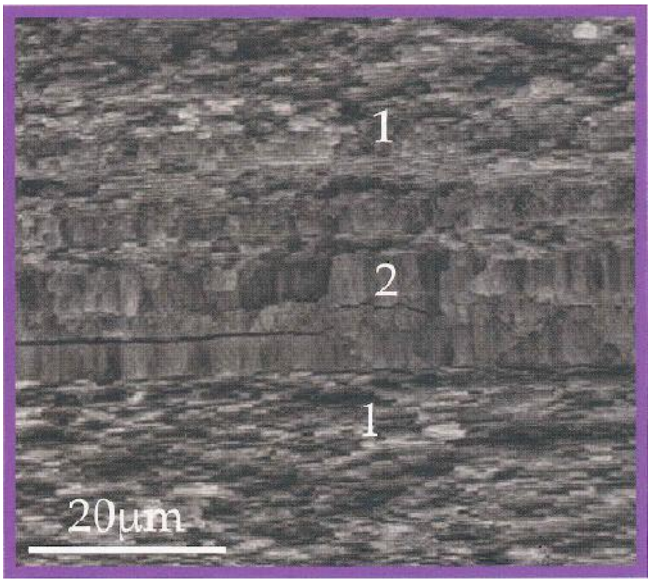

Figure 7: *Prismatic interlayer in nacreous layers: (1) nacreous layer (2) prismatic layer.*

In the section through the shell, the nacreous layer consists of platelets of aragonite crystals *(Figure 6)*, with a total thickness of 1.0-1.5 mm. The aragonite platelets range in thickness from 0.5 to 0.8 µm at the umbo, and from 0.3 to 0.4 µm at the margin of the shell. Additionally, prismatic layers of calcite are visible between nacreous layers *(Figure 7)*.

Prismatic layer: In plan the calcite prisms appear five- or six-sided *(Figure 8)*. Between the calcite prisms are thin films of dark organic material. The pitted texture visible in *Figure 8* indicates that the calcite prisms are composed of many minute calcite crystals rather than only one crystal.

In the transitional growth zone between the nacreous and prismatic layers *(Figure 9)*, aragonite grains first grow along the boundaries of the calcite prisms and then cover the prism layers completely, indicating the organism's control over the growth of aragonite.

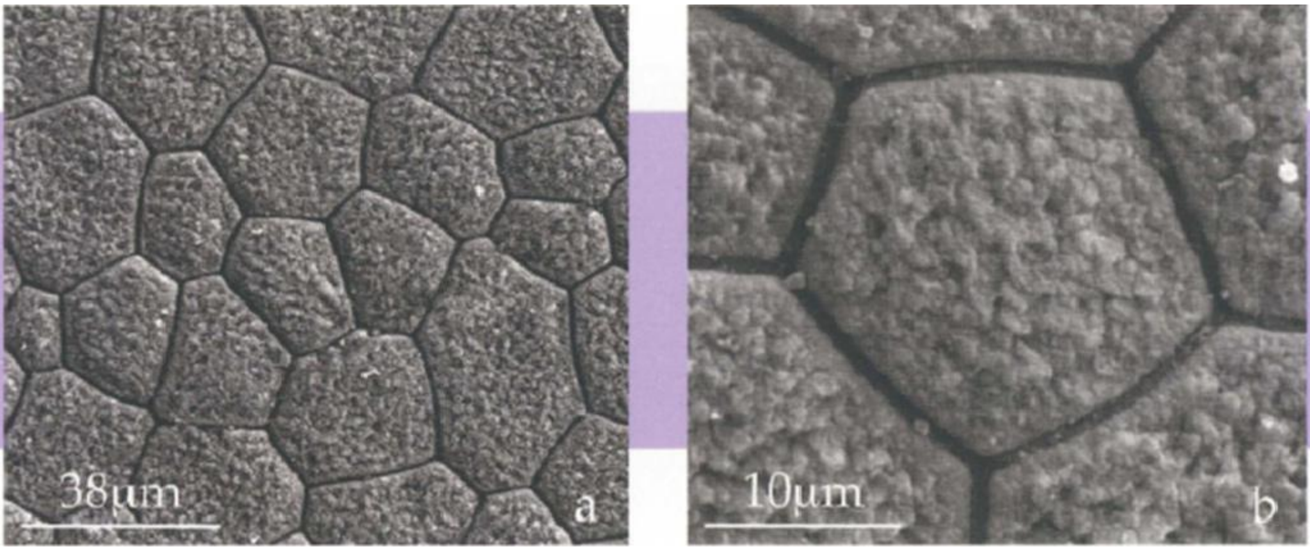

Figure 8a & b: *Five- and six-sided calcite prisms and organic matter at boundaries.*

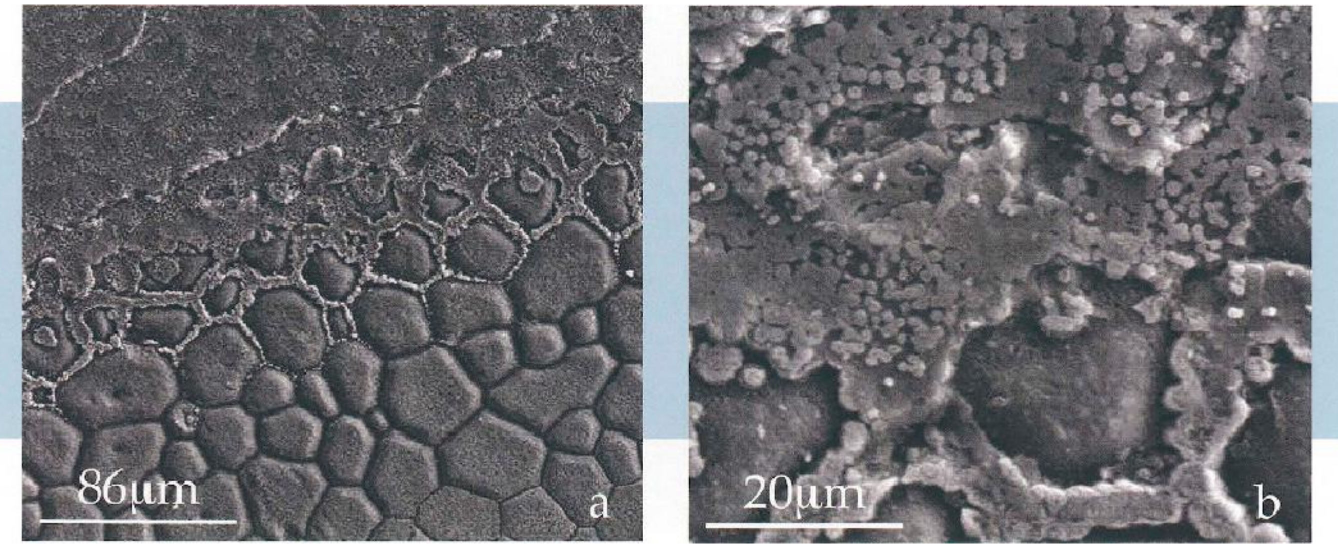

Figure 9a & b: Surface features of the transitional growth zone between the nacreous and prismatic layers:
a. Prismatic calcite (bottom) is penetrated along prism boundaries by aragonite and eventually completely covered (top).
b. Detail of later stages of aragonite growing around calcite.

The initial aragonite grains appear to be poorly defined and to be close-packed,while those grown later appear loose, with round outlines and variable size *(Figure 9b)*.

In section, sharply defined boundaries are visible between the nacreous and prismatic layers *(Figures 7 and 10)* with local development of an organic layer *(Figure 10a)*. However, at the margin of the shell, the nacreous and prismatic layers are interlayed with more complexity *(Figure 10b)*, with the prism layer showing several sub-layers, usually 3–4 *(Figure 11)*. The boundaries are still sharp and the layers range in thickness from 0.30 to 0.80 mm. Each calcite prism has a width of about 13–15 µm *(Figure 12)* and in detail shows an irregular sheet-like overlapping structure *(Figure 13)*. The organic material on the prism surfaces shows a net-like structure *(Figure 14)*.

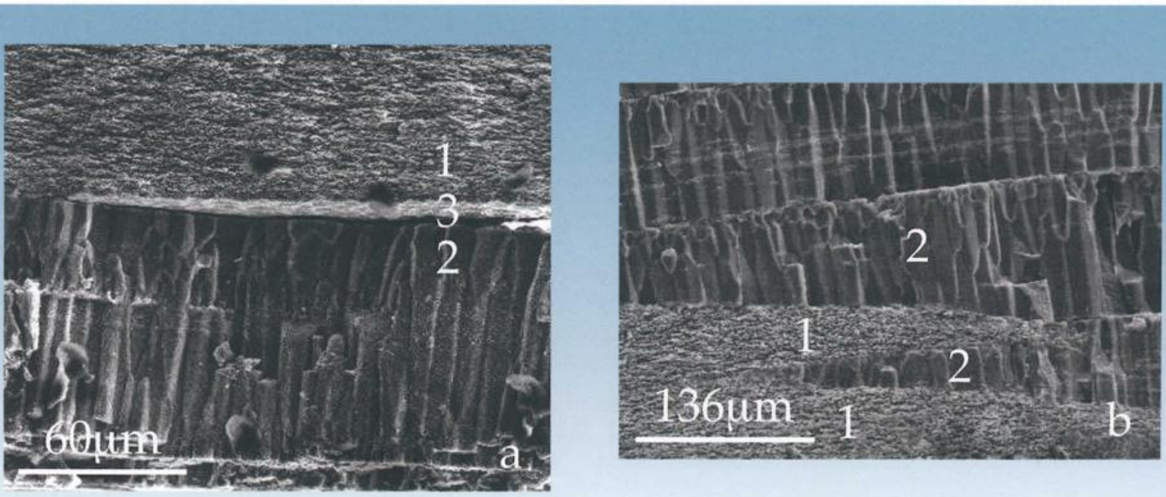

Figure 10a & b: The relationship between the nacreous and prismatic layers: (1) nacreous layer; (2) prismatic layer; (3) organic matrix.

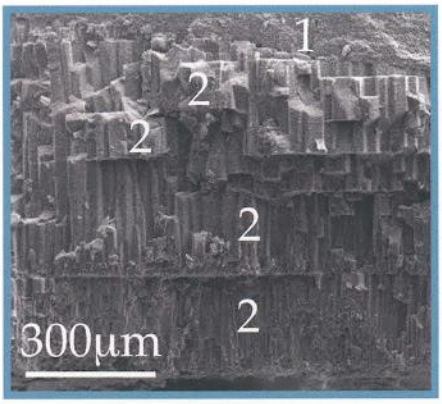

Figure 11: Section showing multiple prism sub-layers (2). A nacreous layer (1) is at the top.

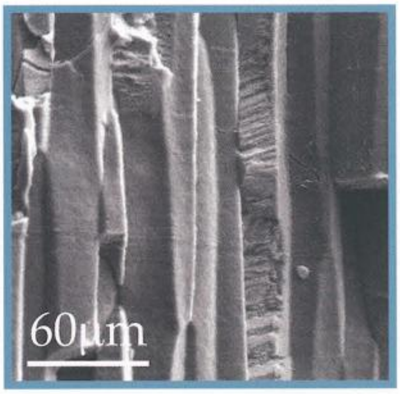

Figure 12: Section showing the boundaries of calcite prisms.

Cultured blister pearl

The cultured blister pearl specimens show mainly step-like and labyrinthic (fingerprint-like) surface structures in the nacreous layer *(Figure 15)*, with no spiral structure visible. The overlap gap in the growth layers of aragonite is wider in the labyrinthic (fingerprint-like) structure compared to that in the step-like structure *(Figure 16)*.

In section, cultured blister pearls also show prismatic and nacreous layers, with a sharply-defined vacant boundary *(Figure 17)*. The nacre consists of regularly arranged aragonite platelets *(Figure 18)*, each approximately 0.5 μm thick. The calcite prisms show prism boundaries, an irregular sheet-like structure and net-like structure of organic material *(Figure 19)*, which, however, are all less distinct than those seen in the prismatic layers of the shell.

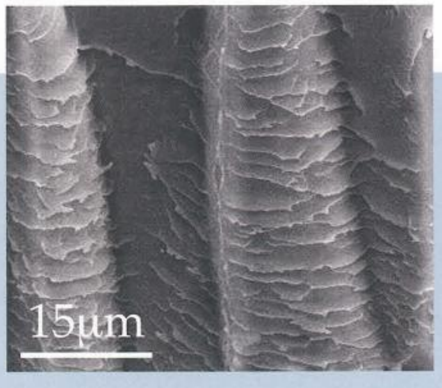

Figure 13: Irregular overlapping sheet-like structure in calcite prisms.

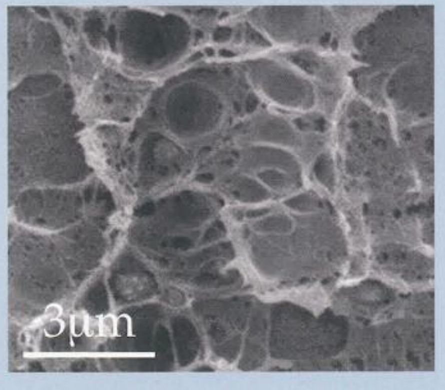

Figure 14: Net-like structure of organic material visible on calcite prisms.

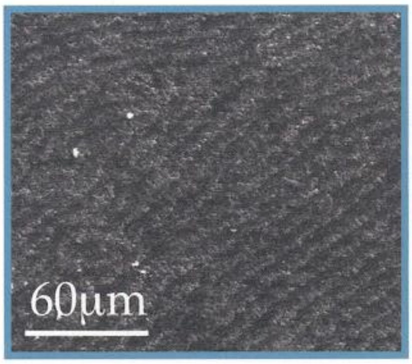

Figure 15: Step-like surface structure of nacreous layer at the top of the cultured blister pearl.

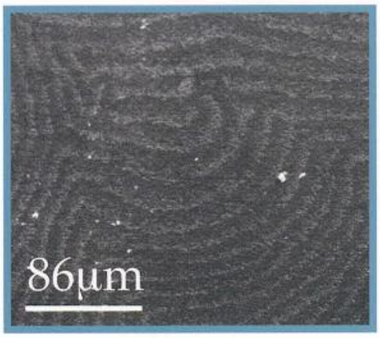

Figure 16: Step-like and labyrinthic surface structure of nacreous layer at the margin of the cultured blister pearl.

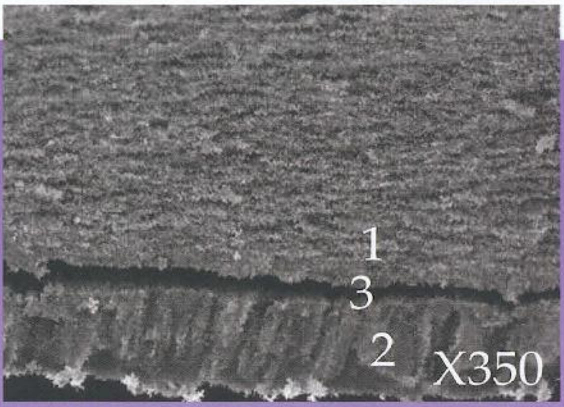

Figure 17: The relationship between the nacreous and prismatic layers of the cultured blister pearl.

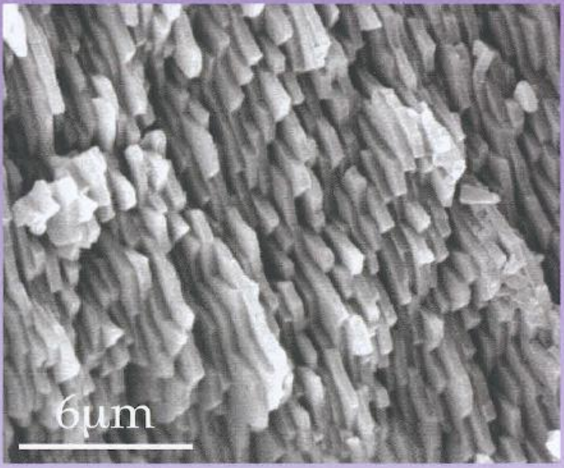

Figure 18: The regular aragonite platelets of the cultured blister pearl.

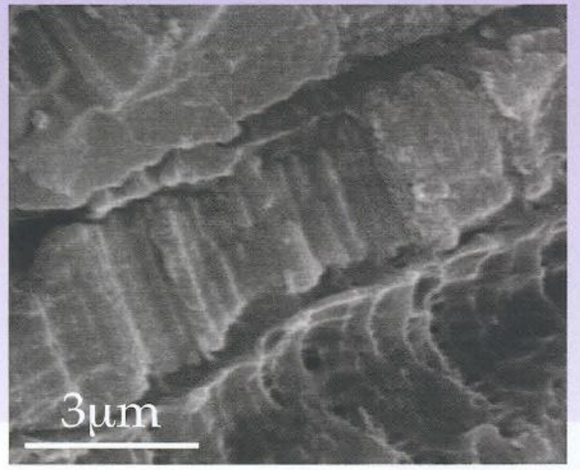

Figure 19: The calcite prisms in the cultured blister pearl; an indistinct sheet-like structure and net-like structure are visible.

Discussion

The aim of this study on the structures of shells and cultured pearls, especially the microstructures, is to learn more about the formation of shells and pearls.

From the descriptions above, the shell of *Pteria penguin* consists of three layers, an outer organic (conchiolin) layer, a middle prismatic layer and an inner nacreous layer. As is generally known, the outer conchiolin layer is mainly composed of horny protein; the middle prismatic layer is dominated by calcite prisms; and the inner nacreous layer consists mainly of aragonite platelets (Zhou, 1993; Xie, 1995; Zhang *et al.*, 1996; Smith, 1998; Li, 2001; Li *et al.*, 2001; Shi and Guo, 2001). The outer conchiolin layer can protect the carbonate layers of the shell from dissolution (Vermeij, 2002; Xie, 1995), and the middle prismatic layer is highly resistant to impact (Tong *et al.*, 2002). The inner nacreous layer acts as a stock for storing Ca^{2+} ions which are then transmitted to the middle prismatic layer (Tong, 2002; Tong *et al.*, 2002). The outer layer of the cultured blister pearl also shows a three-layered structure, the inner conchiolin layer, a middle prismatic layer and an outer nacreous layer, but with an altered arrangement compared with that of the shell *(Figure 20)*. The conchiolin is very thin, approximately 0.02 mm, but is very tough. When cultured blister pearls are cut from the shells, this conchiolin layer is seen to cover the bead nucleus and can easily be separated from the bead below and the prismatic layer above. This similar construction of the shell and the cultured blister pearl implies a similar mode of origin from the same soft body.

The step-like, labyrinthine and spiral growth structures in the shell's nacreous layer represent changes in the manner of growth of the shell. Mao *et al.* (2001) observed the microstructural changes on the inner surfaces of nacreous layers during development of the Polynesian pearl oyster, *Pinctada margaritifera var. cumingii*, from planktonic larval shells to two-year-old adult shells. Five growth zones Z_0, Z_1, Z_2, Z_3

and Z$_4$ were recognized: the Z$_0$ zone shows a homogeneous structure, without any steps or contours, present on one-month-old shells; the Z$_1$ zone shows contour lines parallel to the growing shell edge, which grades into a labyrinthic pattern (Z$_2$) or growth pattern perpendicular to the edge (Z$_3$). The Z$_4$ zone shows spiral growth and was observed in the umbonal region. The three kinds of surface structure, i.e. step-like, labyrinthic and spiral, described above for *Pteria penguin* show regular changes from step-like through labyrinthic to spiral structure from the margin to the umbo of the shell. This indicates that the margin of the shell is the growth front. Step-like growth allows the shell to increase its length and width, while spiral growth allows the shell to increase its thickness (Mao *et al.*, 2001; Vermeij *et al.*, 2002).

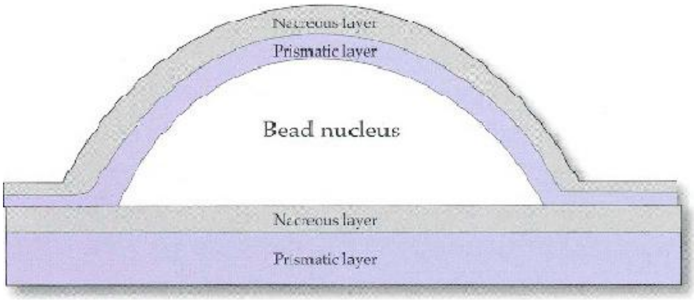

Figure 20: *A diagram showing the construction of cultured blister pearl from* Pteria penguin, *with organic matrix layers not be shown.*

The initial growth of aragonite along the organic matter on the calcite prisms in both shell and cultured blister pearl indicates that the growth of carbonate minerals in shells and pearls may be controlled by the organic matter. Although aragonite would normally change into calcite at normal temperature and pressure (Lippman, 1973, as quoted in Li *et al.*, 1995), these calcium carbonate polymorphs are able to coexist stably in shells and pearls in completely different shapes. It is impossible to explain this fact with an inorganic phase diagram, and it seems that the organism must control the formation of calcite and aragonite in shells and pearls. However, since the organic matter in shells and pearls is complex and in low concentration, there is little published information available. Organic matter in shells is classified into two kinds: soluble matter (SM) and insoluble matter (IM) (Levi *et al.*, 1998; Weiner and Hood, 1975). The insoluble organic matter can provide the network for the formation of soluble organic matrix and crystal nuclei (Falini *et al.*, 1996; Belcher *et al.*, 1996; She and Xie, 1998; Zhang and Xie, 2000b; Jiang *et al.*, 2002). The soluble organic matrix consists mainly of glycoproteins, rich in acidic amino acids such as aspartic acid and glutamic acid. Both aspartic and glutamic acids possess carboxyl groups, which can capture Ca^{2+} ions. Additionally, glutamic acid can regulate the concentration of CO$_3^{2-}$ in water, controlling the formation of aragonite (Miyamoto *et al.*, 1996). However, the details of the control of such organic matter on the formation of shells and pearls are not clear, although several models have been proposed by Watabe, 1981, as quoted in Zhang and Xie, 2000a; Huang and Li, 1991; Arnold, 1992; Dai, 1994; Xie, 1995; Zhang and Xie, 2000b.

Conclusions

The following conclusions may be drawn:

1. The shell of *Pteria penguin* consists of three layers, an outer conchiolin layer, a middle prismatic layer, and an inner nacreous layer.
2. The prismatic layer of the shell consists of multiple sub-layers (usually 3-4), with a total thickness of 0.3-0.9 mm. The calcite prisms are five- or six-sided in cross section, show an irregular overlapping sheet-like structure and have net-like structures on the prism surfaces. Each prism consists of numerous minute calcite grains rather than one calcite crystal. Dark organic matter is visible between calcite prisms.
3. The nacreous layer of the shell shows step-like, labyrinthic (fingerprint) and

spiral surface structures. The step-like structure is typical of the margin of the shell and this changes through labyrinthic to spiral in the umbonal region of the shell. This represents changes in the manner of growth. Step-growth gives rise to the increase in length and width of the shell, and spiral growth increases thickness of the shell. The nacreous layer consists of regular aragonite platelets (0.3-0.8 μm thick) and organic matter, with a total thickness of 1.0-1.5 mm. The single aragonite platelets increase their thickness from the growth edge to the umbonal region of the shell.

4. The cultured blister pearl consists of a bead nucleus with conchiolin, prismatic and nacreous layers. The conchiolin layer is about 0.02 mm thick while both prismatic and nacreous layers total 0.15-1 mm; in the specimen studied, the prismatic layer is about 44 μm and the nacreous layer is about 0.15 mm thick. The nacreous layer consists of regular aragonite platelets about 0.5 μm thick and organic matter. The prismatic layer consists of calcite prisms between 8 and 33 μm wide.
5. The initial growth of aragonite next to organic matter and the similar structures of shell and cultured blister pearl indicate similar causes of growth, probably controlled by organic matter.

Acknowledgements

John Lu and Johnny Lu from Lupearl Aquaculture Co. Ltd. are acknowledged for their help during the collection of *Pteria penguin* shells and cultured blister pearls.

References

Arnold, J.M., 1992. Nautilus embryology: a new theory of molluscan shell formation. *Biol. Bull.*, 183, 373-4

Belcher, A.M., Wu, X.H., Christensen R.J., Hansman, P., Stucky, G.D., and Morse D.E., 1996. Control of crystal phase switching and orientation by soluble mollusc-shell proteins. *Nature*, **381**(2), 56-8

Dai, Y.D., 1994. *Biomineralogy*. Petroleum Industry Publishing House, Beijing

Falini, G., Albeck, S., Weiner, S., and Addadi, L., 1996. Control of aragonite or calcite polymorphism by mollusk shell macromolecules. *Science*, 271(5), 67-9

Fu, Sh., and Liang, F.L., 2000. Experimental cultivation of blister pearl with pearl oyster, *Pteria penguin* (Roding). *Marine Sciences*, **24**(2), 12-14

Huang, L.J., and Li, H.D., 1991. Observation of the phase transition in the growth of a biomineralized calcium carbonate. *Biochem. Biophysic. Res. Communi.*, **176**(2), 654-9

Jiang, G.L., Chen, L., and Liu, Y., 2002. The organic matrix of molluscan shell and its relevance to biomineralization. *Marine Sciences*, **26**(2), 16-18

Levi, Y., Albeck, S., Brack, A., Weiner, S., and Addadi, L., 1998. Control over aragonite crystal nucleation and growth: an in vitro study of biomineralization. *Chem Eur J*, **4**(3), 389-96

Li, H.D., Feng, Q.L., Cui, F.Zh., Ma, Ch. L., Li, W.Z., and Mao, Ch.B,. 2001. Biomimetic research based on the study of nacre structure. *Journal of Tsinghua University (Science and Technology)*, **41**(4/5), 41-47, 62

Li, L.P., 2001. *The structure and composition of Chinese cultured pearls and color changing treatment. Ph.D. dissertation. China University of Geosciences*, 20-5

Li, Sh. F., Yin, Q.F., Kan, Y.H., and Wu, X.L., 1995. Study on crystals of shell by using XRD. *Journal of Yanbian University (Natural Science)*, **21**(2), 57-60

Liang, F.L., Fu, Sh., and Luo, J., 1998. A preliminary study on the grow-out method of *Pteria penguin (Roding). Marine Sciences*, **22**(4), 16-18

Liang, F.L., Mao, Y., and Yu, X.Y., 2001. A preliminary observation on the growth of the artificial spats of Pteria penguin. *Journal of Zhanjiang Ocean University*, **21**(1), 6-9

Mao, Ch.L., Golubic, S., Le Campion-Alumard, T., and Payri, C., 2001. Developmental aspects of biomineralisation in the Polynesian pearl oyster *Pinctada margaritifera var. cumingii. Oceanologica Acta*, **24**(supplement), 37-49

Meng, Z.M., Li, Y.N., and Xing, K.W., 1995. *Theory and technology for culturing pearls.* Science Publishing House, Beijing, 39-41

Miyamoto, H., Miyashita, T., Okushima, M,. Nakano, S., Morita, T., and Matsushiro, A., 1996. A carbonic anhydrase from the nacreous layer in oyster pearls. *Proc. Natl. Acad. Sci.* USA, **93**, 9657-60

She, Y.H., and Xie, A.J., 1998. Interactions between calcium carbonate and organic matrix in pearls. *Journal of Southeast University*, **28**(6), 182-5

Shi, L.Y., and Guo, S.G., 2001. Study on the composition and structure of pearls. *Journal of East China University of Science and Technology*, **27**(2), 205-10

Smith, B., 1998. Studying shells: a growth industry. *Chemistry & Industry*, 17, 649-53

Tong, H., 2002. *Application of modern analysis instrument on the mechanism of biomineralization and bionic synthetic materials.* Ph. D. dissertation. Wuhan University, 3-39

Tong, H., Hu, J.M., Ma, W.T., Zhong, G.R., Yao, S.N., and Cao, N.X., 2002. *In situ* analysis of the organic framework in the prismatic layer of mollusc shell. *Biomaterials*, **23**, 2593-8

Vermeij, G.J., translated by Hao, J.G. and Liu, D.J, 2002. *A natural history of shells.* Shanghai Scientific &

Technological Education Publishing House. 53-63

Weiner S., and Hood L., 1975. Soluble protein of organic matrix of mollusk shells: a potential template for shell formation. *Science,* **190**(5), 987-8

Xie, Y.K., 1995. *Pearl Science.* Oceanic Publishing House, Beijing

Yu, X.Y., Wang, M.F., and Yie, F.L., 2000. Development and artificial propagation of Pteria (Magnavicula) penguin (Roding). *Journal of Hainan University (Natural Science),* **18**(3), 266-9

Zhang, G.Sh., and Xie, X.D., 2000a. Ultrastructure and formation theory of nacre shells. *Journal of Mineralogy and Petrology,* **20**(1), 11-16

Zhang, G.Sh., and Xie, X.D., 2000b. Advances in biomineralization study of biogenic calcium carbonates: control of crystallization by organic matrix. *Advances in Earth Science,* **15**(2), 204-9

Zhang, Q.Y., Ji, X.H., Den, Y.H., and Jiang, Zh.H., 1996. The gemological characteristics and processing technology of cultured pearl in Hepu. *Journal of Shanghai University (Natural Science),* **2**(5) 578-83

Zhang, Zh.Q., Du, T., Fu, Sh., and Luo, J., 1994. A study on the cultivation of blister pearl from pearl shell Pteria penguin (Roding). *Journal of Zhanjiang Fisheries College,* **14**(2), 1-6

Zhou, P.L., 1993. The characteristics of gemology of pearls in Hepu, Guangxi. *Journal of Guilin College of Geology,* **13**(1), 51-9

Abstracts

Diamonds

Exhumation of lower mantle inclusions in diamond: a TEM investigation of retrograde phase transitions, reactions and exsolution.

F.E. BRENKER, T. STACHEL AND J.W. HARRIS. *Earth and Planetary Science Letters*, **198**(1-2), 2002, 1-9.

TEM data on a multiphase inclusion in a diamond from the Kankan deposits, Guinea, show it comprises a large (300 μm) diopside crystal with a small symplectitic intergrowth of olivine and tetragonal almandine pyrope. A ferropericlase inclusion in the same diamond implies a primary origin within the lower mantle. The clinopyroxene formed through the reaction sequence: MgSi-perovskite + CaSi-perovskite MgSi-ilmenite + CaSi-perovskite ringwoodite + stishovite + CaSi-perovskite clinopyroxene + relict ringwoodite. Al-rich bulk symplectite suggests ringwoodite as a coexisting precursor phase with clinopyroxene. SiO_2-depletion during the diopside-forming reaction produces a small amount of relict ringwoodite coexisting with diopside. Subsequent breakdown of ringwoodite to wadsleyite + tetragonal almandine pyrope produces the symplectitic intergrowth. During transformation of wadsleyite to olivine, exsolution of Mg-Al-chromite decreases the original solubility of Al, Cr and Ti, in agreement with experimental data on element partitioning between wadsleyite and olivine. These results suggest tetragonal almandine pyrope forms as a retrograde phase within the mantle transition zone, and is restricted to the upper lower mantle. J.F.

Characteristics of nitrogen and other impurities in diamond, as revealed by infrared absorption data.

F.V. KAMINSKY AND G.K. KHACHATRYAN, *Canadian Mineralogist*, **39**(6), 2001, 1733-45.

Diamond crystals from Siberian, Arkhangelsk, South African, Canadian and South American deposits were analysed for structurally bound nitrogen, hydrogen and 'platelet' defects using IR absorption spectroscopy. Wide variations in total nitrogen and hydrogen contents and in the state of nitrogen aggregation were established from different areas and deposits. On this basis, three groups were distinguished: (1) low-nitrogen, highly aggregated-nitrogen diamond, (2) intermediate diamond crystals and (3) high-nitrogen, poorly-aggregated-nitrogen diamond (occasionally with high contents of hydrogen and 'platelets'). These represent, in general terms, three major stages of diamond formation: (1) the initial stage at high *P-T* conditions which occasionally occur in super-deep areas (e.g. lower mantle and transition zone), (2) the main stage and (3) the final stage, which represents the latest episodes of magmatic evolution and is characterized by high oversaturation of the crystallization medium and high internal T-gradients. These data may be used for 'fingerprinting' diamonds, in prospecting for new deposits in diamondferous areas and in the evaluation of diamond crystals from newly discovered deposits. R.A.H.

Kimberlites from the Wawa area, Ontario.

F.V. KAMINSKY, S.M. SABLUKOV, L. SABLUKOVA V.S. SHCHUKIN AND D. CANIL. *Canadian Journal of Earth Sciences*, **39**(12), 2002, 1819-38.

Two newly discovered kimberlites from the Wawa area, Ontario, are group-1 kimberlites in their petrographic, mineralogical, geochemical and isotopic features. They contain mantle minerals and xenoliths of the Fe-Ti-association (magnesian ilmenite, iron-rich olivine, orange Ti-pyrope garnet, augite and ferroan enstatite) and of the Cr-association (chromian spinel, forsteritic olivine, purple Cr-pyrope garnets, chromian diopside and enstatite); minerals of Fe-Ti-association are much more abundant. Minerals of eclogitic association are absent. Both G-10 pyrope garnets and high Cr-spinels typically associated with diamond are represented in the Cr-association. The average age of the kimberlites is 1097 ± 7 m.y., i.e. contemporaneous with other alkaline igneous rocks in the Wawa area. Equilibration *P* and *T* of mantle xenoliths plot close to a 40-45 mW/m^2 geotherm. On the basis of the Ni-in-garnet geothermometer, garnets from the Wawa kimberlites equilibrated at 800-1350°C, and at least in part within the diamond stability field. It is likely that kimberlitic magma was derived from *LREE*-enriched asthenospheric mantle. G.L.B.

An important exhibition of seven rare gem diamonds.

J.M. KING AND J.E. SHIGLEY. *Gems & Gemology*, **39**(2), 2003, 136-43.

A temporary display at the Smithsonian Institution in Washington DC contained one colourless 203.04 ct diamond (the De Beers Millennium Star) and six coloured diamonds (the 101.29 ct Fancy Vivid yellow Allnatt, the 59.60 ct Fancy Vivid pink Steinmetz pink, the 27.64 ct Fancy Vivid blue Heart of Eternity, the 5.54 ct Fancy Vivid orange Pumpkin, the 5.51 ct Fancy Deep blue-green Ocean Dream and the 5.11 ct Fancy red Moussaieff), all of which are shown in coloured illustrations. R.A.H.

The pressures and temperatures of formation of diamond based on thermobarometry of chromian diopside inclusions.

P. NIMIS. *Canadian Mineralogist*, **40**(3), 2002, 871-84.

The *T* and *P* of formation have been calculated for >100 inclusions of chromian diopside (mostly isolated) in diamond crystals also containing inclusions of peridotite material, and for peridotite xenoliths from worldwide occurrences, using single-clinopyroxene thermobarometers. The results provide constraints on the conditions and relative timing of diamond genesis. Inclusions in diamonds and xenoliths from the same source commonly yield similar *P-T* values,

ISSN: 1355–4565

suggesting that diamond crystals formed when the lithospheric mantle had already attained a conductive thermal regime comparable to or even colder than that extant at the time of emplacement of the host kimberlite or lamproite. Some inclusions record thermal or metasomatic events, which can be ascribed to the ascent of hot C-rich fluids from which the diamond precipitated. In general, there is no evidence for the occurrence of diamond being concentrated at particular levels in the lithosphere. R.A.H.

Growth habit of needle crystals in coats of coated diamonds.

N. Shimobayashi and M. Kitamura. *Journal of Mineralogical and Petrological Sciences*, **96**(5), 2001, 188-96.

Needle diamond crystals constituting the coat portion of coated diamond from Zaire are bounded by curved {100} faces (cuboid) and small {111} facets, showing distinct sector zoning in CL brightness under CL microscopy. It is argued that the needle morphology is responsible for 'random walk model', which can also explain the whole external morphology of coated stones. The needle crystals were formed by co-precipitation of inclusions and due to the rapid growth controlled by the kinetic roughening of the octahedral faces and the kinetic smoothing of the cuboid faces. It is suggested that both coated stones and mixed-habit growth were grown under similar conditions, except for the co-precipitation of inclusions in the former. I.S.

Gems and Minerals

Sir Victor Sassoon and his ivories.

P. Allen. *Transactions of the Oriental Ceramic Society*, **66**, 2003, 95-105.

Brief description of the collection of Chinese ivory artefacts formed by Sir Victor Sassoon (1881-1961). Accounts of some of the vicissitudes of the collection and comments on the catalogues are included. M.O'D.

The Bishop copper prospect.

H. Barwood. *Mineralogical Record*, **34**, 2003, 215-22.

The Bishop copper prospect is the source of the world's best crystals of turquoise. Situated about one mile west of Lynch Station in Campbell County, Virginia, USA, the prospect produces turquoise crystals either on a mica schist or on a white quartz brèccia. Crystals are too small for ornamental use but are sought by collectors who still find specimens on the mine dumps. M.O'D.

An unusual crystal from the Central Queensland sapphire fields.

R. Beattie. *Australian Gemmologist*, **21**(10), 2003, 408, 4 illus.

An unusual crystal fragment of around 17 carats was recovered from the Great Northern Mining's Subera sapphire mine located 5 km east of Rubyvale. The pyramidal crystal displayed the distinct features of both ruby and sapphire. Light transmitted along its c-axis made it glow bright red and revealed the hexagonal orientation of 'silk' included sapphire in the base of the crystal. When this transmitted light was analysed with a hand-held spectroscope the identifying spectrum of both ruby (fine lines in the red and a broad absorption in the green-yellow) and sapphire (strong absorption band at 450nm) were revealed. P.G.R.

Jewelled gifts of the Mughal court.

S. Canby. *Transactions of the Oriental Ceramic Society*, **66**, 2003, 57-64.

Text of a lecture given by the author to the Society on 4 December 2001. The tradition of presenting expensive and elaborate gifts characterized the courts of the first five Mughal emperors from 1526 to 1658 and some of the rituals of giving and receiving are described. Some of the gifts were set with important gemstones. M.O'D.

Rare gem mineral deposits from Brazil – Part 2: Lazulite and scorzalite.

M.L.C. Chaves, J. Karfunkel, A.H. Horn and D.B.Hoover. *Australian Gemmologist*, **21**(10), 2003, 390-9, 6 illus., 4 maps, 3 tables.

The lazulite group members, lazulite and scorzalite, form a solid solution series between the magnesium and iron end members and are valued because of their fine blue colour. However, their relatively low hardness and rarity as gem-quality specimens make them collectors' stones. Brazil is the main source of these two minerals and this paper identifies the deposits and regions where they occur, discusses their genesis, and describes their gemmological characteristics. P.G.R.

Beryllium diffusion of ruby and sapphire.

J.L. Emmett, K. Scarratt, S.F. McClure, T. Moses, T.R. Douthit, R. Hughes, S. Novak, J.E. Shigley, Wuyi Wang, O. Bordelon and R.E. Kane. *Gems & Gemology*, **39**(2), 2003, 84-135.

Although initially only orange to orange-pink ('padparadscha'-like) sapphires were seen, it is now known that a full range of corundum colours, including yellow and blue as well as ruby, have been produced or altered by the heat treatment of corundum involving lattice diffusion of Be at $T >$ 1800°C. An extension of the current understanding of the causes of colour in corundum is presented to help explain the colour modifications induced by Be diffusion. The examination of hundreds of rough and faceted Be-diffused sapphires reveals that standard gemmological testing will identify many of these treated corundums, though in some cases MS analysis may be necessary. Potential new methods to provide additional aids in their identification are being investigated. A fold-out colour chart is provided to assist in appreciating visual diagnostic clues. R.A.H.

The Rogerley mine, Weardale, County Durham, England.

J. Fisher and L. Greenbank. *UK Journal of mines and minerals*, **23**, 2003, 9-20.

The Rogerley mine is producing very fine green crystals of fluorite, many of which are gem quality. The history of mining in the area, with the local geology and mineralization, is described with notes on the chemistry. REE, though present in the crystals, are not thought to cause the colour on their own. M.O'D.

CO_2-H_2S-COS-S_8-AlO(OH)-bearing fluid inclusions in ruby from marble-hosted deposits in Luc Yen area, North Vietnam.

G. Giuliani and 10 others. *Chemical Geology*, **194**(1-3), 2003, 167-85.

Fluid inclusions have been studied in rubies from marble-hosted deposits in the Luc Yen mining distinct, N. Vietnam. Raman and IR spectroscopy combined with microthermometry investigations on primary and secondary fluid inclusions provided evidence of CO_2-H_2S-COS-S_8-AlO(OH)-bearing fluids with native sulphur and diaspore daughter minerals without visible water. Diaspore formed as an invisible film 2-3 μm thick coating the walls of the fluid inclusion cavity, and native sulphur was generally nucleated during Raman irradiation. The presence of diaspore and COS in the fluid inclusions indicates that water was present in the palaeofluid. The mole fractions of H_2O and CO_2 are ~10^{-2} and the expected concentration in the fluid inclusions is in the 1-10 mol.% range. Crush-leach identified sulphates and chlorides that are assigned to the presence of anhydrite and Na-Ca-Cl salts found by SEM in the ruby crystals. The CO_2-rich inclusions which do not coexist with an aqueous phase by immiscibility process demonstrate that ruby grew from this CO_2-rich and water-poor fluid at equilibrium with Na-Ca-Cl salts. Thermal reduction of evaporitic sulphates based on an initial assemblage of anhydrite, calcite and graphite, originating from the metamorphism of organic matter is proposed to explain the original fluid chemistry of these marble-hosted rubies. The marbles acted as a closed system and the carbonic composition of the parent fluids in ruby indicates that aluminium can be transported in CO_2-rich fluids at high *T* and *P*. G.L.B.

Über Amethystvorkommen in Sachsen.

R. Haake. *Mineralien Welt*, **14**(4), 2003, 12-25.

Amethyst of ornamental and sometimes near-gem-quality is described from different locations in Saxony, Germany. Details of the local geology are given for some locations. M.O'D.

The distribution of rare earth elements in north Pennine fluorspar and fluorite.

R.A. Ixer. *UK Journal of mines and minerals*, **23**, 2003, 21-6.

Though fluorite from the north Pennine orefield is REE-rich, it is not thought that they are the cause of the range of colours shown. Details of experiments are given. M.O'D.

Imilchil.

S. Jahn. *Mineralien Welt*, *14*(**4**), 2003, 42-64.

Geological and mineralogical survey of the Imilchil region of Morocco. A full descriptive species list is given. Transparent gem-quality apatite crystals over 2.5 cm are noted. M.O'D.

Amazonitization in granite resulting from the intrusion of pegmatites.

H. Jordt-Evangelista, J. César-Mendes and A.L.C. Lima. *Revista Brasileira de Geociências*, **30**(4), 2000, 693-98.

Borrachudos-type granite from Santa Maria do Itabira, in Minas Gerais is cut by amazonite-bearing pegmatites, being marginally transformed into a green granite due to amazonitization. This paper deals with the processes and the mineralogical and chemical variations involved in the transformation of the normal granite into a green granite. The metre-wide pegmatite is composed of decimetre size amazonite crystals of intense green colour, cleavelandite, biotite, quartz and small amounts of black tourmaline, galena, fluorite and anatase. The alkaline anorogenic granite is composed of quartz, nearly pure albite, microcline with triclinicities of 0.68–0.93, Fe-biotite and accessory minerals. The mean SiO_2 content is 74 wt.%, but in quartz-poor samples it decreases to 62%. MgO is very low (<0.05 wt.%), Fe_2O_{3total} reaches 4.4% and alkalis 8.5%. A strong negative Eu anomaly could be due to the retention of Eu in the calcic plagioclases left over in restitic rocks which generated the alkaline magma by partial melting. The intensity of the green colour in the granite increases towards the pegmatite contact. Chemically this colour variation is accompanied by an increase in the Pb (and to a lesser extent also in Rb) contents, while no difference could be registered for the major and other trace elements. Pb varies from 37 to 302 ppm, reaching 406 ppm in the amazonite. It is possible that the subsolidus introduction not only of Pb but also of water from the pegmatite into the country rock was responsible for the generation of H_2O–Pb pairs in the microcline, which are postulated as the cause of the green colour of amazonites. Considering the relatively low *T* of pegmatitic magmas and the massive structure of the granite, the metasomatic process of amazonitization was very efficient since the aureoles locally reached a width equal to the width of the pegmatite. H.A.H.

Gem News International.

B.M. Laurs (ed.). *Gems & Gemology*, **39**(2), 2003, 152-65.

Items mentioned include a 1372 ct faceted pink fluorite from Pakistan, chatoyant reddish-brown cabochons of Na-meionite with abundant inclusions of hematite, an 83.53 ct quartz cabochon from Kola containing stalks and fibres of astrophyllite, and a bi-coloured synthetic diamond showing both blue and yellow zones (due to B-induced absorptions). R.A.H.

Sapphire in diamond alluvial deposits at Coxim River region, Mato Grosso do Sul, Brazil.

A. Liccardo and J.E. Addad. *Revista Brasileira de Geociências*, **31**(3), 2001, 635-8.

Alluvial diamondiferous deposits of Coxim, Mato Grosso do Sul, contain corundum grains (sapphire type) in association with diamonds. These sapphires were analysed by electron microprobe for Al, Fe, Ti, Cr and Ga. The relation Cr/Ga < 1 indicates an alkaline basaltic source for the corundum and the Coxim sapphires presented values around 0.25-0.5. High iron content, between 1.03 and 1.26%, and low Ti, from 0.0 to 0.31%, suggests the cause of colour by charge transfer between Fe^{2+} and Fe^{3+}, typical basaltic sapphires. High levels of resistance to chemical attack through hardness and density of both corundum and diamond, point to sedimentary reworking survival and depositional convergence at fluvial traps. The high roundness of the sapphires from Coxim indicates a long distance vector. H.A.H.

Relationship between the groove density of the grating structure and the strength of iridescence in mollusc shells.

Y. Liu, K.N. Hurwit and L. Tian. *Australian Gemmologist*, **21**(10), 2003, 405-7, 2 illus.

A scanning electron microscope and a laser were used to study the iridescence of a shell of the mollusc *Pinctada margaritifera* and to measure the groove structure which acts as a reflection diffraction grating. The studies have shown that the range of groove density in a shell is between 80 grooves-per-mm for the weakest iridescence and 300 grooves-per-mm for the strongest iridescence. If two shells have the same groove density, the one with the higher quality diffraction grating will produce the stronger iridescence. P.G.R.

Fibrous nanoinclusions in massive rose quartz: HRTEM and AEM investigations.

C. Ma, J.S. Goreva and G.R. Rossman. *American Mineralogist*, **87**(2-3), 2002, 269-76.

Examination of pink fibrous crystals within massive rose quartz from localities in California, South Dakota, Brazil, Madagascar and Namibia with high-resolution transmission electron microscopy (HRTEM) and analytical electron microscopy (AEM) reveals that the nanofibres in all samples are related to dumortierite. Selected-area electron diffraction (SAED) patterns and HRTEM images indicate that the dumortierite-related fibres have a superstructure with a doubled periodicity along the a and b axes of dumortierite, giving cell parameters $a = 2a_{\mathrm{dum}} = 2.36$ nm, $b = 2b_{\mathrm{dum}} =$ 4.05 nm, $c = c_{\mathrm{dum}} = 0.47$ nm. Computer simulations suggest that periodic arrangements of two different *M1* site occupancies in the octahedral face-sharing chains give rise to the superstructure. One type of *M1* site is occupied mainly by Al, whereas the other type is dominated by Ti and Fe. Simulated HRTEM images based on the proposed model match the experimental images. Most of the fibres, elongated along the *c*-axis, are free of defects. AEM analysis shows that the dumortierite-related fibres have a composition similar to well-characterized dumortierite, but that they contain a greater amount of Fe substituting for Al and the *M1* sites. Boron was detected in all fibres examined by electron energy loss spectroscopy as well as in sillimanite crystals found as a minor component in one rose quartz from Brazil. P.M.W.

Pressure, temperature and fluid conditions during emerald precipitation, southeastern Yukon, Canada: fluid inclusion and stable isotope evidence.

D. Marshall, L. Groat, G. Giuliani, D. Murphy, D. Mattey, T.S. Ercit, M.A. Wise, W. Wengzynowski and W.D. Eaton. *Chemical Geology,* **194**(1-3), 2003, 187-99.

The Crown emerald veins are somewhat enigmatic, displaying characteristics that are common to emerald deposits of tectonic-hydrothermal origin and of igneous origin. The veins cut the Fire Lake mafic metavolcanic rocks, occurring within 600 m of an outcrop of Cretaceous S-type granite. Fieldwork and vein petrography are consistent with a polythermal origin for the veins. The primary vein mineralogy is quartz and tourmaline with variable sized alteration haloes of tourmaline, quartz, muscovite, chlorite and emerald. The veins weather a buff brown colour due to jarosite, scheelite and minor lepidocrocite, which were precipitated during the waning stages of vein formation. Microthermometric studies of primary fluid inclusions within emerald growth zones are consistent with emerald precipitation from H_2O-CO_2-CH_4 (± N_2 ± H_2S)-bearing saline brines. The estimated fluid composition is ~ 0.9391 mol.% H_2O, 0.0473 mol.% CO_2, 0.0077 mol.% CH_4 and 0.0059 mol.% NaCl (~2 wt.% NaCl eq.). Fluid inclusion and stable isotope studies are consistent with vein formation in the *T* range 365-498°C, with corresponding *P* along fluid inclusion isochore paths ranging from 700 to 2250 bar. These data correlate with a very slow uplift rate for the region of 0.02-0.07 mm/year. Emerald deposits are generally formed when geological conditions bring together Cr (± V) and Be. Cr and V may have been derived locally from the mafic and ultramafic rocks during hydrothermal alteration. The Be was most likely derived from the nearby Cretaceous granite intrusion. G.L.B.

Lab notes.

T.M. Moses, I. Reinitz, S.F. McClure and M.L. Johnson (eds). *Gems & Gemology,* **39**(2), 2003, 144-51.

Notes are given on a green cut stone of chrysoberyl with V as chromophore, a Guatemalan jade with inclusions of reddish-brown lawsonite, a 'red' spinel whose pink body colour was increased to orange-red by exsolved inclusions of hematite along octahedral planes and two natural marquise-cut brown-yellow diamonds with strong parallel pink lamellae. R.A.H.

Proceedings, 4th Indian Gemmological Seminar.

Udaipur, 2002. In: *Indian Gemmologist,* **11**(1/2), 2003, 2-64.

Papers presented include Understanding colour in diamonds; Padparadscha, natural or treated?; Priority areas for exploration of gem minerals in India; The Kashmir sapphire; Identification of fracture filled diamonds; Gemstones of Orissa – an overview. M.O'D.

What's new in minerals?

J. Scovil and T. Moore. *Mineralogical Record,* **34**, 2003, 275-85.

Specimens of gem interest seen in the Tucson and Carnegie [Pittsburgh] shows of 2002 included an emerald theme at the Carnegie show, fine almandine from the Two Fat Guys mine, Erving, Massachusetts, deep rose-coloured beryl from Mandrasonora, west of Ambatofinandronara, Madagascar, aquamarine from Taplejung, Taplejung district, Nepal, diopside from Xinjiang Uygur province, China, spessartine in a deep raspberry-red colour from the Urucum mine, Galileia, Minas Gerais, Brazil and elbaite from the Terra Corrida mine near Coronel Murta in the same state. Some of the crystals were deep red at both ends with a deep green in the centre. M.O'D.

First finding of sapphire from Cenozoic alkali-basaltic volcanoes in the Primor'e region.

S.V. Vysotskii, S.A. Shcheka, V.P. Nechaev, V.P. Soroka, A.V. Barker and A.I. Khanchuk. *Doklady, Russian Academy of Sciences, Earth Sciences Section,* **387A**(9), 2002, 1100-3 (English translation).

To test the hypothesis that rare metal pegmatites, greisens and granite-related metasomatites were the source of the corundum in this region, extensive heavy concentrate sampling of alluvial sediments and talus in the Cainozoic alkali-basaltic fields was carried out. The chemical compositions of basalt, garnet, pyroxene, spinel, amphibole and biotite from the Konfetka and Podgelbanochnyi volcanoes are tabulated, together with TiO_2, Al_2O_3 and FeO analyses of sapphires from these localities and also from the Nezametnaya placer and the Kedrovka River placer. The authors regard this region as the N segment of the Australian and East Asian sapphire-bearing belt. A.M.C.

Gem quality petalite from Myanmar (Burma).

U.K.K. Win and T. Themelis. *Australian Gemmologist,* **21**(10), 2003, 409, 1 illus.

Petalite, a lithium aluminium silicate, occurs in Khet-chal, Molo district near Momeik, Myanmar as gem-quality transparent colourless crystals having a glassy appearance and as water-worn pebbles with a characteristic waxy lustre. Although confused locally with quartz, petalite has a distinctively different SG, RI and habit. This is the first report of Myanmar gem-quality petalite in the literature, and only a handful of these rare gemstones are known. P.G.R.

Instruments and Techniques

Limitations of the pavilion depth rapid sight estimates method.

G. HOLLOWAY. *Australian Gemmologist*, **21**(10), 2003, 400-3, 5 illus., 3 tables.

The *Rapid sight estimates* method, as proposed by Liddicoat (*Gems & Gemology*, 1962) is a way of estimating the pavilion depth of a brilliant cut diamond by visually assessing the relative size of the table reflection compared with the actual size of the table facet. However, if either the crown angle is very steep, or the girdle is very thick, then Liddicoat's visual depth estimation leads to an underestimate of the pavilion depth. Research by the author also reveals that diamonds with combined steep crowns and slightly deep pavilions can cause a significant amount of light entering the crown to leak out of the pavilion, resulting in reduced brilliance. This increases the possibility of incorrect appraisal when assessing the cut proportions of a brilliant cut diamond. In the author's opinion, the most effective alternative is to use a Sarin™ proportion measurement analyser, although this is an expensive option at US$6,000. P.G.R.

Large OPL™ diffraction grating spectroscope.

T. LINTON, A. CUMMING AND K. HUNTER. *Australian Gemmologist*, **21**(10), 2003, 410-12, 3 illus.

This report by the GAA Instrument Evaluation Committee compares results obtained with the well known small OPL diffraction grating spectroscope with those obtained on the new larger version. Both models employ a fixed slit which is set for maximum resolution of fine line absorption spectra. This fixed slit has the disadvantage of requiring stronger illumination when checking the absorption spectra of darker gemstones. Although diffraction grating spectroscopes are supposed to be in focus across the complete spectrum, one member of the Evaluation Committee noted differences in focus between red and blue on the larger model. The new instrument's size made it easy to use, and the spectroscope's large eyepiece lens provided easy viewing of the bigger spectrum available, features making it particularly suitable for teaching purposes. The image quality of complex absorption spectra was better than that obtained with the smaller version and matched the quality of those produced by most prism spectroscopes. The report includes general recommendations for the use of spectroscopes in the identification of gemstones. P.G.R.

Diamond cut grading based on red reflection instruments.

T. LINTON AND G. HOLLOWAY. *Australian Gemmologist*, **21**(10), 2003, 413-19, 4 illus., 2 tables.

Four instruments designed for diamond cut grading are compared and their methodologies described. Each instrument, the Brandt, Schindler, Fire Scope and the Ideal-Scope, is based on a 10× lens surrounded by a red reflector. Comparisons are made by using the instruments to analyse four diamonds of differing proportions. Neither the Brandt nor the Schindler instruments functioned as effectively as the Fire Scope and the Ideal-Scope in allowing the user to make a good subjective judgement of diamond cut quality, light return and light leakage. P.G.R.

Synthetics and Simulants

50th anniversary of first successful diamond synthesis.

R. CAVENEY. *Industrial Diamond Review*, **2003**(1), 2003, 13-15.

After a brief review of earlier unsuccessful attempts to synthesize diamond, an account is given of the successful experiment by the Swedish company ASEA on 15th February 1953. Iron carbide and graphite were used, with a thermite; the latter was activated by an electric pulse sent through a wire between the anvils in a spherical P intensifier (the Quintus press) which started the exothermic reaction to provide the required T. The crystals were confirmed as diamond by XRD. The yields in the successful runs were 20-50 crystals, from 0.1 to 0.5 mm in size; they had irregular faces and were mostly transparent and colourless, but a few were green, yellow or grey. R.A.H.

Spectroscopy of natural silica-rich glasses.

E. FAULQUES, E. FRITSCH & M. OSTROUMOV, *Journal of Mineralogical and Petrological Sciences*, **96**(3), 2001, 120-28.

By means of IR and Raman spectroscopy and optical microscopy, impactites, tektites and obsidian have been investigated and compared with artificial glasses with silica-rich and alkali-rich compositions. IR spectra are strongly dependent on silica content: frequencies of the ν_3 and ν_D bands increase with the silica content. Raman spectra of tektites show relationship between silica, alumina, sodium contents and the presence of vibrational bands peaked at very specific energies. Raman spectra of Libyan desert glass, Darwin glass and vitreous silica are almost identical with the typical doublet at 440-490 cm^{-1}, whereas in tektites the band at 440 cm^{-1} has a relatively less pronounced doublet structure. A common character of Raman spectra of tektites and obsidians is the appearance of broad bands centred around 1000 and 1600 cm^{-1} due to substitutions of Si by metals. Tektites have a strong absorption band at 1100 cm^{-1} due to Fe^{2+} ions. In the other glasses, this absorption is slightly shifted towards 1100-1130 nm. Additional sharp features of impactites and obsidians at 1380, 2210-2250 nm are completely absent in the absorption spectra of tektites. These bands are the signature of molecular water trapped inside the structure. I.S

Abstractors

G.L. Barron	G.L.B.	H.A. Horn	H.A.H.	P.G. Read	P.G.R.
A.M.Clark	A.M.C.	R.A. Howie	R.A.H.	I. Sunagawa	I.S.
J. Flinders	J.F.	M.O'Donoghue	M.O'D.	P.M. Whelan	P.M.W

For further information on many of the topics referred to, consult *Mineralogical Abstracts*

Book Reviews

Gem and ornamental materials of organic origin.

M. CAMPBELL PEDERSON, 2004. Elsevier, Oxford. pp xiv 268, illus. in colour. Hardcover, ISBN 0 7506 58525. £33.25.

This is a very interesting book which draws together a vast amount of information which would otherwise require delving into many sources from a wide range of disciplines. The author advocates identification by visual observation (if necessary aided by a 10× hand lens) since she feels that standard gemmological tests are often not feasible on account of the shape and size of many 'organic' objects, and that some tests might damage delicate surfaces. She could be correct.

The book is well bound and the overall design is admirable. The author's photographic skills show through in the prolific illustrations, but the fine details in some of the pale coloured objects (notably the ivories) is often poorly reproduced, which may be caused by inadequacies in the printing processes. The magnification is not given in many enlarged photographs.

There are fourteen chapters, which in the case of the amber chapter (38 pages) is divided into sections on localities and species, structures and properties, treatments and uses, identification and history. Some chapters may have fewer sections while conservation status and availability are also discussed in others. Other chapters are Jet (17 pages), Ivory (29), Bone (8), Antler (9), Rhino horn (6), Horn (17), Tortoiseshell (17), Pearl (27), Coral (27), and Miscellaneous organics (18) which includes such diverse materials as baleen, byssus, calabash, coconut, feathers, fossilised molluscs, hair, hornbill ivory, insect wings, lacquer, shagreen, vegetable ivory and others. The chapter on Plastics (12) is excellent. The final chapter is a series of seven identification charts (tables) which compare and contrast the properties of similar species described in the book.

The book does not deal with some methods which might be conducted in a gemmological laboratory, but it does list three seemingly simple tests which individuals might be able to use; (1) the hot-point – not recommended by this reviewer except by those with *very* considerable expertise, (2) the burning test, using a tiny scraping from an inconspicuous part of the object – again much experience is needed and (3) ultraviolet light which can be a useful indication, but this apparatus can be expensive although there are now some small UV lights which fit into the pocket and cost much less.

There is a useful glossary and a good bibliography, but surprisingly, this does not mention R. Webster's book *Gems* which does describe many simple and useful gemmological tests on organic materials. For the antique dealer, jeweller and gemmologist this book would be a most useful addition to their bookshelves. E.A.J.

Diamonds. Revised edn.

F. WARD, 2003. Fred Ward Gem Series. Gem Book Publishers, Bethesda, MD. pp 64, illus. in colour. Softcover ISBN 1 887 651 09 8. £10.95.

Well-written and illustrated as readers have come to expect from this excellent series, this new member of the Gem Books series includes up-to-date information on synthetic diamond and some of the recent developments in the sale of rough by the De Beers organization. Photographs of diamonds in jewellery are particularly effective and the whole page illustrating pink to near-red Argyle stones is one of the first to catch the eye. The author's continuing services to gemmology and jewellery are most welcome. M.O'D.

Rubies & sapphires. 4th edn.

F. WARD, 2003. Fred Ward Gem Series. Gem Book Publishers, Bethesda, MD. pp 65, illus. in colour. Softcover ISBN 1 887 651 10 1. £10.95.

Along with the fine photographs come up-to-date details of synthesis and treatment. In particular there is an account of beryllium diffusion and other treatments, one showing the before and after state of Montana sapphires. Traditional corundum examples have not been forgotten and, as always in this series, many specimens are shown set in jewellery. All students should buy this. M.O'D.

Proceedings of the Gemmological Association and Gem Testing Laboratory of Great Britain and Notices

The Presentation of Awards ceremony held in the magnificent Livery Hall at Goldsmiths' Hall, London.
(Photo: Lewis Photos Ltd.)

Presentation of Awards

The Presentation of Awards gained in the 2003 examinations was held at Goldsmiths' Hall, Foster Lane, London EC2, on Monday 3 November. Professor Alan Collins, President of the Association, presided and welcomed those present, particularly students who had travelled from as far away as Canada, Colombia, Hong Kong, Sri Lanka and the U.S.A., as well as from the UK and Europe. He announced that in January and June 2003 a total of 861 students had sat the Preliminary and Diploma Gemmology and Gem Diamond Diploma examinations.

Professor Collins introduced Anthony Hirsh who presented the awards.

Anthony Hirsh then delivered his address (see below) and a vote of thanks was given by Ian Thomson who also thanked the Goldsmiths' Company for kindly permitting Gem-A to hold the ceremony at the Hall.

A reception was held following the ceremony, attended by over 200 members, students and their guests.

Anthony Hirsh's Address

First off, congratulations! This evening is for all of you wonderful and clever students who passed your FGA/DGA exams, so give yourselves a hand. You deserve it!

ISSN: 1355-4565

Have you ever stood back and pondered why? Why do teachers instruct us in various skills which we will probably never use in our everyday lives? They ask us all sorts of questions and then we must present the answers. Well I am here to tell you that you will use these skills; it is just a question of time and place.

In life – that is in the real business world – everything that you have learned in the past and will continue to learn in the future will benefit you at some point in your lives. You may not agree now, but believe me, this is true. All that you have learned, studied and read will eventually bear fruit. Realize the only ingredient you have not acquired thus far is *experience*. That really is the crux of the matter.

The work that you have input, along with your teachers aid and guidance, are so that you will not only know the answers but also so that you will understand and begin to know why.

For better understanding, let us break down those key components which will lead you to a successful career in any given field: first, comes the learning; second, comes the studying; and third and most importantly, comes the *application*. With that in mind, then ask yourselves three vital questions: what can I... and what should I do with all of that knowledge? Will I be able to make an impact on the business and in what aspect of the business can I apply myself?

Naturally, you want a job, but as you will find out or may have already discovered, it is not so easily obtainable – even with having expert knowledge and qualifications. Possessing a diploma does not automatically guarantee you a job. You and you alone must work at it continuously. Simply replying to advertisements, sending out CVs, emailing, phoning or pounding the pavement alone can, and often will, prove ineffective unless you know someone or are recommended by someone reputable. Today, networking is crucial for securing yourself a position within an organization. During the interview process try and meet with either the boss or senior manager in order to develop a positive rapport and make an unforgettable impression.

Just remember, no matter how large or small the company, good people are hard to come by and most employers know this to be the case. *You* know how good you are – but they do not. Bear in mind that you probably are better informed, more skilled and certainly better qualified than most of the people that will be conducting the interview. So what is the problem? Basically, there are far too many clever people out there competing for similar jobs. By the way, it is the same in every country all over the world today.

Therefore, it is up to you to prove yourself! You must invest in yourself before anyone else will do the same. Start by subscribing to the trade presses. Constantly be aware of the trends, the competition and the current happenings within your chosen industry. By continuing to grow and being receptive to new ideas, you will be adding to your job credibility and marketability. If you pace yourself and choose the businesses which are right for you – whether it be in design, manufacturing or selling – you should have no trouble locating

Anthony Hirsh presenting the Anderson-Bank Prize to Jessica Banks. (Photo: Lewis Photos Ltd.)

Anthony Hirsh presenting the Anderson Medal and the Preliminary Trade Prize to Antoinette Jackson. (Photo: Lewis Photos Ltd.)

that perfect job in which you can shine. Consider you have three very important assets: yourself, your knowledge and do you know what the third asset is?... your certificate!

Now, some helpful tips you may wish to consider at this time on your careers. Finding employment at a small company rather than a large firm will provide you with the opportunity to hone up on your skills and learn all aspects of the industry. Also, allow your employer to train you in their personal style of working instead of having them conform to your work traits. Likewise, be familiar with the difficulties that go into creating your own business and the amount of capital that goes into making a successful company. Always remember that your reputation will follow you throughout your career, whether you are just beginning or at the top of the corporate ladder, maintain your integrity, practice a high work ethic and be trustworthy to all those around you.

The best advice I can give you today, according to my personal experience, is that your enthusiasm about your work will play the most important role in how you achieve success in your careers. Naturally when you radiate enthusiasm, whether in your personal or professional lives, you become a positive influence on those around you. This kind of passion will be contagious. Your employer, your peers and the public will automatically sense this enthusiasm about you and share in your excitement toward a particular product or jewellery design.

You are probably asking yourselves, so how did I end up in this wonderful and challenging business? In 1969, I met a young (we were all young then - some of you were not even thought of, let alone, born) dynamic man by the name of Lawrence Graff. He asked me to change the direction of my career and come and work for him at the then Graff Diamonds Ltd. In a matter of months, I became a sales director. Even though I found the gem side very interesting, especially since we handled and sold some of the largest gems in the world, my main job was to increase the sales side of the company. I accomplished this by travelling all over the world, meeting people and establishing valuable business contacts. The excitement of selling, travelling and creating were so exhilarating. Graff then went on to create the largest jewellery company which today is recognized as the leader in the field. Opening a store in Knightsbridge in 1974, at the time of the Arab boom, demonstrated great timing. It not only showed impeccable vision, but proved very profitable as well.

As with most companies that grew rather large, there arose differences of opinion. As a result, I resigned and began my own company in 1980. I began in wholesale and then in 1986, I took over a lease at no. 10 Hatton Garden. It was there that I started retailing under my own name *Hirsh*. Then, in 2001, I opened our flagship store in Burlington Arcade located in the West End.

I am very proud to stand before you today and say that our company is known throughout the world for our fine handmade jewellery, for our one-of-a-kind designs and for our exceptional sales service. However, I cannot take all the credit. Our team is lucky to be led by one of the UK's finest gemmologists, Anne Bailey FGA DGA. Anne came to us in 1992 at 19. Through her ingenious and original designs and establishing a solid client-base; she can now call herself Director of Hirsh – in charge of purchasing loose diamonds and gemstones, as well as, creating the beautiful jewellery designs.

In addition, my staff and I have established our own in-house manufacturing, design and PR facility. Over the past 24 years we have worked very hard to build up a highly reputable and competitive business. When we began, we constantly underwent changes regarding the upgrading of our quality and services. Whether we were selling wholesale within the trade or later to the public, we knew the only way to make a name for ourselves was to deliver an exceptional piece of jewellery and to establish an impeccable reputation amongst the industry and public. Once those factors were in place, we turned our attention toward selling – one of the most difficult and unpredictable aspects of this business. In the end, if you follow these ethical guidelines, you too can have a rewarding and profitable career in this industry.

I am fortunate to have established in my company a team-oriented work environment where fresh ideas and an open-door policy are encouraged. For these reasons, I have a loyal and content staff; therefore, my company will continue to grow and flourish.

It is vital to keep the lines of communication open at all times. Although I am the boss in my company that does not automatically mean that I am correct in all my decisions. I must always remember to listen to any advice or criticism in order to improve my quality of management or the overall welfare of my staff.

Of course, I would not be here today without the continual love and support that I receive from my family. They say that behind every great man is a fine woman. That can be said of my lovely wife, Diane. Likewise, I could not be any prouder of my two daughters, Tracy and Lianne, and of my two sons, Mark and Jason. Only last month, Jason, my youngest, began working for Asprey in New York where he already is proving to be one of their top salesmen.

I hope you are still listening because I want to wish you all much success and happiness in all your future endeavours. Please feel free to ask me any questions or advice this evening. I look forward to hearing only great things about you in the years to come.

Thank you.

Members' Meetings

Gem-A Conference 2003

The Gem-A Annual Conference was held on Sunday 2 November at Kempton Park Racecourse, Sunbury-on-Thames, Middlesex. Keynote speaker was William E. Boyajian, President of the Gemological Institute of America.

The Conference was followed on Monday 3 and Tuesday 4 November by visits to the Diamond Trading Company and the Julius Werhner Collection at the Ranger's House, Greenwich, and a private viewing of the Crown Jewels with David Thomas, the Crown Jeweller.

A full report of the Conference was published in the December 2003 issue of *Gem & Jewellery News*.

Midlands Branch

On 31 October at The Earth Sciences Building, University of Birmingham, Edgbaston, Brian Dunn gave a talk entitled 'The Naughty Nineties (1890s)'.

On 28 November at the Earth Sciences Building, Brian Jackson gave a talk on 'British gemstones with a Scottish flavour'.

On 6 December the 51st Anniversary Branch Dinner was held at Barnt Green.

The Midlands Branch has a new Gem Club which meets monthly for informal practical sessions at Elliott's Deli in Birmingham's Jewellery Quarter. The inaugural meeting was held on Friday 3 October when the topic was inclusions. The November and December meetings focused on gem treatments and synthetics respectively.

Gifts to the Association

The Association is most grateful to the following for their gifts for research and teaching purposes:

Selim Besli, London, for a large collection of rough and cut gemstones.

David Kent FGA, London, for his boxed collection of 46 cut and polished colourless gemstones. Details of the collection were published in *The Journal of Gemmology*, 1987, 20(6), 344-5 and 1996 25(2), 87-9

Aung Kyaw Khaing, Myanmar, for amphiboles from Mogok, Myanmar

Rosemary Ross, FGA, Islington, London, for treated sponge coral beads

North West Branch

On 15 October at Church House, Hanover Street, Liverpool 1, Stephen Kennedy gave a talk entitled 'Notes from the laboratory – detection, disclosure and false descriptions'.

On 19 November at Church House the Branch Annual General Meeting was held when Deanna M. Brady, Raymond I. Rimmer and Elizabeth Franks were re-elected Chairman, Secretary and Treasurer respectively. The AGM was followed by a social evening.

Scottish Branch

On 15 October at the British Geological Survey, Murchison House, West Mains Road, Edinburgh, James Gosling gave a talk on 'The Cheapside Hoard'.

On 17 November at the British Geological Survey, Tracey Jukes spoke on her experiences in the trade in a talk entitled 'Tales of a gemstone dealer: thoughts from a broad'.

South East Branch

On 7 December at Christie's South Kensington the Branch AGM was held when Colin Winter, Sally Hudson and Lawrence Hudson were re-elected Chairman, Secretary and Treasurer respectively. The AGM was followed by a presentation by Terry Davidson, Chief Executive Officer of Gem-A, entitled 'Cartier: the 20th century'.

Membership

Between 1 October and 30 November 2003 the Council of Management approved the election to membership of the following:

Fellowship and Diamond Membership (FGA DGA)

Hadden, Elizabeth Anne, Stotfold, Hertfordshire. 1987/88
Kanaan, Dominique, London. 2003/2003

Fellowship (FGA)

Cherchi, Sonia, Zurich, Switzerland. 2003
Cheung, Wing Man Cynthia, Hong Kong. 2003
Ching Mei Kit, Jennifer, Kowloon, Hong Kong. 2003
Deprez, Guillaume, London. 2003
Fitzgerald, John, Peoria, Illinois, USA. 2003
Fleuranceau, Annie M., Brossard, Quebec, Canada. 2003
Ku Kai Leung, Kowloon, Hong Kong. 1992
Kwong Yi Hang, Agnes, Kowloon, Hong Kong. 1992
Li Wenjian, Nanshan, Shenzhen, P.R. China. 2003
McMillan, Emma Louise, Leamington Spa, Warwickshire. 2003
Mak Sio In, Joey, Hong Kong. 2003
Mathiesen, Lisbeth S. C., Virum, Denmark. 2003
Ng Chee Keong, Quarry Bay, Hong Kong. 1991
Phillips, Gregory, Toronto, Ontario, Canada. 2003
Phillips, Patrick Edward, Toronto, Ontario, Canada. 2003
Rosas, Manuel, Maria Ramos Pinto, Porto, Portugal. 1949
Schwabe, Arnold R., Burnaby, British Columbia, Canada. 2003
Su Chen-Hui, Taiwan, Taipei, R.O. China. 2003
Thornhill, Helen Victoria, Sheffield, South Yorkshire. 2003

Tsang, Judy, Kwai Chung, Hong Kong. 2002
Vélez Meléndez, Ana Maria, Bogota, Colombia. 2003
Westling, Jonny Anders, Stockholm, Sweden. 2003
Wijetunga, Lettietia Chandra, Colombo, Sri Lanka. 2003

Diamond Membership (DGA)

Deligiannis, Marios, Athens, Greece. 2003
Facey, Emma, Solihull, West Midlands. 2003
Georma, Titika, Pireaus, Greece. 2003
Hadley, John William, Stratford-upon-Avon, Warwickshire. 2003
Haycock, Ian Phillip, Sheldon, Birmingham, West Midlands. 2003
Hayward, Johnathon, Oldbury, West Midlands. 2003
Kelly, Christopher, High Wycombe, Bucks. 2003
Koraki, Christina, Athens, Greece. 2003
Lam Siu Wing, Hamilton, Ontario, Canada. 2003
Lee Ka Yan, Audrey, New Territories, Hong Kong. 2003
Lee Lok Chi, Kowloon, Hong Kong. 2003
Lindsay, Antony Peter, Blackheath, London. 2000
Manchanda, Anu Dippal, Smethwick, West Midlands. 2003
Rafter, Jacinta Maree, Kensington, London. 2003
Rynhold, Emma N.C., London. 2003
Singh, Harjit, Bilston, West Midlands. 2003
Suen Ka Kwan, Athena, Kowloon, Hong Kong. 2003
Tse Chui Yin, Angela, Causeway Bay, Hong Kong. 2003
Wells, Miranda E.J., Hartlebury, Worcestershire. 2003
Yip Siu Ling, New Territories, Hong Kong. 2003

Gem-A Photo Competition 2004

Imaginative Images

Creative gem cuts and mineral carvings, fanciful inclusions, gems as the inspiration in jewellery design; let your imagination run away with you in this year's Photo Competition.

All entries will be judged for originality, beauty and gemmological interest.

Prizes

First prize:	£100.00
Second Prize:	£75.00
Third Prize:	£50.00

To enter, send prints or slides of pictures taken by yourself together with the entry form to reach Gem-A by not later than 30 April 2004.

Professor Bob Howie

We send our congratulations to Gem-A Vice-President Professor Bob Howie on his election as a Foreign Member of the Lynxes – the Accademia Nazionale dei Lincei. This body became the Italian national academy of sciences (and was founded in 1603 before even the Royal Society). Professor Howie won the honour for his work in fostering the international promulgation of mineralogical knowledge via his books and 40 years' Editorship of *Mineralogical Abstracts*.

Associate Membership

Allen, Duane Owen, London
Ashton, Sandré Kay, Rayleigh, Essex
Bardehle, Petra Christina, Munich, Germany
Cushman, Tom, Sun Valley, Idaho, U.S.A.
Das, D.A., Muswell Hill, London
Ilunga, Dieudonne, Wallington, Surrey
Khan, Sanaullah, Forest Gate, London
Lee, Christopher, Pontypridd, South Wales
McFadden, Lisa, Rancho Mirage, California, U.S.A.
Morrison, Victoria, Sunningdale, Berkshire
Ng Chau Ping, New Territories, Hong Kong
Nichol, Camilla, Partick, Glasgow
Samuels, Clinton, London
Smith, Brian Donald, Canterbury, Kent
Stevens, Janet Connors, Bellevue, WA, U.S.A.
Thida, Tika Maya, Yangon, Myanmar
Tribe, Jennifer, Fetcham, Surrey
Visvanathan, Sokkalingam, Singapore
Walker, Guy, Southwark, London
Webb, Stephen Charles, Nelson, New Zealand

Yasa, Muhammad, Lahore, Pakistan
Yeoman, Michael Charles, Kingsbridge, Devon

Transfers

Fellowship to Fellowship and Diamond Membership (FGA DGA)

Watanabe, Tomoko, Ibaraki, Japan. 2003

Associate Membership to Fellowship (FGA)

Domec, Cedric, Forest, Belgium. 2003
Ecknauer, Marc, Stein, Switzerland. 2003
Inagaki, Yuko, Kawaguchi-shi, Saitama-Ken, Japan. 2003
Shikatani, Kohei, Yudogawaku, Osaka, Japan. 2003
Sykes-Gomez, Heidi, Cornelius, North Carolina, U.S.A. 2003

Obituary

We very much regret to announce the death of **Alexander E. Farn FGA**, a Vice President of the Gemmological Association since 1992. A full obituary will appear in the April issue of *The Journal.*

Roy De Rosa FGA (D.1950), Southgate, London, died on 19 September 2003.

Edward J. Soukup FGA (D.1955), San Diego, California, U.S.A., died on 19 November 2003 aged 95. Mr Soukup was an avid rockhound, silversmith, facetor and teacher, but will be best remembered for his work and publications in gemmology and jewellery. He was an active member of the Gemological Society of San Diego and the San Diego Lapidary Society.

Errata

In *J.Gemm.*, 2003, **28**(8), 505, under Obituary, for Nikola read Nikolas. We do apologize for this error.

In *J.Gemm.*, 2003, **28**(8), pp. 479-81, due to a technical error, figures 5, 6 and 7 were printed in black-and-white; a leaflet replacing those pages was circulated in December. We apologize for the error.

Pearls Coral Amber Bead Necklaces Carvings Cameos Mineral Specimens

The World of Gemstones

Ruppenthal (U.K.) Limited

Gemstones of every kind, cultured pearls, coral, amber,
bead necklaces, hardstone carvings, objets d'art and
18ct gold gemstone jewellery.

We offer a first-class lapidary service.

By appointment only
1a Wickham Court Road, West Wickham, Kent BR4 9LN
Tel: 020-8777 4443, Fax: 020-8777 2321, Mobile: 07831 843287
e-mail: roger@ruppenthal.co.uk, Website: www.ruppenthal.co.uk

Opal Precious Topaz Ruby Star Ruby Sapphire Star Sapphire Tourmaline

Gemstones Aquamarine Alexandrite Amethyst Emerald Jade Lapis-Lazuli

Modern 18ct Gem-set Jewellery

FELLOWS & SONS

Auctioneers & Valuers of Jewels, Silver & Fine Art

Established in 1876 Fellows & Sons are one of the UK's leading provincial auction houses, specialising in the sale and valuation of jewellery & watches, silver, furniture and collectables.

We hold over 30 auctions per annum of fine diamond and gem set jewellery; loose gemstones; memorial jewellery; novelties; and wrist and pocket watches, including Rolex, Piaget & Patek Phillipe.

Fully illustrated catalogues are available on our website
www.fellows.co.uk
and our Antique & Modern Jewellery & Watches auctions are available live on the internet to bidders around the world on
www.ebayliveauctions.com

Contact us now for further information on our services.

Augusta House, 19 Augusta Street, Hockley, Birmingham B18 6JA
Tel: 0121 212 2131 Fax: 0121 212 1249


2

Museums,
Educational Establishments,
Collectors & Students

I have what is probably the largest range of genuinely rare stones in the UK, from Analcime to Wulfenite. Also rare and modern synthetics, and inexpensive crystals and stones for students. Computerised lists available with even more detail. Please send 12 1st class stamps refundable on first order (overseas free).

Two special offers for students:
New Teach/Buy service and free stones on an order.

A.J. French, FGA
7 Orchard Lane, Evercreech
Somerset BA4 6PA
Telephone: 01749 830673
Email: french@frencht.freeserve.co.uk
www.ajfrenchfga.co.uk

PROMPT LAPIDARY SERVICE!

Gemstones and diamonds cut to your specification and repaired on our premises.
Large selection of gemstones including rare items and mineral specimens in stock.
Valuations and gem testing carried out.
Mail order service available.

R. HOLT & CO. LTD

98 Hatton Garden, London EC1N 8NX
Telephone 020-7405 0197/5286
Fax 020-7430 1279

ROCK 'n' gem SHOWS

Exhibitors displaying & selling a huge range of minerals, fossils, crystals & jewellery

HATFIELD HOUSE
Hatfield, Herts, Jct 4 A1M
31 JANUARY - 1 FEBRUARY

YORK RACECOURSE
York, North Yorks, Off A64
28 - 29 FEBRUARY

BRIGHTON RACECOURSE
Freshfield Road, Brighton
6 - 7 MARCH

KEMPTON PARK RACECOURSE
Sunbury-On-Thames, Middx (A308)
20 - 21 MARCH*

CHELTENHAM RACECOURSE
Prestbury Park, Cheltenham, Glos
3 - 4 APRIL

NEWARK SHOWGROUND
Winthorpe, Newark, Notts, (Off A46)
24 - 25 APRIL

ALEXANDRA PALACE
Wood Green, London
8 - 9 MAY*

KEMPTON PARK RACECOURSE
Sunbury-On-Thames, Middx (A308)
5 - 6 JUNE

NEWCASTLE RACECOURSE
High Gosforth Park, Tyne and Wear
12 - 13 JUNE

All shows open 10am - 5pm (Trade & Public)
Kempton Park only: Sat 10am - 6pm, Sun 10am - 5pm

Admission:
Alexandra Palace & Kempton Park *: Adults £3.50, Seniors £2.75
All other Kempton Park Shows: Adults £3.25, Seniors £2.75
Brighton, York & Cheltenham: Adults £2.75, Seniors £2.00
All other shows: Adults £2.50, Seniors £2.00
Children (8-16 yrs) £1.25
For further information please contact:
HD Fairs Ltd 01628 621697
Email: info@rockngem.co.uk www.rockngem.co.uk

Forthcoming Events

30 January	**Midlands Branch**: Annual Bring and Buy and Team Quiz
18 February	**North West Branch:** Gems in Space: An introduction to the world of meteorites. *Alan Bowden*

Midlands Branch One-day Conference

22 February – Barnt Green
Stephen Dale – Keynote speaker
Carl Fabergé – a Russian Revolution
Where are they now? *Michael O'Donoghue*
The minerals of Scotland. *Roy Starkey*

23 February	**Scottish Branch (Edinburgh)**: Quiz and Bring and Buy
27 February	**Midlands Branch**: The latest from the SSEF and the University of Basel. *Professor Henry Hänni*
25 February	**South East Branch**: Tavernier and his stones. *Nigel Israel*
17 March	**North West Branch**: Cartier: the 20th Century. *Terry Davidson*
23 March	**Scottish Branch (Glasgow)**: The feldspar family. *Brian Jackson*
26 March	**Midlands Branch**: The hallmark. *Chris Tarratt*
30 April	**Midlands Branch**: Branch AGM followed by Bond Street jewellers of the 19th and 20th centuries. *Terry Davidson*

Scottish Branch Conference

30 April to 3 May – Lovat Hotel, Perth
Speakers will include:
John I. Koivula – Keynote speaker
Peter Buckie, Alan Hodgkinson, Elisabeth Strack,
Colin Trowler and Chris Walton

contact details

When using e-mail, please give Gem-A as the subject:

London:	Mary Burland on 020 7404 3334; e-mail gagtl@btinternet.com
Midlands Branch:	Gwyn Green on 0121 445 5359; e-mail gwyn.green@usa.net
North East Branch:	Neil Rose on 0113 2070702; e-mail gema.northeast@gemro.com
North West Branch:	Deanna Brady 0151 648 4266
Scottish Branch:	Catriona McInnes on 0131 667 2199; e-mail scotgem@blueyonder.co.uk
South East Branch:	Colin Winter on 01372 360290; e-mail info@ga-seb.org
South West Branch:	Richard Slater on 01635 553572; e-mail rslater@dreweatt-neate.co.uk

Gem-A Website

For up-to-the-minute information on Gem-A events visit our website on www.gem-a.info

Guide to the preparation of typescripts for publication in *The Journal of Gemmology*

The Editor is glad to consider original articles shedding new light on subjects of gemmological interest for publication in *The Journal*. Articles are not normally accepted which have already been published elsewhere in English, and an article is accepted only on the understanding that (1) full information as to any previous publication (whether in English or another language) has been given, (2) it is not under consideration for publication elsewhere and (3) it will not be published elsewhere without the consent of the Editor.

Typescripts Two copies of all papers should be submitted on A4 paper (or USA equivalent) to the Editor. Typescripts should be double spaced with margins of at least 25 mm. They should be set out in the manner of recent issues of *The Journal* and in conformity with the information set out below. Papers may be of any length, but long papers of more than 10 000 words (unless capable of division into parts or of exceptional importance) are unlikely to be acceptable, whereas a short paper of 400-500 words may achieve early publication.

The abstract, references, notes, captions and tables should be typed double spaced on separate sheets.

Title page The title should be as brief as is consistent with clear indication of the content of the paper. It should be followed by the names (with initials) of the authors and by their addresses.

Abstract A short abstract of 50-100 words is required.

Key Words Up to six key words indicating the subject matter of the article should be supplied.

Headings In all headings only the first letter and proper names are capitalized.

A This is a first level heading

B *This is a second level heading*

First and second level headings are in bold and are ranged left on a separate line.

Third level headings are in italics and are indented within the first line of text.

Illustrations High resolution digital files, for both colour and black-and-white images, at 300 dpi TIF or JPG, and at an optimum size, can be submitted on CD or by email. Vector files (EPS) should, if possible, include fonts. Match proofs are essential when submitting digital files as they represent the colour balance approved by the author(s).

Transparencies, photographs and high quality printouts can also be submitted. It is recommended that authors retain copies of all illustrations because of the risk of loss or damage either during the printing process or in transit.

Diagrams must be of a professional quality and prepared in dense black ink on a good quality surface. Original illustrations will not be returned unless specifically requested.

All illustrations (maps, diagrams and pictures) are numbered consecutively with Arabic numerals and labelled Figure 1, Figure 2, etc. All illustrations are referred to as 'Figures'.

Tables Must be typed double spaced, using few horizontal rules and no vertical rules. They are numbered consecutively with Roman numerals (Table IV, etc.). Titles should be concise, but as independently informative as possible. The approximate position of the Table in the text should be marked in the margin of the typescript.

Notes and References Authors may choose one of two systems:

(1) The Harvard system in which authors' names (no initials) and dates (and specific pages, only in the case of quotations) are given in the main body of the text, (e.g. Collins, 2001, 341). References are listed alphabetically at the end of the paper under the heading References.

(2) The system in which superscript numbers are inserted in the text (e.g. ... to which Collins refers.[3]) and referred to in numerical order at the end of the paper under the heading Notes. Informational notes must be restricted to the minimum; usually the material can be incorporated in the text. If absolutely necessary both systems may be used.

References in both systems should be set out as follows, with *double spacing* for all lines.

Papers Collins, A.T., 2001. The colour of diamond and how it may be changed. *J.Gemm.*, **27**(6), 341-59

Books Balfour, I., 2000. *Famous diamonds*. 4th edn. Christie's, London. p. 200

Abbreviations for titles of periodicals are those sanctioned by the *World List of scientific periodicals* 4th edn. The place of publication should always be given when books are referred to.

The Journal of
Gemmology

Contents

Cover Picture: *Polished quartz crystal with numerous coiled 'rutile' whiskers. (See Coiled 'rutile' whiskers in a quartz single crystal pp 1-7).*

The Gemmological Association and Gem Testing Laboratory of Great Britain
Registered Office: Palladium House, 1-4 Argyll Street, London W1F 7LD

Designed & Produced by Harley UK

ISSN: 1355–4565